

**CHARACTERIZATION OF *PLASMODIUM FALCIPARUM* PFF1010c AND  
SCREENING OF PYRIMIDINE-QUINOLINE HYBRIDS AS INHIBITORS OF HSP70-  
HSP40 FUNCTIONAL PARTNERSHIPS OF THE MALARIA PARASITE**

**A dissertation submitted in fulfilment for the requirements**

**of**

**MASTERS OF SCIENCE (MSc) IN BIOCHEMISTRY**

**School of Mathematics and Natural Sciences**

**University of Venda**

**THOHOYANDOU, LIMPOPO**

**SOUTH AFRICA**

**by**

**Candidate: Pertunia T. Mudau**

**Student number: 17015657**

**Supervisor: Prof A. Shonhai**

**Co-supervisor: Dr. T. Zininga**

**May 2021**

## Abstract


With nearly half the world's population at risk of malaria infection, 229 million new cases were recorded in 2019 with Sub-Saharan Africa accounting for most of these cases. In 2020, 384 000 malaria deaths were reported in the WHO African region. *Plasmodium falciparum* is the most virulent species responsible for over 90 % of all malaria infections. The *P. falciparum* life cycle occurs through multiple stages in humans and mosquitoes. Many advances have been made in the fight against malaria through vector control and treatment against infection by the parasite. However, resistance of *P. falciparum* to antimalarial medicines/treatment has hindered global efforts to control and eliminate malaria. A multidimensional approach to fighting malaria by targeting its essential protein machinery is needed. Heat shock proteins (Hsp) are molecular chaperones that are upregulated in response to stress and have long been projected as antimalarial drug targets. *P. falciparum* Hsp70-1 (PfHsp70-1; PF3D7\_0818900) is an essential heat shock protein involved in the folding of newly synthesized and misfolded polypeptides and is also implicated in protein trafficking. PfHsp40 (PF3D7\_1437900.1) is a type I Hsp40 co-chaperone of PfHsp70-1 that presents substrates to PfHsp70-1 and stimulates its ATPase activity, while PFF1010c (PF3D7\_0620700.1) is a type IV Hsp40 found in the gametocytes that is yet to be characterized. The current study explored pyrimidine-quinoline hybrid (PQH1-4) compounds as possible inhibitors of PfHsp70-1 interaction with PfHsp40. Furthermore, this study sought to characterize the structure and function of PFF1010c. Notably, PFF1010c possess SVN residues in place of the HPD motif located in the so-called J domain of this Hsp40 co-chaperone. For this reason, PFF1010c is an atypical Hsp40 which may lack the capability to interact with PfHsp70-1. To characterise the role of PFF1010c, and consequently, its SVN motif, the SVN motif of PFF1010c was switched with the HPD motif of PfHsp40. The structure-function features of the mutants were characterized relative to the wild type Hsp40s. Bioinformatics based analysis was employed to predict the fold of the mutants relative to the wild type Hsp40s. Recombinant proteins were expressed in *E. coli* cells and purified using nickel affinity chromatography. Fluorescence spectroscopy was used to map out the tertiary structure of the Hsp40 proteins. It was noted that the HPD motif confers thermostability to the proteins. Possible interaction of PFF1010c with PfHsp70-1 was evaluated using

ATPase assay and SPR analysis. Furthermore, the same study was repeated for the motif switch mutants. PFF1010c was found to interact with PfHsp70-1, though the interaction would not be as conventional as the one between PfHsp40 and PfHsp70-1 because PFF1010c does not have the HPD motif. SPR analysis was also employed to investigate binding of the pyrimidine-quinoline hybrid compounds to PfHsp70-1. Compounds PQH1 and PQH4 were found to have high binding affinities for PfHsp70-1. The compounds also inhibited binding of PfHsp40 to PfHsp70-1. The study provides the first evidence that PfHsp70-1 interacts with a type IV Hsp40, where PfHsp70-1 and PFF1010c could be a druggable complex to reduce transmission of malaria from humans to mosquito. The pyrimidine-quinoline hybrid compounds would play a role in the proliferation of the malaria parasite by inhibiting the chaperone activities of PfHsp70-1 and PfHsp40.

**Keywords: HPD/SVN motif, Malaria, *P. falciparum*, PFF1010c, PfHsp40, PfHsp70-1, pyrimidine-quinoline hybrids**

## Declarations

I, Pertunia Thendo Mudau, declare that the dissertation submitted to the University of Venda is my own, that has been submitted to the University of Venda. The dissertation does not contain any other person's writing unless specifically acknowledged and referenced accordingly.

Signature (Candidate):  Date: 04/05/2021

## Dedication

I dedicate this thesis to my parents, Munyadziwa and Madume Mudau, who have been my constant support and the biggest cheerleaders of all my hopes, dreams and aspiration. I hope that in everything I do I make you proud.

## Acknowledgements

I thank my supervisor Prof. Addmore Shonhai and co-supervisor Dr. Tawanda Zininga for their guidance, mentorship and expertise throughout the project and a whole lot of patience they had with me. Their professional input and advice has been invaluable and I have learned a lot from them.

I wish to extend acknowledgement to Dr G Chakafana, Mr LM Mathomu and Dr A Burger for their advice, invaluable input, assistance and encouragement.

I wish to extend further acknowledgement to the following:

- National Research Foundation (NRF South Africa) for funding this research project
- University of Venda research fund
- Department of Pharmaceutical Chemistry, College of Health sciences, University of KwaZulu-Natal for the antimalarial compounds

I would also like to express my gratitude to my lab mates, the Protein Biochemistry & Malaria (ProBioM) research team and the staff of the Biochemistry department (University of Venda). A special thanks Ms ZS Thenga as well.

And above all, I thank God Almighty for seeing me through.

## Table of Contents

Abstract .....	i
Declarations .....	iii
Dedication .....	iv
Acknowledgements .....	v
List of Figures .....	ix
List of Tables .....	xi
List of Symbols .....	xii
List of Outputs .....	xiii
Chapter 1: Introduction and literature review .....	1
1.1. Malaria: Still a devastating disease .....	1
1.2. Malaria parasite and it's life cycle .....	1
1.3. Treatment of malaria .....	3
1.4. The gametocyte stages .....	6
1.5. Molecular chaperones .....	8
1.6 Heat shock proteins .....	8
1.6.1 Heat shock protein 100 .....	9
1.6.2 Heat shock protein 90 .....	11
1.6.3 Heat shock protein 70 .....	12
1.6.3.1 Hsp70 interaction with co-chaperone (Hsp40) .....	13
1.6.4 Heat shock protein 40 .....	15
1.7 Molecular chaperones as drug targets .....	17
1.8 Pyrimidine-quinoline hybrids as antimalarials .....	19
1.8.1 Role of heat shock proteins in drug resistance .....	19
1.9 Study rationale and problem statement .....	20
1.10 Hypothesis .....	21
1.11 Aim .....	22
1.12 Objectives .....	22
Chapter 2: Methodology .....	23
2.1 Bioinformatics .....	24
2.1.1 Multiple sequence alignments .....	24
2.1.2 Prediction of the PFF10101c interactome .....	25
2.1.3 3D model generation .....	25
2.1.4 Hydropathy profile of Hsp40s .....	25

2.2 Expression of recombinant protein in E. coli XL1 Blue and JM109 .....	26
2.3 Purification of the recombinant protein.....	26
2.4 Investigation of the tertiary structure of the recombinant protein.....	27
2.5 Surface plasmon resonance (SPR) analysis .....	28
2.5.1 Investigating protein-protein interactions .....	28
2.5.2 Investigating drug-protein interactions .....	28
2.6 ATPase assay .....	29
Chapter 3: Results.....	31
3.1 Bioinformatics and in silico studies .....	31
3.2 Confirmation of plasmid constructs used in this study .....	38
3.3 Expression and purification of recombinant proteins.....	41
3.4 Biophysical characterisation of Hsp40 proteins.....	46
3.4.1 Hydrophobicity of proteins .....	46
3.4.2. Effects of denaturants on tertiary structure stability .....	47
3.4.3 Thermostability of the proteins.....	49
3.5 Interactions studies between Hsp40s and PfHsp70-1.....	50
3.5.1 ATPase activity .....	50
3.3 SPR Analysis .....	51
3.6 Screening of quinoline-pyrimidine hybrid compounds using SPR .....	54
Chapter 4: Discussion .....	57
Conclusions and future perspectives .....	61
References.....	63
Soulard, V., Bosson-Vanga, H., Lorthiois, A., Roucher, C., Franetich, J., Zanghi, G. 2015. Plasmodium falciparum full life cycle and Plasmodium ovale liver stages in humanized mice, <i>Nature Communications</i> , 1-9.....	72
Appendix A.....	75
A1. Preparation of competent E. coli JM109 and XL1 Blue cells .....	75
A2. Transformation of competent cells.....	75
A3. Plasmid DNA extraction.....	76
A4. Restriction digest of plasmid DNA .....	76
A5. Agarose gel electrophoresis .....	76
A6. Determination of protein solubility.....	77
A7. Sodium dodecyl sulphate-polyacrylamide gel electrophoresis (SDS-PAGE)..	77
A8. Western blot analysis.....	78
A9. Protein concentration determined using Bradford assay .....	79



A10. Immobilization of ligand (PfHsp70s) on GLC sensor chip.....	79
Appendix B: Supplementary data .....	81
Appendix C: List of Reagents.....	100

## List of Figures

- Figure 1.1. Plasmodium falciparum life cycle
- Figure 1.2. Gametocytes stages of P. falciparum in the human host
- Figure 1.3. Structure of PfClpB2 chaperones
- Figure 1.4. Predicted structure of PfHsp90 with its functional domains
- Figure 1.5. Typical structure of PfHsp70
- Figure 1.6. Chaperone mediated folding by the Hsp70-Hsp40 chaperone complex
- Figure 1.7. Schematic representation of the different types of Hsp40 proteins
- Figure 1.8. Basic chemical structure of pyrimidine and quinoline
- Figure 2.1. Alignment of PfHsp40 J-domain with PFF1010c J-domain
- Figure 2.2. Step by step process of ATPase assay
- Figure 3.1. Protein sequence alignments of J domain of Hsp40s
- Figure 3.2. Predicted tertiary structures of PFF1010c and its mutant PFF1010c-HPD
- Figure 3.3. Predicted tertiary structure of PfHsp40 and its mutant PfHsp40-SVN
- Figure 3.4. Prediction of hydrophobicity in PFF1010c and Hsp40 *versus* their mutants
- Figure 3.5. Restriction digest of the pQE30/*PFF1010c* and pQE30/*PFF1010c-HPD* plasmid construct
- Figure 3.6. Restriction digest of the pQE30/*PfHsp40* and pQE30/*PfHsp40-SVN* plasmid construct
- Figure 3.7. Restriction digest of the pQE30/*PfHsp70-1* plasmid construct
- Figure 3.8. Expression and purification of PFF1010c
- Figure 3.9. Expression and purification of PFF1010c-HPD
- Figure 3.10. Expression and purification of PfHsp40
- Figure 3.11. Expression and purification of PfHsp40-SVN
- Figure 3.12. Expression and purification of PfHsp70-1
- Figure 3.13. Analysis of the tertiary structure of wildtype Hsp40s and mutants using ANS fluorescence
- Figure 3.14. Effect of denaturants, urea and guanidine hydrochloride, on the tertiary structure of Hsp40s
- Figure 3.15. Investigating the thermostability of Hsp40s

Figure 3.16. Comparative analysis of ATPase activity stimulation by wildtype vs mutant Hsp40s

Figure 3.17. Sensograms for PfHsp70-1 association with Hsp40s in presence and absence of nucleotides

Figure 3.18. Relative affinities of Hsp40s to PfHsp70-1

Figure 3.19. Sensograms of PfHsp70-1 association with quinoline-pyrimidine hybrid compounds in the presence and absence of its co-chaperone, PfHsp40

Figure A1. Protein standard curve

Figure B1. Full sequence alignment of PFF1010c with canonical Hsp40s

Figure B2. Full sequence alignment of PFF1010c with other parasitic Apicomplexa species

Figure B3. Full sequence alignment of PFF1010c with other *P. falciparum* type IV Hsp40s

Figure B4. Secondary structure prediction of PFF1010c

Figure B5. Secondary structure prediction of PFF1010c-HPD

Figure B6. Secondary structure prediction of PfHsp40

Figure B7. Secondary structure prediction of PfHsp40-SVN

Figure B8. Effect of urea on PFF1010c and PFF1010c-HPD tertiary structures.

Figure B9. Effect of urea on PfHsp40 and PfHsp40-SVN tertiary structures.

Figure B10. Effect of guanidine hydrochloride on PFF1010c and PFF1010c-HPD tertiary structures.

Figure B11. Effect of guanidine hydrochloride on PfHsp40 and PfHsp40-SVN tertiary structures.

Figure B12. Investigating the thermostability of PFF1010c and PFF1010c-HPD.

Figure B13. Investigating the thermostability of PfHsp40 and PfHsp40-SVN.

Figure B14. SPR curve.

## List of Tables

Table 1.1. Classification of antimalarial drugs and their mode of action

Table 1.2. Functions, localization and size of different heat shock proteins

Table 2.1. List of plasmid constructs and bacterial expression strains used

Table 2.2. Formulas of the pyrimidine-quinoline hybrids

Table 3.1. Proteins predicted through co-expression patterns to interact with PFF1010c

Table 3.2. ATPase kinetics for PfHsp70-1 with Hsp40s

Table 3.3. Kinetics for the interaction of PfHsp70-1 with Hsp40s

Table 3.4. Kinetics for the interaction of PfHsp70-1 and quinoline-pyrimidine hybrid compounds

Table A1. Reagents added per tube for digestion of plasmid DNA

Table A2. Preparation of 12% separating gel and of stacking gel

Table B1. Properties of amino acid residues in HPD and SVN motif

Table B2. Peptide properties of Hsp40s

## List of Symbols

<b>Abbreviations of units</b>	<b>Symbol Interpretation</b>
%	percent
$\mu\text{l}$	microlitre
A595	absorbance at 595 nanometres
A600	absorbance at 600 nanometres
bp	base pair
kDa	kilodalton
$\mu\text{M}$	micromolar
$^{\circ}\text{C}$	degree celsius
$\mu\text{l}$	microlitre
ml	millilitre
l	litres
w/v	weight per volume
v/v	volume per volume
$\mu\text{g}$	microgram
g	gram
$\alpha$	alpha
$\beta$	beta

## List of Outputs

### Journal articles

Kayamba, K., Malimabe, T., Ademola, I.K., Pooe O.J., Kushwaha, N.D., Mahlalela, M., van Zyl, R.L., Gordan, M., Mudau, P.T., Zininga, T., Shonhai, A. and Nyamori, V.O. 2021, Design and synthesis of quinoline-pyrimidine inspired hybrids as potential *Plasmodial* inhibitors, *European Journal of Medicinal Chemistry*, 217, 1-20

Chakafana, G., Mudau, P.T., Zininga, T. and Shonhai, A. 2021, Characterisation of a unique linker segment of the *Plasmodium falciparum* cytosol localised Hsp110 chaperone, *International Journal of Biological Macromolecules*, 180, 272-285

### Conference Proceedings

Mudau, P.T., Zininga, T. and Shonhai, A. Biochemical characterization of *Plasmodium falciparum* Hsp40 type IV protein, PFF1010c. 5<sup>th</sup> Annual Southern Africa Malaria Research Conference, 30 – 01 August 2019

## Chapter 1: Introduction and literature review

### 1.1. Malaria: Still a devastating disease

Infectious diseases are caused by pathogenic microorganisms such as bacteria, viruses or parasites and the spread of these diseases can be through direct or indirect contact with another person (Cortez and Weitz, 2013; WHO, 2017). Direct transmission occurs when the infectious agent is directly transferred through personal contact as in the case of Human Immune deficiency Virus (HIV) and through tiny droplets of spray causing Tuberculosis and Influenza. Indirect transmission occurs when a susceptible host has been exposed to a pathogen in the environment through free living pathogens or through other infected host species as in the case of malaria or rabies. Malaria, HIV and TB are three of the world's most common infectious diseases (Irene *et al*, 2016).

Nearly half of the world's population is at risk of malaria infection, with 229 million new cases of malaria being recorded in 2019 (WHO, 2020). It is estimated that in 2018, the WHO African Region accounted for about 93% of all deaths caused by malaria (WHO, 2019). Furthermore, 70% of these deaths are usually children under the age of five (WHO, 2017). Children between 6 months and 5 years of age are most vulnerable because they have lost maternal immunity and have not yet developed specific immunity to infection (Schumacher and Spinelli, 2012). Although the global mortality rate has decreased significantly between 2010 and 2018, malaria related deaths are still high, with approximately 405 000 deaths being reported in 2018 (WHO, 2019).

Five species of the single cell parasites of the genus *Plasmodium* cause malaria in humans (Rug and Maier, 2011; Srinivas, 2015). These species are *P. vivax*, *P. malariae*, *P. knowlesi*, *P. ovale* and *P. falciparum*. *P. falciparum* is responsible for over 90% of the malaria infections, as this is the most virulent species (Tiburcio *et al*, 2015).

### 1.2. Malaria parasite and its life cycle

The *P. falciparum* has a complex, multistage life cycle occurring within two living organisms, mosquitoes and humans. Mosquitoes are the insect vectors of the parasite

while humans are the main vertebrate host. Malaria infection in humans is initiated when an infected female *Anopheles gambiae* mosquito injects sporozoites (Figure 1.1.), into the blood stream during a blood meal. The sporozoites then actively invade the hepatocytes (liver cells) and start the asexual exo-erythrocytic schizogonic cycle (Figures 1.1). At the end of the liver cycle, merozoites are released into the sinusoids of the liver through budding of merozoites, which are merozoite-filled vesicles (Soulard *et al*, 2015). Merozoites are capable of hiding from the immune system as they are derived from the host hepatocyte plasma membrane (Vaughn and Kappe, 2017). It is these released merozoites that then invade erythrocytes (Matteelli and Castelli, 2015; Soulard *et al*, 2015). Inside the erythrocytes, the merozoites develop into the trophozoite stage and nuclear division of the trophozoites generates about 16-32 merozoites (Figure 1.1.; Soulard *et al*, 2015). Some of the merozoite infected erythrocytes leave the asexual multiplication cycle. Alternatively, these merozoites develop into female and male gametocytes, which are the sexual forms of the parasite (Figure 1.1.; Matteelli. and Castelli, 2015). During a blood meal, the mosquito ingests the mature gametocytes present in the microvasculature of the human host (Figure 1.1.; Alano, 2007). Once the ingested gametocytes make their way to the gut of the mosquito, maturation of the female and male gametocytes occurs, preceded by fertilization which results in the formation of ookinete (motile zygote). The resulting ookinete then invades the gut wall of the mosquito and matures into an oocyst, which enter a multiplication phase and develop into sporozoites. The resulting invasive sporozoites travel into the salivary glands of the mosquito and infect a new host during the mosquito's next blood meal (Cox, 2010).



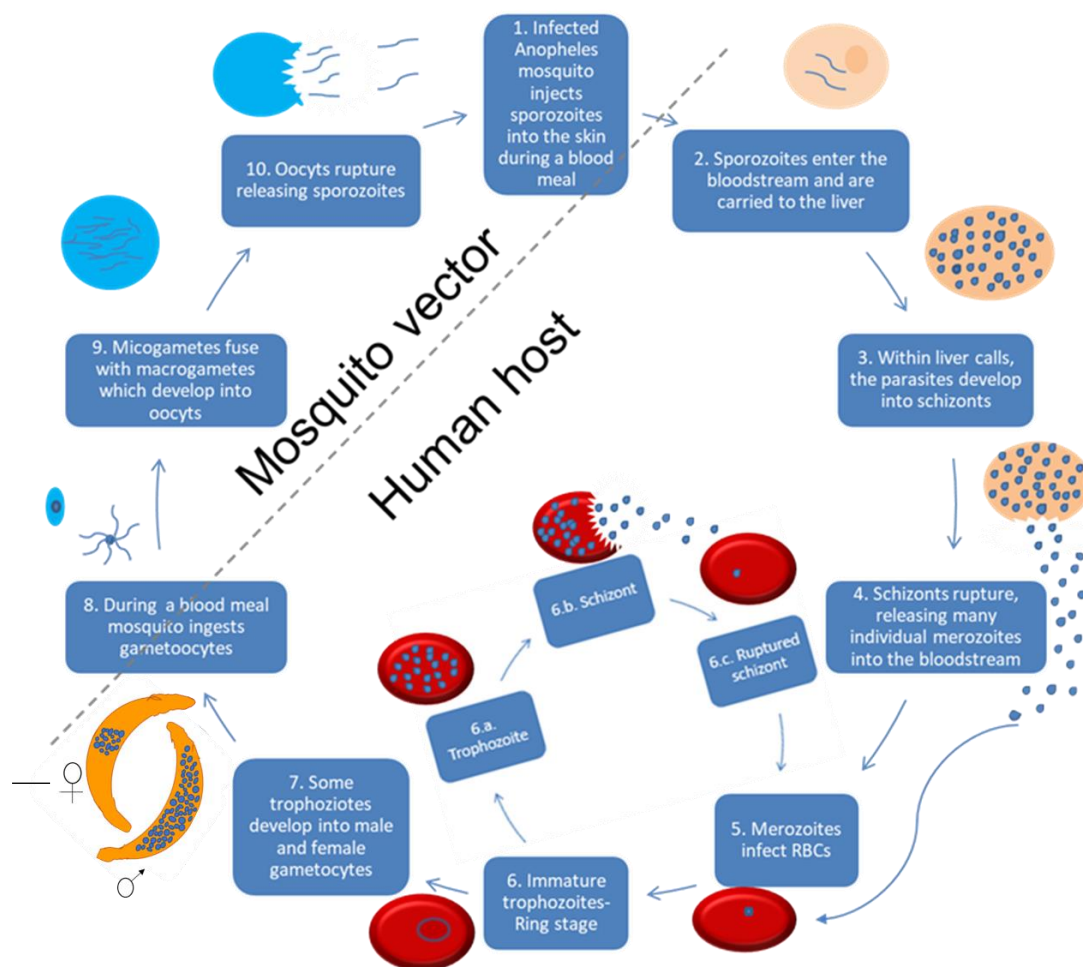


**Figure 1.1:** The life cycle of *Plasmodium falciparum*, showing the development stages as they occur in the mosquito vector and human host. (Siciliano and Alano, 2015).

### 1.3. Treatment of malaria

For thousands of years, traditional/herbal medicines were relied on in the treatment of malaria (Willcox and Bodeker, 2004). That is because the phytochemicals highly efficacious in treating malaria are abundantly found in herbal plants (Okello and Kang, 2019). The two main groups of modern antimalarial drugs, quinine and artemisinin derivatives, are derived from traditional/herbal plants (Willcox and Bodeker, 2004). There are more than 1200 plant species that can be used in treating malaria (Willcox and Bodeker, 2004). Effective modern-day treatment of malaria is dependent on successful identification of the infecting *Plasmodium* species, clinical status of patient and drug susceptibility of the infecting parasite determined through susceptibility drug phenotyping (Kaddouri *et al*, 2006; Srinivas, 2015). Anti-malarial drugs can be classified according to their efficacy and the structure of the target tissue (Srinivas, 2015). Various antimalarial classes are known that are delineated based on tissue

specificity and include, tissue schizonticides (prophylaxis and relapse prevention), blood schizonticides, gametocytocides and sporontocides (Srinivas, 2015). The commonly used antimalarials can also be grouped according to classes of compounds (Table 1.1; Saifi et al, 2013).

**Table 1.1:** Classification of antimalarial drugs and their mode of action

Drug group	Drug	Mode of action	References
Quinolines	Chloroquine	Inhibits DNA and RNA biosynthesis, induces degradation of ribosomes and inhibits the detoxification of heme.	Slater, 1993 Saifi <i>et al</i> , 2013 Thome <i>et al</i> , 2013
	Quinine	Causes clumping of the malaria pigment, hemozoin	
	primaquine	Generates the accumulation of H <sub>2</sub> O <sub>2</sub> . This leads to the generation of superoxide and hydroxyl radicals or damage of Fe <sup>+</sup> and FeS-containing proteins and through oxidation of sulphhydryl groups on proteins.	Camarda <i>et al</i> , 2019 Chotivanich <i>et al</i> , 2006
	Mefloquine	Inhibits polymerization of heme <i>in vitro</i>	Slater, 1993, Saifi <i>et al</i> , 2013
Antifolates	Pyrimethamine	These drugs interfere with folate metabolism by inhibiting either dihydropteroate synthase or dihydrofolate reductase	Saifi <i>et al</i> , 2013
	Proguanil		
	sulfadoxine		
Artemisinin derivatives	Artemisinin	Artemisinins undergo bioactivation to generate the biologically active metabolite, dihydroartemisinin with reactive oxygen species	Chotivanich <i>et al</i> , 2006
	Artesunate		
	artemether		
Hydroxynaphthaquinones	Atovaquone	Acts primarily on mitochondrial functions and inhibits cytochrome c reductase activity in <i>P. falciparum</i>	Fry and Pudney, 1992 Saifi <i>et al</i> , 2013
Antibiotics	Tetracycline	May inhibit mitochondrial protein synthesis directly and decrease activity of mitochondrial enzyme involved in <i>de novo</i> synthesis of pyrimidine	Gaillard <i>et al</i> , 2015
	Doxycycline	Inhibits synthesis of nucleotides and ribonucleotides	
Synthetic dye	Methylene blue	Inhibits glutathione reductase, prevents polymerization of haem into hemozoin and has the potential to reverse chloroquine resistance	Schirmer <i>et al</i> , 2003 Suwanarusk <i>et al</i> , 2015

Chloroquine is used to treat uncomplicated malaria (CDC, 2013). Chloroquine is a quinoline-containing drug, which is known to accumulate by a weak base mechanism in the acidic food vacuoles of intraerythrocytic trophozoites. This prevents the degradation of haemoglobin. Chloroquine and related quinolines such as quinine inhibit the heme polymerase enzyme, an enzyme that is also present in trophozoite food vacuole and is responsible for the biosynthesis of the beta-hematin (malarial pigment; Chou and Fitch, 1992; Slater, 1993). Chloroquine and quinine both have gametocytocidal activity against *P. vivax* and *P. Malariae* (Srinivas, 2015). However, the heavy use of chloroquine over the decades eventually led to chloroquine resistance in *P. falciparum* (Wellem and Plowe, 2001). Primaquine has gametocytocidal effect against all *plasmodia*, including *P. falciparum*. Pyrimethamine competitively inhibits dihydrofolate reductase, a key enzyme within the redox cycle of tetrahydrofolate that reduces dihydrofolic acid to tetrahydrofolic acid, and functions together with primaquine to block the erythrocytic stage (Srinivas, 2015; PubChem, 2017). Chloroquine, quinine, halofantrine, mefloquine, sulfadoxine, pyrimethamine, sulfones and tetracyclines are all important drugs in anti-malarial chemotherapy. These drugs target clinical malaria by acting on the blood forms (merozoites, trophozoites and schizonts) of the parasite (Srinivas, 2015). In most countries, artemisinin-based combination therapy (ACT) is used as the first-line treatment for *P. falciparum* (WHO, 2008). Artemisinins act by inhibiting a *P. falciparum*-encoded sarcoplasmic-endoplasmic reticulum calcium ATPase (Dahlstrom *et al*, 2008). Artemisinin prevents progression of the disease by inhibiting the development of the trophozoites (Portugaliza *et al*, 2020). Artemisinin compounds (artesunate and artemether) have also been reported to reduce gametocytogenesis by reducing the sexual conversion rate of trophozoites to gametocytes which directly reduces the transmission of malaria (Sutherland *et al*, 2005; Portugaliza *et al*, 2020). But patients treated with ACTs remain infectious for several days contributing to transmission despite the drugs' efficacy in reducing gametocytemia (gametocyte density in blood) (Portugaliza *et al*, 2020).

#### 1.4. The gametocyte stages

Transmission of the malaria parasites heavily relies on the gametocyte stages of the parasite (Tibúrcio *et al*, 2015). *P. falciparum* gametocytes mature over five stages and have been shown to exhibit a different pattern of gene expression than asexual stages (Talman *et al*, 2004; Delves *et al*, 2013). This could be attributed to the fact that approximately 20% of all plasmodial genes are expressed specifically in the sexual stages (Ngwa *et al*, 2016). This may account for how anti-malarial drugs are less effective on gametocytes, which includes artemisinin derivatives. Primaquine is the only drug recognized thus far to attack *P. falciparum* gametocytes (Henry *et al*, 2019). Haematological disruptions have been suggested to be linked to the production of gametocytes. This includes red blood cell lysis and anaemia (Baker, 2010). In recent studies, epigenetics and transcriptional regulation have been associated with gametocyte commitment (Ngwa *et al*, 2016). *P. falciparum* gametocytes develop from stage I to stage V over a period of 7 to 12 days and develop from the erythrocytic asexual stages of the parasite's life cycle (Delves *et al*, 2013; Talman *et al*, 2004; Figure 1.2). These five stages are morphologically recognisable, and as they grow, the parasites elongate to gradually occupy the majority of the host erythrocytes (Baker, 2010). Stage I gametocytes are roundish with a pointed end and are difficult to distinguish from young trophozoites in a Giemsa-stained blood film. Giemsa solution is a type of Romanowsky stain that is composed of eosin and methylene blue and stains the parasite nucleus red and the cytoplasm blue (Baker, 2010; WHO, 2016). There are no visible alterations on the erythrocyte plasmalemma of stage I gametocytes compared to that of the knobbed (surface protrusions) asexual parasite infected erythrocyte (Talman *et al*, 2004). Gametocyte stages II-V are easily differentiated using Giemsa-stained blood films (Baker, 2010). In stage II, the subpellicular membrane and microtubule complex expand to give rise to an asymmetrical cell (Figure 1.2; Talman *et al*, 2004). During stage III, further development of the subpellicular membrane complex distorts the cell. Notably, the male nucleus is larger than that of the female. During stage IV of gametocyte development, the membrane and microtubule complex completely surrounds the gametocyte which restores the cells symmetry. Immature gametocytes (stage I-IV) are sequestered into internal organs (primarily the bone marrow and spleen) of the human host (Tibúrcio *et al*, 2015; de Jong *et al*, 2020). By stage V, the subpellicular

microtubules are lost by depolymerisation while the inner membrane remains (Talman *et al*, 2004). The only stage that circulates within the host's blood stream are the mature stage V gametocytes. This makes the mature stage V gametocytes available for uptake by the mosquito vector during a blood meal (Gardiner and Trenholme, 2015; de Jong *et al*, 2020).

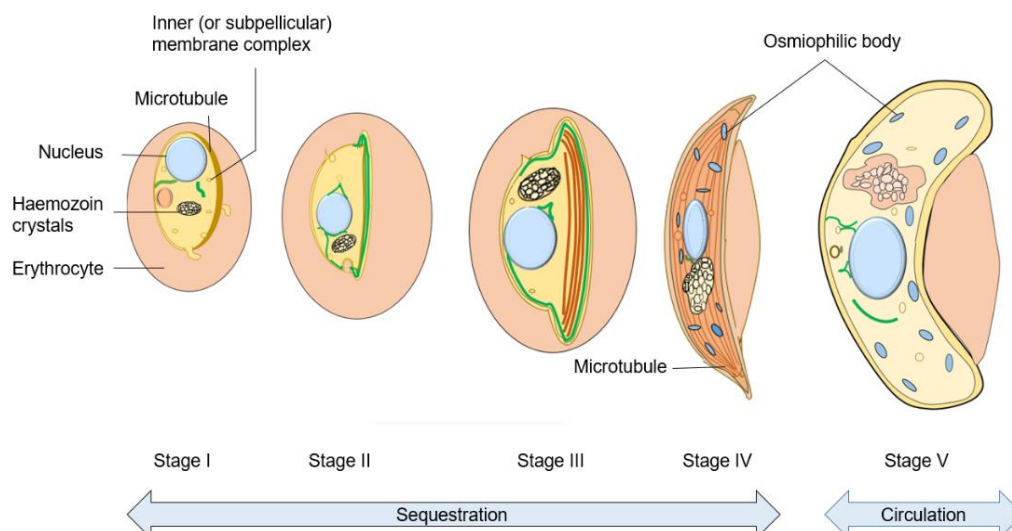


**Figure 1.2. Gametocyte stages of *P. falciparum* in the human host.** Stage I to stage IV are sequestered while stage V gametocytes are found in circulation (Dixon *et al*, 2012).

*Plasmodium* asexual parasites form gametocytes at a low frequency (0.2 to 1%), with sexually committed merozoites from one pre-committed schizont all forming gametocytes of the same sex (either male or female) (Delves *et al*, 2013; Ngwa *et al*, 2016). Mature gametocytes are “primed” for rapid and complex development into gametes upon sensing a change in environment when taken up into the mosquito during a blood feed. Once in the gut of the mosquito, the formation of gametes is induced by a decrease in temperature as well as the presence of a gametocyte-activating factor (xanthurenic acid) (Delves *et al*, 2013). In order to survive the transition from a warm-blooded human host to a cold-blooded mosquito vector, the gametocytes need to be able to maintain protein homeostasis (proteostasis) (Shonhai, 2010; Hartl *et al*, 2011). To reverse protein misfolding that arises from the stressful conditions, cells have developed a complex network of protein quality control machines including molecular chaperones (Hartl *et al*, 2011). Aside from gene expression and protein synthesis, other changes that occur include changes in the

parasites cell biology and metabolism ensuring development, drug resistance and transmission of the gametocytes (Ngwa *et al*, 2016).

### **1.5. Molecular chaperones**

Molecular chaperones are abundant and highly conserved proteins that assist other macromolecules assemble into higher order structures, without themselves being part of these final structures (Miyata *et al*, 2011; Saibil, 2013). Molecular chaperones are also employed to stabilize non-native protein conformations (Patterson and Höhfeld, 2006). Most of the major chaperones make use of ATP binding and hydrolysis cycles to act on non-native polypeptides to facilitate their folding or unfolding. Some chaperones simply have a 'handover' role where they protect nascent subunits during the assembly process (Saibil, 2013). The classical function of chaperones is to facilitate protein folding, inhibit misfolding and prevent aggregation (Patterson and Höhfeld, 2006). Molecular chaperones can be further divided into three functional subclasses: folding, holding and disaggregase chaperones (Baneyx, 2008). In the first class are folding chaperones which rely on ATP-driven conformational changes to mediate the net refolding and unfolding of the substrates (Baneyx, 2008). Holdases act *via* reversible complex formation, binding client proteins in an ATP-independent manner to prevent protein aggregation and for further action by other chaperones, commonly a foldase (Morky *et al*, 2015; Hall, 2019; Begeman *et al*, 2020). Disaggregases liberate protein clients from aggregates (Morky *et al*, 2015).

### **1.6 Heat shock proteins**

Some molecular chaperones that are upregulated in response to stress are termed heat shock proteins (Hsps) (Lindquist, 1984; Miyata *et al*, 2011). In both prokaryotic and eukaryotic cells, Hsps are essential components contributing to cellular homeostasis under optimal and detrimental growth conditions (Park and Seo, 2015). Hsps are a family of structurally related proteins that are classified according to their molecular weight. The Hsps that have been well characterized from many organisms,

are Hsp20, Hsp40, Hsp60, Hsp70, Hsp90 and Hsp100 (Neckers and Tatu, 2008, Table 2).

**Table 1.2:** Function, localization and average size of the different Heat shock protein families in *P. falciparum*

Hsp family (size in kDa)	Location	Functions	References
Hsp100 (~100 kDa)	Apicoplast Parasitophorous vacuole (PV) mitochondria	Involved in secretion of malarial proteins into the PV	El Bakkouri <i>et al</i> , 2010 AhYoung <i>et al</i> , 2015
Hsp90 (~90 kDa)	Cytosol Endoplasmic reticulum (ER) Apicoplast Mitochondria	Signal transduction, partners with Hsp70 to fold proteins, antigen processing, protein trafficking and secretion, RNA processing role in cell cycle and proliferation	Jolly and Morimoto, 2000 Banumathy <i>et al</i> , 2003 Zininga <i>et al</i> , 2015
Hsp70 (~70 kDa)	Cytosol Nucleus Mitochondria ER PV Erythrocyte cytosol Maurer's cleft	Folding newly synthesized polypeptides, interorganellar transport, signal transduction, refolding denatured proteins and maintenance of proteins <i>in vitro</i> , role in cell cycle and proliferation, anti-apoptotic activity	Jolly and Morimoto, 2000 Kityk <i>et al</i> , 2012 Zininga <i>et al</i> , 2015
Hsp60 (~60 kDa)	Apicoplast Mitochondria	Refolding and preventing aggregation of denatured proteins <i>in vitro</i>	Liu and Houry, 2014 Yeo <i>et al</i> , 2015
Hsp40 (~40 kDa)	Cytosol, nucleus Apicoplast ER Erythrocyte cytosol J-dots, knob	Important co-chaperone activity with Hsp70, binds and presents substrates to Hsp70, modulates ATPase activity of Hsp 70 and regulates functional specificity of Hsp70	Rug and Maier, 2011 Pesce <i>et al</i> , 2014 Makhoba <i>et al</i> , 2016
Small Hsps (~20 kDa)	Cytosol	<i>In vitro</i> suppression of aggregation and heat inactivation of proteins, confers thermotolerance through stabilization of microfilaments, anti-apoptotic activity	Jolly and Morimoto, 2000

Proteins belonging to a particular family share functional similarity and structural homology across species (Jolly and Morimoto, 2000).

### 1.6.1 Heat shock protein 100

The Hsp100 class of chaperones belong to the AAA+ superfamily of ATPases that are defined by the presence of a ~200-250 amino acid basic core comprised of a  $\alpha$ -helical domain a walker-type nucleotide domain (Kirstein *et al*, 2009). The Hsp100 proteins

are divided into two major classes. Members of the first class of Hsp100 contain two highly conserved nucleotide-binding domains (NBD) that are flanked by amino-terminal middle and carboxy-terminal regions (Schirmer *et al*, 1996). Members of the second class are shorter in length as they only contain a single NBD that closely resembles the second NBD of class 1 Hsp100. Class 2 members also possess the carboxy-terminal region (Schirmer *et al*, 1996). The Hsp100 family/Clp chaperones disassemble protein aggregates (Neckers and Tatu, 2008). The *P. falciparum* parasite contains five Clp ATPases: *PfClpB1*, *PfClpB2*, *PfClpC*, *PfClpM* and *PfClpY* (*PFHsIU*) (El Bakkouri *et al*, 2010; Liu and Houry, 2014). These proteins were found to be localized within the apicoplast, a non-photosynthetic organelle that functions to accommodate several metabolic pathways in *P. falciparum*. However, *PfClpB2* (also known as Hsp101; Figure 1.2) was also found in the parasitophorous vacuole (PV) and is proposed to be involved in the secretion of malarial proteins into the PV (El Bakkouri *et al*, 2010; Liu and Houry, 2014). *PfClpB1* is located in the apicoplast (AhYoung *et al*, 2015). Hsp101 comes together with PTEX150 and EXP2 (a PVM protein) to form a membrane protein complex known as PTEX, the *Plasmodium* translocon of exported proteins (Ho *et al*, 2018). Malarial effector proteins are transported across the PVM into the host erythrocytes through the PTEX, a process essential for parasite survival (Chrisholm *et al*, 2018; Ho *et al*, 2018). Hsp104 is a homolog of Hsp101 that collaborates with other Hsps to disaggregate proteins. It is highly conserved in eubacteria and eukaryotes and is essential for cell viability in stressful conditions when proteins tend to aggregate more (Torrente *et al*, 2014). Hsp101 is also essential for *P. falciparum* survival and is a prominent drug target (Torrente *et al*, 2014).

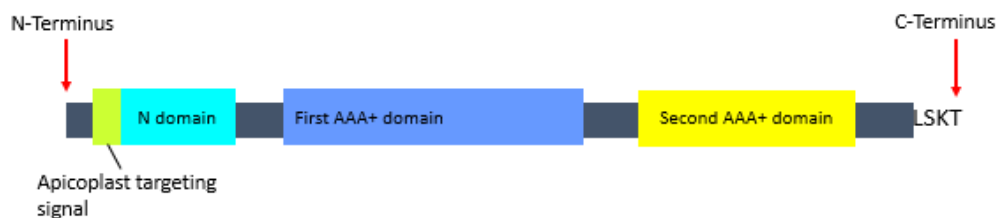


**Figure 1.3. Structure of *PfClpB2* chaperones.** *PfClpB2* possesses an apicoplast targeting signal and N-domain on the N-terminus, followed by the first AAA+ domain. The second AAA+ domain is positioned towards the C-terminus. *PfClpB2* has a LSKT domain on the C-terminus.



*P. falciparum* also contains a proteolytic subunit, PfClpP. The inactive version of this protease is PfClpR (El Bakkouri *et al*, 2010). Experimental data showing the functions of PfClpB1, PfClpC and PfClpM is not available and furthermore, PfClpB1, PfClpB2 and PfClpM do not bind a proteolytic component responsible for degrading or hydrolysing proteins into smaller peptides (Liu and Houry, 2014).

### 1.6.2 Heat shock protein 90

Hsp90 is a molecular chaperone that is important for normal growth and development in eukaryotes and is involved in protein folding (Banumathy *et al*, 2003; Neckers and Tatu, 2008). Hsp90 also regulates activities of protein kinases and transcription factors (Banumathy *et al*, 2003). It is known to form a partnership with Hsp70 coordinated by Hsp70-Hsp90 organising protein which is an adapter protein (Gitau *et al*, 2012). All Hsp90 proteins consist of an N-terminus ATP binding site, a charged linker region, a middle domain and a C-terminus dimerization domain. The predicted network of the malaria heat shock protein suggests that Hsp90 chaperones might be involved in chromatin remodelling, protein trafficking and cytoadherence, though it has not been experimentally proven (Shahinas and Pillai, 2014). In addition, there exists a mitochondrial-compartmentalized Hsp90-like chaperone, TRAP-1 (tumor necrosis factor receptor associated protein 1), and an endoplasmic reticulum Hsp90-like protein, Grp94/96 (glucose-regulated protein 94) (Altieri *et al*, 2012; Beibl and Buchner, 2019). Grp94 has a specialized role in the maturation process of particular secretory membrane-bound proteins such as integrins and Toll-like receptors (TLRs; Yang *et al*, 2007; Beibl and Buchner, 2019). Some of the functions of TRAP-1 include conferring antioxidant properties to the cell, regulate mitochondrial permeability as well as functioning as a metabolic switch that regulates the balance between oxidative phosphorylation and aerobic glycolysis (Yoshida *et al*, 2013; Beibl and Buchner, 2019).

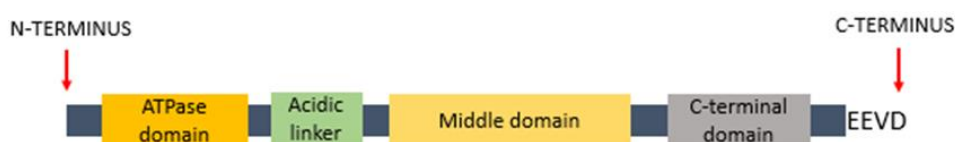


**Figure 1.4 Predicted structure of PfHsp90\_C with its functional domains.** PfHsp90 has an ATPase domain on the N-terminus, followed by an acid linker that connects to the middle and C-terminus domain. The C-terminus has a EEVD motif.

The common features found on the Hsp90 chaperones are the ATPase domain, middle domain and C-terminal domain (Figure 1.4). Hsp90 functions as a dimer and has a highly conserved N-terminal domain (NTD) that is responsible for ATP binding and hydrolysis (Prodromou *et al*, 1997; Liu and Houry, 2014).

### 1.6.3 Heat shock protein 70

Hsp70 is one of the major heat shock protein families, is present in virtually all organisms, and is the most highly conserved Hsp family (Shonhai, 2014). Hsp70 play well defined roles in folding newly synthesized polypeptides, protein translocation, signal transduction and protein degradation (Botha *et al*, 2010). Under normal and stressful conditions, both constitutive and inducible Hsp70s are vital in maintaining proteostasis. *P. falciparum* encodes six Hsp70s: PfHsp70-1 (PF3D7\_0818900), PfHsp70-2 (PF3D7\_0917900), PfHsp70-3 (PF3D7\_1134000), PfHsp70-x (PF3D7\_0831700), PfHsp70-y (PF3D7\_1344200) and PfHsp70-z (PF3D7\_0708800). Hsp70 chaperones typically have an ATPase domain, substrate binding domain (SBD) and a C-terminal lid subdomain (Figure 1.4; Shonhai *et al*, 2007). However, PfHsp70-y and PfHsp70-z have an ATPase domain that relatively conserved but display very low conservation in the substrate binding domains (Shonhai *et al*, 2007).

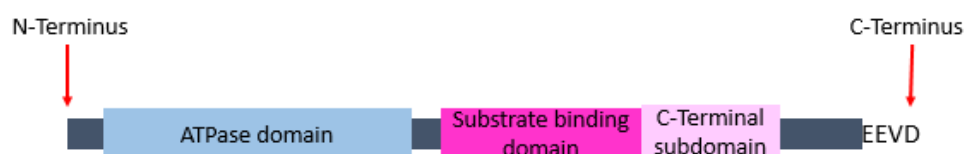


**Figure 1.5 Typical structure of PfHsp70.** PfHsp70 possesses an ATPase domain on the N-terminus and substrate binding domain towards the C-terminus. The two domains are connected by a linker region and the C-terminus has a EEVD motif.

PfHsp70-y (PfGRP170) and PfHsp70-2 (GRP78) are predicted to be localized in the ER. PfHsp70-2 is responsible for the translocation of proteins in the ER, directing proteins targeted for degradation (Przyborskei *et al*, 2015; Kudyba *et al*, 2019). PfHsp70-2 is proposed to be a signalling receptor in the plasma membrane and an ER chaperone in the intracellular compartment (Chen *et al*, 2018). PfHsp70-y is thought to act as a nucleotide exchange factor for PfHsp70-2 (Shonhai *et al.*, 2007; Shonhai,

2014; Przyborskei *et al*, 2015; Kudyba *et al*, 2019). PfHsp70-y is an ER resident protein essential for the growth of asexual forms of *P. falciparum* (Kudyba *et al*, 2019). PfHsp70-3 is predicted to be localized in the mitochondria where it is responsible for the translocation of proteins into the mitochondrion (Przyborskei *et al*, 2015; Nyakundi *et al*, 2016).

PfHsp70-x is exported into the erythrocyte cytosol and is also secreted into the PV. PfHsp70-x is not essential for survival but is implicated in host cell invasion and host immune evasion (Charnaud *et al*, 2017; Mabate *et al*, 2018). Analysis of the crystallized SBD of PfHsp70-x suggests that the protein takes on the architecture of a canonical Hsp70 chaperone SBD (Schmidt and Vakonakis, 2020).

PfHsp70-z is localized in the cytosol and is an essential protein that is involved in folding proteins that possess asparagine-rich repeats (Zininga *et al*, 2015). PfHsp70-z is an ATPase that is heat stable and interacts with PfHsp70-1 in a nucleotide-dependant manner (Zininga *et al*, 2015). PfHsp70-z interacts with the nucleotide binding domain of PfHsp70-1 and is likely to be the sole nucleotide exchange factor of PfHsp70-1 (Zininga *et al*, 2016).

PfHsp70-1 is known to play an important role in the development and survival of *P. falciparum* and has been implicated in antimalarial drug resistance (Lebepe *et al*, 2020). PfHsp70-1 (Figure 1.4) is the canonical Hsp70, and its C-terminal contains the EEVD motif and a set of Gly-Gly-Met-Pro (GGMP) repeats (Acharya *et al*, 2007). This repetitive GGMP motif is absent from other *P. falciparum* Hsp70 isoforms (Gong *et al*, 2018; Makumire *et al*, 2021).

### **1.6.3.1 Hsp70 interaction with co-chaperone (Hsp40)**

The canonical Hsp70 group to which PfHsp70-1 belongs interacts with Hsp40 (Section 1.6.4) in order to carry out its function (Botha *et al*, 2010). The Hsp40 co-chaperones present substrates to the Hsp70 chaperones and regulates ATP-dependent binding of substrates by Hsp70 (Neckers and Tatu, 2008; Shonhai, 2014).

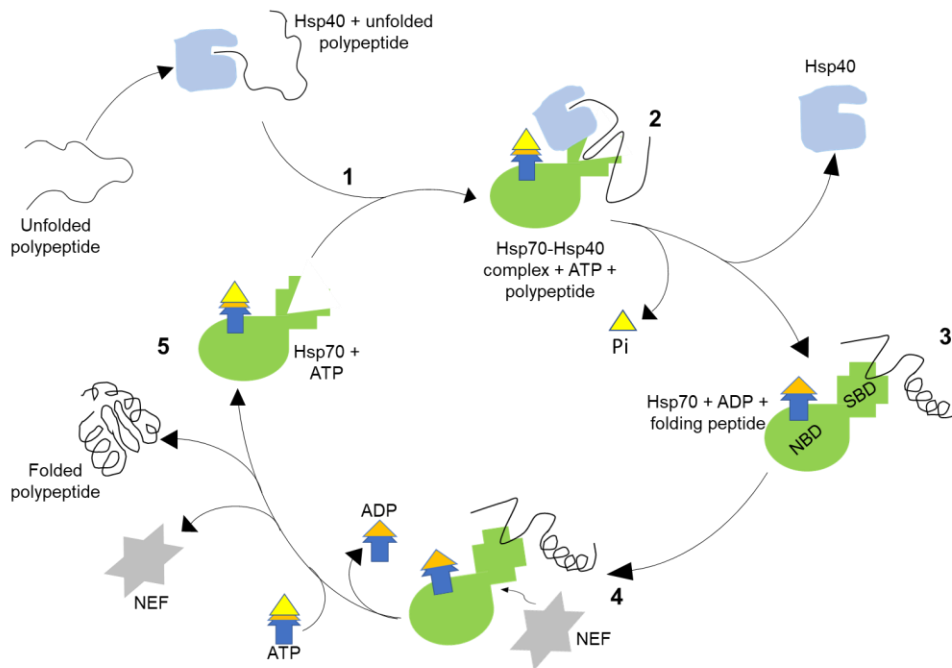


**Figure 1.6 Chaperone mediated folding by the Hsp70-Hsp40 chaperone complex.** The Hsp70-Hsp40 cycle shows how a substrate is presented to Hsp70 by Hsp40 and the downstream processes that lead to the substrate (unfolded polypeptide) being folded. 1, Hsp40 binds a unfolded polypeptide. 2, Hsp40 presents the unfolded polypeptide to the ATP bound Hsp70 and stimulates Hsp70s ATP hydrolysis activity. 3 and 4, Nucleotide exchange factor mediates the nucleotide exchange when binding to the Hsp70-substrate protein complex. 5, the replacement of ADP with ATP causes a conformational change that allows the release of a folded polypeptide or unfolded polypeptide that can re-enter the cycle until it reaches proper folded state (Kityk *et al*, 2012; Sousa, 2014).

Hsp70 switches between the ATP- and ADP- bound conformations. In the ATP-bound conformation of Hsp70, the chaperone displays fast on-and-off rates of peptide binding which results in a low affinity for substrate (Kityk *et al*, 2012; Edkins and Boshoff, 2014). The ADP-bound conformation of the chaperone in turn has a high affinity for substrate (Figure 1.5; Kityk *et al*, 2012). Firstly, Hsp40 delivers specific clients to Hsp70 and secondly, it stabilizes the Hsp70-polypeptide complexes by driving the conversion ATP-bound Hsp70 to the ADP-bound Hsp70 form (Fan *et al*, 2003). Nucleotide exchange factors (NEF) are involved in modulating Hsp70 peptide substrate binding and the subsequent release by interacting with the ATPase domain (Botha *et al*, 2010; Zininga *et al*, 2015). Selectively targeting a species-specific Hsp70-Hsp40 partnerships might be possible, due to the fact that the substrate binding domain of Hsp70 is highly divergent between species, and in addition, Hsp40 vary in scope and structure across species (Botha *et al*, 2007; Rug and Maier, 2011).

## 1.6.4 Heat shock protein 40

The *P. falciparum* genome encodes for more than 49 Hsp40 like proteins (Rug and Maier, 2011; Njunge *et al*, 2013). Hsp40s are molecular co-chaperones defined by the presence of a highly conserved J-domain of approximately 70 amino acids. *P. falciparum* Hsp40s are classified into four classes, Type I-IV (Figure 2.1; Botha *et al*, 2007; Rug and Maier, 2011). The Hsp40 proteins are classified according to their functional domains (Figure 1.6).

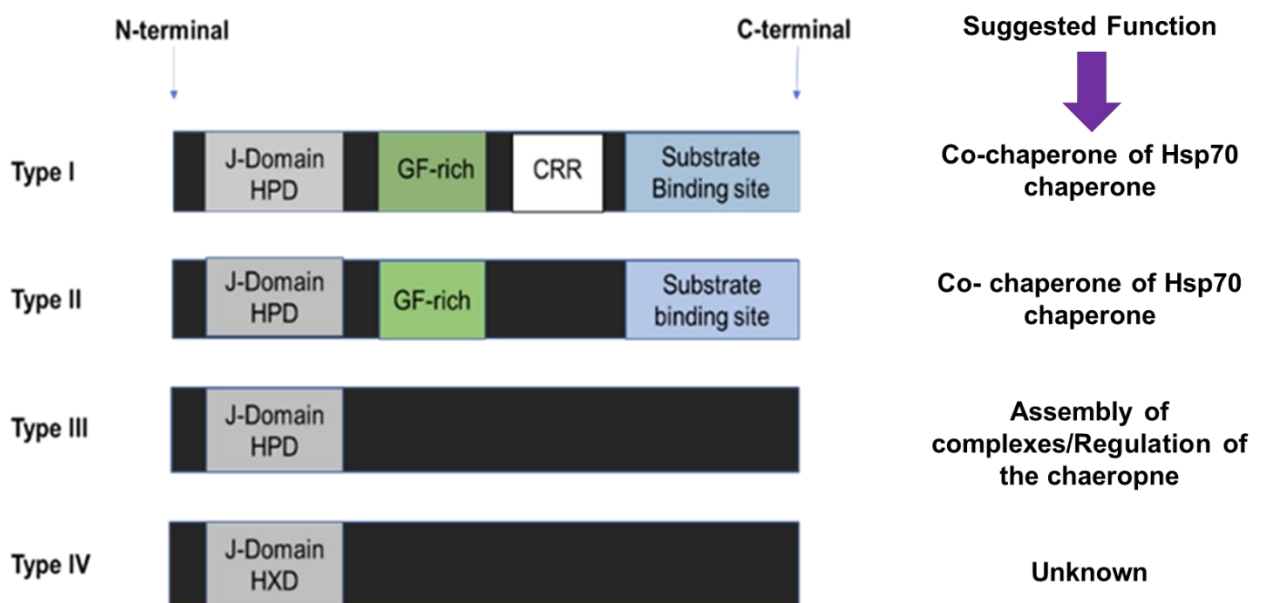


**Figure 1.7. Schematic representation of the four different types of Hsp40 proteins.** From the figure one can see where the proteins have similarities and where the proteins are different from each other. Represented are the functional domains for Hsp70 interaction and substrate binding: (Adapted from Rug and Maier, 2001).

### 1.6.4.1 Type I Hsp40

Type I Hsp40s are characterized by 4 regions: the J-domain, the glycine/phenylalanine rich region, a C-terminal region substrate binding site and the cysteine-repeat region (Rug and Maier, 2011). Only two type I Hsp40 proteins have been identified in *P. falciparum*, one of which is PF3D7\_1437900.1. This protein is thought to function in 'house-keeping' co-chaperone processes such as normal protein folding along with Hsp70 (Botha *et al*, 2007; Pesce *et al*, 2014). The other Type I Hsp40 is Pfj1 (PF3D7\_0409400.1) that is 672 amino acids-long with an extended C-terminus. The C-terminus of Pfj1 is lysine and proline residues rich. In thermo-sensitivity studies, Pfj1

has been found to slightly increase the capacity of PfHsp70-1 to reactivate heat denatured glucose-6-phosphate dehydrogenase and enhance its ATPase activity (Pesce *et al*, 2014). This suggests that Pfj1 plays a role in helping reactivate denatured proteins when the parasite encounters heat stress.

#### 1.6.4.2 Type II Hsp40

Type II Hsp40 proteins consist of 9 proteins that are similar to type I Hsp40 proteins but, lack the cysteine-rich domain (Rug and Maier, 2011; Njunge *et al*, 2013). Three of the type II Hsp40 proteins were predicted to be exported to the host erythrocyte (Botha *et al*, 2007; Rug and Maier, 2011). For example, the type II Hsp40, Pfj2 (PF3D7\_1108700.1) is a 540 amino acid-long protein that possess a putative PEXEL (*Plasmodium* export element) motif that falls within the J-domain of the protein. Furthermore, it has been found to be associated with the apicoplast genome and is predicted to have an apicoplast target sequence (Botha *et al*, 2011; Pesce *et al*, 2014). It also contains a thioredoxin domain, containing the cysteine-serine-histidine-cysteine (CSHC) active site, that potentially allows Pfj2 to function as a disulphide bond reductase (Pesce *et al*, 2014). Other type II Hsp40 proteins that have a PEXEL motif are PF3D7\_0113700.1 and PF3D7\_0201800.1 and they have been found to be localised in so-called J-dots which are cholesterol-containing, mobile vesicle-like structures located in the erythrocyte cytosol (Pesce *et al*, 2014).

#### 1.6.4.3 Type III Hsp40

The type III Hsp40 proteins are the most diverse and largest group of Hsp40 protein in *P. falciparum* with 26 proteins. These proteins are known to have more specialized functions in other species (Rug and Maier, 2011; Njunge *et al*, 2013). Two members of this group, the proteins PF3D7\_1318800.1 and PF3D7\_0823800.1 are non-PEXEL type III Hsp40 proteins that are localized in the endoplasmic reticulum (ER) and display similarities with ER resident proteins of other species (Sec63 (protein translocation protein in *Saccharomyces cerevisiae*) and ERdj5 (ER resident protein containing DnaJ). Sec63 plays a role in ER translocation while ERdj5 exhibits elevated mRNA levels upon heat shock (Rug and Maier, 2011). Similarities with proteins from other species could indicate function similarities too.

#### 1.6.4.4 Type IV Hsp40 proteins

Of the 13 type IV Hsp40 proteins, 11 are predicted to contain a PEXEL/host targeting (HT) signal sequence (Botha *et al*, 2007). For this reason, it is thought that these molecules might play important roles in the remodelling process that takes place after parasite invasion. The host cell remodelling process mediated by the trafficking of several hundred effector proteins to the erythrocyte compartment leads to cytoadherence (Rug *et al*, 2014). One of the most intensely studied type IV Hsp40 protein is the ring-infected erythrocyte surface antigen (RESA; PF3D7\_0102200.1). RESA reinforces the resistance of the parasite to heat stress by protecting spectrin (a cytoskeletal protein that lines the intracellular of the plasma membrane) against thermally induced stress (Rug and Maier, 2011). One other Hsp40 type IV that has been characterized is PF3D7\_1039100.1, which is important for knob formation (Watermeyer *et al*, 2013). Knobs are parasite-induced protuberances found on the surface of erythrocytes (Mbengue *et al*, 2012). *P. falciparum* seems to be the only *Plasmodium* species that has PEXEL/HT containing Hsp40 proteins. Thus, suggesting that there might be parasite-host interactions unique only to *P. falciparum* (Botha *et al*, 2007). PFF1010c (PF3D7\_0620700.1) is type IV Hsp40 that is only expressed in the early and late gametocyte stages (Mutavhatsindi, 2016). PFF1010c does not contain the PEXEL motif.

#### 1.7 Molecular chaperones as drug targets

Parasite chaperones have been studied and identified to be important in the growth, development and proliferation of parasites. The important role of chaperones in *P. falciparum* is to maintain the proteome as the parasite cycles between the poikilothermic mosquito vector and the homeothermic human host (Acharya *et al*, 2007). During its life cycle, *P. falciparum* experiences heat shock over 10°C while being transmitted from a mosquito to a human. Furthermore, during clinical malaria the parasite is repeatedly exposed to heat shock as a result of febrile episodes (Acharya *et al*, 2007). Aside from maintaining proteostasis during stressful conditions such as heat shock, chaperones play a major role in remodelling infected erythrocytes (Acharya *et al*, 2007; Hartl *et al*, 2011). Parasite proteins are exported to the

erythrocyte to alter the host cell structure and rigidity coupled with the formation of protrusions (knobs) (Day *et al*, 2019).

After the isolation of quinine in the 1820s, a number of other natural and synthetic compounds have been developed. As time passed, parasite strains began to develop resistance towards the developed drugs, rendering them less effective (Tse *et al*, 2019). This then drives a high unmet need for the development of new drugs with molecular chaperones as drug targets. The treatment should also have a low propensity for the development of resistance (Ashley and Phyto, 2018). PfHsp70-1 would make a good drug target as it is essential and shown to be expressed during all the life stages of the parasites including the sexual gametocyte stages (Acharya *et al*, 2007). PfHsp70-1 function can be inhibited by targeting the co-chaperones that increase its functional efficiency (Grover *et al*, 2014). It is plausible that PF1010c may play a significant role in Hsp70-1 functional cycle despite the HXD motif. It has been shown that PfHsp70-1 interaction with Hsp40 requires both the NBD and the SBD. It is tempting to speculate that the EEVD or the GGMP motifs of PfHsp70-1 may facilitate its interaction with the untypical type IV Hsp40s.

Synthetic pyrimidinones and naturally occurring ATP mimics are chemical scaffolds that have in the past been evaluated (Grover *et al*, 2014). In a study by Chiang *et al* (2009), it was observed that one of the designed pyrimidinone inhibitors affected the ATPase activity of PfHsp70-1 more significantly than its human homolog. Furthermore, in the same study, one of the pyrimidinone-based inhibitors of breast cancer cell proliferation compromised the ability of J-domain containing co-chaperones (Hsp40s) to enhance ATP hydrolysis (Chiang *et al*, 2009). In another study by Kang *et al* (2014), pyrimidine inhibitors were found to bind an active site of cysteine embedded within the allosteric pocket of a human Hsp70. Pyrimidinone-peptoid compounds have been found to possess potent effects on *P. falciparum* metabolism, with some potencies being similar to those of other antimalarial drugs that have been reported (Chiang *et al*, 2009). A study by Taldone *et al* (2014), sought to investigate the inhibition of Hsp70 with co-chaperones with several synthetic compounds including pyrimidine derived compounds. The study proposed the use of allosteric Hsp70 inhibitors towards development of novel targeted anticancer therapeutics (Taldone *et al*, 2014).



## 1.8 Pyrimidine-quinoline hybrids as antimalarials

A fast-emerging strategy in combating resistance to anti-malarial drugs is the synthesis of hybrid drugs where two distinct chemical pharmacophores are covalently linked. In a study by Pretorius *et al* (2013), a series of quinoline-pyrimidine hybrids whose *in vitro* anti-malarial activity and cytotoxicity were evaluated. Two of the hybrids were found to be more potent against *P. falciparum* than pyrimidine and quinoline on their own (Pretorius *et al*, 2013). A study by Singh *et al* (2012) also reported quinoline-pyrimidine hybrids with potent antimalarial activity.

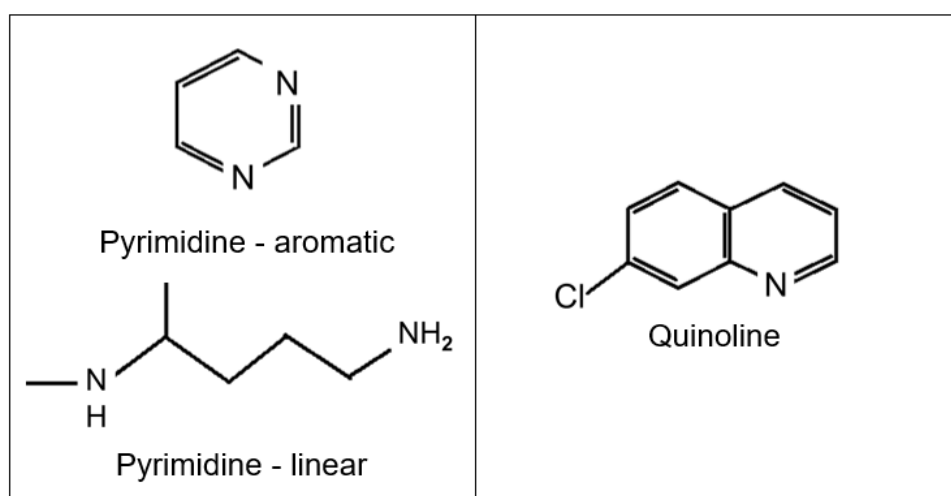


Figure 1.8. Basic chemical structure of pyrimidine and quinoline.

An advantage to this approach is the reduced risk of drug-drug interaction due to the hybrid drugs being distributed, metabolised and excreted at a single rate (Nqoro *et al*, 2017). The hybrids can be synthesized through three approaches: the pharmacophores can be conjugated by a distinct linker group, cleavage conjugates separated by metabolized linker or through a reduced linker that produces a fused hybrid (Muregi and Ishih, 2010). Another advantage is the cost effectiveness of this approach (Nqoro *et al*, 2017).

### 1.8.1 Role of heat shock proteins in drug resistance

Some well-established antimalarials have been observed to induce a stress response which leads to heat shock proteins helping the cells overcome the stressful conditions (Pesce *et al*, 2010). One such example is artemisinin and its derivatives that exert their antimalarial activity through the generation of carbon centered radicals. These carbon

centered radicals end up causing oxidative stress and the subsequent alkylation of proteins (Lu *et al*, 2020). PfHsp70-1 is one of the proteins whose upregulation protects the *P. falciparum* parasite partly from drug treatment (Daniyan *et al*, 2019). Thus, the dilemma becomes how to abrogate *P. falciparum* Hsp70 to allow the antimalarials to effectively kill the parasite? In a review by Daniyan *et al* (2019), the idea was put forth of possibly combining artemisinin treatment with a *P. falciparum* Hsp70 inhibitor. Quinoline-pyrimidine hybrids have the potential to be such inhibitors as needed to inhibit PfHsp70-1 activity. Pyrimidinones have been identified as Hsp70 inhibitors effective at killing the malarial parasite and being largely specific for the parasite Hsp70 (Chaing *et al*, 2009; Daniyan *et al*, 2019)

### 1.9 Study rationale and problem statement

Transmission of the *Plasmodium* parasite between the host and vector is accomplished by two specialized parasite cell types. These cell types are the gametocytes and the sporozoites (Alano, 2007). Initially, gametocytes are susceptible to schizonticidal antimalarials, but for the final part of their maturation process they become broadly insensitive to most antimalarial drugs, except for primaquine and methylene blue (Delves *et al*, 2013). Mature gametocytes have reduced targetable biology for drug discovery as they are minimally metabolically active, making them insensitive to most schizonticidal drugs (Delves *et al*, 2013). To overcome malarial resistance and transmission there is a high unmet demand for new treatment solutions. Malaria medication must evolve, as the parasite evolves to successfully combat the malaria epidemic.

Heat shock proteins have long been a focus as possible antimalarial drugs. The Hsp40 family presents substrates to the Hsp70 chaperones and regulate ATP-dependent binding of substrates by Hsp70 (Neckers and Tatu, 2008). Hsp70s are involved in protein folding (Neckers and Tatu, 2008). The mechanism of interaction (ATPase activity activation and substrate presentation) which Hsp40 Type I and II uses to interact with Hsp70 is fairly understood. This is also an interaction that is targeted in drug development as maintenance of parasite proteostasis is heavily dependent on Hsp70-Hsp40 cooperation (Botha *et al*, 2010). Pyrimidine inhibitors have been reported to compromise Hsp70-Hsp40 interaction (Chiang *et al*, 2009). However, the

role of type III and IV Hsp40 and their role in the pathogenesis of the parasite is not well understood. Type IV Hsp40 are the least studied. Type IV Hsp40s possess a modified J-domain that has corrupted HXD motif (Rug and Maier). PFF1010c is an uncharacterized type IV Hsp40 that has an SVN motif in place of the HPD motif. This SVN motif can also be seen in a few other *Apicomplexa* parasites (e.g. *Plasmodium knowlesi*). Investigating whether this protein (PFF1010c) with its SVN motif can interact with PfHsp70-1 would bring some understanding of the protein's function and maybe that of other type IV Hsp40s. Mutations in the HPD motif have been reported to block the ability of Hsp40s in regulating the ATPase activity of Hsp70, thus the speculation that type IV PfHsp40s may interact on a different site on PfHsp70-1 than where canonical PfHsp40s interact (Sojourner *et al*, 2018). PfHsp70-1 possesses a GGMP repeats motif whose yeast homologue has been implicated in being a secondary peptide binding site. In a study by Gong *et al* (2018), the yeast equivalent of PfHsp70-1 GGMP motif, Ssa1 GGAP motif, in combination with the EEVD motif, was found to exhibit increased interaction with Ydj1 (Hsp40) (Gong *et al*, 2018). Therefore, this suggested a secondary peptide binding site in PfHsp70-1 might not only require canonical Hsp40s as co-chaperones but, may also bind non-canonical Hsp40s such as the type IV PFF1010c.

According to Botha *et al* (2007), very few of the *P. falciparum* Hsp40 proteins have human homologs, and with PFF1010c being a type IV Hsp40, it most likely does not have a human homolog. This is further supported by the fact that humans only have three classes of Hsp40s, type I-III. Thus, PFF1010c would be important as a drug target to prevent transmission and PfHsp70-1 would be an important drug target to inhibit the proliferation of *P. falciparum* after the initial infection. Therefore, this study sought to characterize PFF1010c and screen for possible inhibitors of Hsp40 and Hsp70 interaction as a druggable complex.

### 1.10 Hypothesis

PFF1010c functions as a co-chaperone interacting with PfHsp70-1 which is a druggable complex and pyrimidine-quinoline hybrids can inhibit the chaperone function of PfHsp70-1 and PfHsp40.

## 1.11 Aim

To investigate the role of the SVN motif of PFF1010c in the protein interaction with PfHsp70-1 and to evaluate the anti-plasmodial activities of select pyrimidine-quinoline hybrids on the PfHsp70-1 Hsp40 chaperone function.

## 1.12 Objectives

1. Bioinformatic prediction of PFF1010c structure and generation of SVN mutant proteins of PfHsp40 and PFF1010c
2. Expression of recombinant PFF1010c and PfHsp40, their HPD/SVN motif switch mutants (PFF1010c-HPD; PfHsp40; PfHsp40-SVN) and PfHsp70-1 in *E. coli* followed by purification of proteins using nickel affinity chromatography
3. Biochemical analysis of the role of the SVN/HPD motif on PFF1010c and investigate the effect of Hsp40 HPD/SVN mutation on the interaction of PfHsp70-1 with PfHsp40
4. Biophysical analysis of the SVN motif on PFF1010c
5. Screen potential pyrimidine-quinoline hybrids against PfHsp70-1 and PfHsp40 interaction

## Chapter 2: Methodology

### Materials

All reagents used in this study are listed in Appendix A. The following antibodies were used: rabbit raised  $\alpha$ -PFF1010c antibody previously described (Mutavhatsindi, 2016), rabbit raised  $\alpha$ -PfHsp70-1 antibody previously described (Gitau *et al*, 2012), mouse raised  $\alpha$ -DnaK antibody, HRP conjugated  $\alpha$ -Histidine,  $\alpha$ -rabbit secondary (Thermo Scientific, USA) and  $\alpha$ -mouse secondary (ThermoFischer Scientific, USA) antibodies were used to validate the expression and purification of the recombinant proteins. The plasmids and strains of expression systems used for the production of the recombinant proteins are listed in Table 2.1.

**Table 2.1:** List of plasmid constructs and bacterial expression strains used

Plasmids	Description	Supplier
pQE30/ <i>PFF1010c</i>	pQE30 expression vector encoding <i>PFF1010c</i> , Amp <sup>R</sup>	Mutavhatsindi, 2016
pQE30/ <i>PFF1010c-HPD</i>	pQE30 expression vector encoding <i>PFF1010c-HPD</i> , Amp <sup>R</sup>	GenScript (USA)
pQE30/ <i>PfHsp40</i>	pQE30 expression vector encoding <i>PfHsp40</i> , Amp <sup>R</sup>	Lebepe, 2018
pQE30/ <i>PfHsp40-SVN</i>	pQE30 expression vector encoding <i>PfHsp40-SVN</i> , Amp <sup>R</sup>	GenScript (USA)
pQE30/ <i>PfHsp70-1</i>	pQE30 expression vector encoding <i>PfHsp70-1</i> , Amp <sup>R</sup>	Chakafana <i>et al</i> , 2021
<b>Bacteria strains for expression</b>		
<i>E. coli</i> JM109	e14 <sup>-</sup> (McrA <sup>-</sup> ) <i>recA1 endA1 gyrA96 thi-1 hsdR17 (r<sub>k</sub>-m<sub>k</sub><sup>+</sup>) supE44 relA1 <math>\Delta</math>(lac-proAB) (F'<i>ntraD36nproAB</i> <i>lacI<sup>q</sup></i> <math>\Delta</math>ZAM15)</i>	Thermofischer scientific (USA)
<i>E. coli</i> XL1 Blue	<i>recA1 endA1 gyrA96 thi1 hsdR17 supE44 relA1 lac</i> (F' <i>proAB lacI<sup>q</sup></i> $\Delta$ ZAM15 Tn10 (Tetr)	Thermofischer scientific (USA)

## 2.1 Bioinformatics

### 2.1.1 Multiple sequence alignments

Bioinformatics studies were conducted to predict the structure and functions of PFF1010c. The protein sequences for the *Plasmodium* proteins were obtained on Plasmodb (<https://www.plasmodb.org>) while other protein sequences used were obtained on the NCBI (<https://www.ncbi.nlm.nih.gov>) website. Multiple sequence alignments to assess conservational and functional feature were performed. To assess if PFF1010c (PF3D7\_0620700) has any conserved domains, PFF1010c was aligned with other Hsp40 proteins within the *Apicomplexa* phylum; *P. ovale* (SCP05061.1), *P. malariae* (SBT79714.1), *Toxoplasma gondii* (KFG34430.1) and *Babesia bovis* (BAN65055.1). And PFF1010c was aligned with other *P. falciparum* type IV Hsp40s (PF10\_0381, PF11\_0034, PFB0925w, PFB0085c and PFA110w). To assess if PFF1010c had any known functional domain, PFF1010c was aligned with Hsp40 proteins that are better understood from other species: *Escherichia coli* (DnaJ), *Saccharomyces cerevisiae* (Ydj1), *Homo sapiens* (DNJB1) and *P. falciparum* (PfHsp40/PF3D7\_1437900.1). The alignments were generated on Clustal omega (<https://www.ebi.ac.uk/Tools/msa/clustalo/>) and viewed using Boxshade ([https://embnet.vital-it.ch/cgi-bin/BOX\\_form.html](https://embnet.vital-it.ch/cgi-bin/BOX_form.html)). The sequence for PFF1010c and PfHsp40 (PF3D7\_1437900.1) were obtained from Plasmodb ([www.plasmodb.org](http://www.plasmodb.org)). Having aligned the protein sequences of the canonical Hsp40s with the type IV Hsp40, PFF1010c, the HPD motif of the Hsp40s responsible for activating the ATPase activity of PfHsp70-1 was found to be an SVN motif in PFF1010c (Figure 2.1). To investigate the functional significance of the SVN motif, the HPD amino acid residues of PfHsp40 (residues 55 – 57) were substituted into PFF1010c (residues 96 - 98) and the SVN amino acid residues of PFF1010c (residues 96 – 98) were substituted into PfHsp40 (residues 55 – 57). Thus, resulting in a motif switch that gives rise to PfHsp40-SVN mutant and PFF1010c-HPD mutant.

PFF1010c	56	KIKYMRSSYSKFKYYEILNVNVKSDAKTIRKSYLALSKEI	SVN	KKLSREYEECYYLIOKS
PFF1010c-HPD	56	KIKYMRSSYSKFKYYEILNVNVKSDAKTIRKSYLALSKEI	HPD	KKLSREYEECYYLIOKS
PfHsp40	15	QQARRKREVNNNKFFYEVLNLIKKNCTTDEVKKAYRKLAI	HPDKG	---GDPEKFKETISRA
PfHsp40-SVN	15	QQARRKREVNNNKFFYEVLNLIKKNCTTDEVKKAYRKLAI	SVNKG	---GDPEKFKETISRA

PFF1010c	116	YKILLNKFEKFFYYDVLNINNYIDENTI-----EQRYMLEKEADIIYANKIEELKDIYEIK
PFF1010c-HPD	116	YKILLNKFEKFFYYDVLNINNYIDENTI-----EQRYMLEKEADIIYANKIEELKDIYEIK
PfHsp40	72	YEVLSDEEKRKLYDEYGEENLENGEQPADATLDFDFILNAGKG----KKKRGEDIVSEVK
PfHsp40-SVN	72	YEVLSDEEKRKLYDEYGEENLENGEQPADATLDFDFILNAGKG----KKKRGEDIVSEVK

**Figure 2.1 Alignment of PfHsp40 J-domain with PFF1010c J-domain and their mutants.** J-domain alignment that shows the amino acids on PFF1010c that corresponds to the HPD motif PfHsp40. The alignment shows that the specific motif in PFF1010c has the SVN amino acid. The wildtype SVN/HPD motifs are highlighted in red and the mutant SVN/HPD motifs are highlighted in green.

### 2.1.2 Prediction of the PFF1010c interactome

String ([www.string-db.org](http://www.string-db.org)) was used to extract predicted PFF1010c interactors. The string database aims to provide a critical assessment and integration of protein-protein interactions which include direct as well as indirect associations (Szklarczyk *et al*, 2014). In string, function association is the basic interaction unit, where proteins need not interact physically but have some part of their functional roles within the cell overlap (Szklarczyk *et al*, 2019)

### 2.1.3 3D model generation

Furthermore, Phyre2 ([www.sbg.bio.ic.ac.uk/phyre2](http://www.sbg.bio.ic.ac.uk/phyre2)) was used to develop 3D models of PFF1010c, PfHsp40, PFF1010c-HPD and PfHsp40-SVN. Phyre2 generates a 3D model through 4 underlying technical stages: gathering homologous sequences; fold library scanning; loop modelling; and multiple template modelling with Poing (Kelley *et al*, 2015). The 3D structures obtained were superimposed using SuperPose (<http://superpose.wishartlab.com>) to reveal any structural differences that may have arisen as a result of the motif switch.

### 2.1.4 Hydropathy profile of Hsp40s

The protein structure and fold are governed by the hydrophilic and hydrophobic properties of the amino acids in the protein sequence (Damodharan and Pattabhi, 2004). The Kyte and Doolittle programme (<https://wed.expasy.org/protscale/>) systematically evaluates the hydrophilic and hydrophobic tendencies of a polypeptide chain where each amino acid is assigned a value that reflects its relative hydrophilicity

and hydrophobicity (Kyte and Doolittle, 1982). The hydropathy profile was employed to investigate variations in the hydrophobicity and hydrophilicity of the mutant proteins PFF1010c-HPD and PfHsp40-SVN from PFF1010c and PfHsp40, respectively.

## 2.2 Expression of recombinant protein in *E. coli* XL1 Blue and *E. coli* JM109 cells

After having confirmed the plasmid DNA constructs (Appendix A3 and A4), recombinant proteins were produced. The recombinant proteins were heterologously expressed in *E. coli* following a previously described protocol (Zininga et al, 2015). *E. coli* XL1 Blue competent cells that were transformed with pQE30 plasmid containing the gene of interest (*PfHsp70-1*, *PFF1010c* or *PFF1010c-HPD*) and *E. coli* JM109 competent cells transformed with pQE30/PfHsp40 or pQE30/PfHsp40\_SVN (Table 2.1, Appendix A2). The transformed cells were then inoculated in 50 ml 2x YT broth (1.6 g tryptone, 1.0 g yeast, 1.5 g agar, 0.5 g NaCl per 100 ml preparation in distilled water with 100 µg/ml ampicillin) and incubated overnight at 37°C in a shaker incubator. The overnight cultures were diluted into fresh 2x YT broth (450 ml containing 100 µg/ml ampicillin) and grown to an optical density of OD<sub>600</sub> between 0.5 – 0.6. A concentration of 1 mM Isopropyl-1-thio-β-D-galactopyranoside (IPTG) was used to induce protein expression. An aliquot was taken before induction and every hour for six hours after induction. Each aliquot was centrifuged for 5 minutes at 1500 g and the supernatant was discarded. The pellet was resuspended in phosphate buffered saline (PBS) (137 mM NaCl, 2.7 mM KCl, 10 mM Na<sub>2</sub>HPO<sub>4</sub>, 2 mM KH<sub>2</sub>PO<sub>4</sub>, pH 7.5), in a volume equivalent to OD<sub>600</sub>/0.5\*150 µl and was treated with SDS-PAGE loading buffer (0.25 % Coomassie Brilliant blue [R250], 2 % SDS, 10 % glycerol [v/v], 100 mM Tris, 1 % β-mercaptoethanol). The samples were boiled for 10 minutes and analyzed by 12 % SDS-PAGE (Appendix A7) and Western blot analyses (Appendix A8). The protein sizes were obtained from ExPASy (<https://web.expasy.org>) which computes the theoretical molecular weight of protein sequences.

## 2.3 Purification of the recombinant protein

To purify the recombinant protein, cells are harvested and sonicated to facilitate cell lysis (Zininga et al, 2015). Lysis buffer was used to resuspend the harvested cell



cultures which contained 10 mM Tris, 300 mM NaCl, 10 mM Imidazole, 8 M urea, pH 8.0, 1 mM PMSF (phenylmethylsulfonyl fluoride and 1mg/ml lysozyme). The cells were stored at -80 °C overnight and thawed the following morning followed by mild sonication at amplitude setting of 30 for 7 cycles with 15 seconds pulse and 30 seconds pause after each cycle and centrifuged at 5000 xg for 20 minutes at 4 °C. The supernatant containing the recombinant protein was suspended in nickel-chelating sepharose beads and incubated for 1 hour on ice. Purifying the protein immobilized on the nickel-chelating sepharose beads, involves washing off unbound and contaminating proteins with wash and elution buffers with varying concentrations of imidazole. Unbound protein was removed by washing the beads twice in denaturing buffer (300 mM NaCl, 25 mM imidazole [wash I], and 100 mM Tris, pH 8.0 and also 80 mM Imidazole [wash II]). The bound protein was eluted using Elution buffer (300 mM NaCl, 250 mM Imidazole [elution I], 350 mM Imidazole [elution II, 500 mM Imidazole [elution III] and 100 mM Tris, pH 8.0). The proteins are then resolved using SDS-PAGE and analysis to confirm the presence of the recombinant PFF1010c protein is done using Western blot. With BSA as the standard, protein yield was estimated using the Bradford assay (Appendix A9; Zininga et al, 2015).

## **2.4 Investigation of the tertiary structure of the recombinant protein**

Furthermore, fluorescence spectrometry was also conducted to investigate the tertiary structure of the proteins. Fluorescence occurs when a molecule or an atom absorbs light and goes into the excited stage and thereafter re-emits the absorbed light and returns to its ground state (Neha and Priyanka, 2017). First, extrinsic ANS fluorescence was used to determine the level hydrophobicity in the proteins (Achilonu *et al*, 2014). ANS (100 mM) was briefly mixed with 2 µM of the recombinant proteins (PfHsp40, PfHsp40-SVN, PFF1010c, PFF1010c-HPD). Following excitement at 390nm resultant emission spectrum was recorded between 400 and 600 nm using the JASCO FP-6300 spectrofluorometer (JASCO, Tokyo, Spain). The data was analysed by subtracting the emission spectrum of free ANS from the ANS: protein spectra. Secondly, intrinsic fluorescence was used to investigate tertiary structure stability of the proteins when exposed to denaturants and thermal stress. Tryptophan and tyrosine constitute naturally occurring fluorophores in protein. Tryptophan has the

highest quantum yield and its emission maximum is sensitive to the polarity of its environment hence it is the most commonly used intrinsic fluorescent probe when studying protein folding and dynamics (Munishkina and Fink, 2007). The recombinant proteins (PfHsp40, PfHsp40-SVN, PFF1010c, PFF1010c-HPD) were incubated in assay buffer (10 mM Phosphate, 137 mM NaCl, 3 mM KCl; pH 7.5) at varying concentrations of urea (1 M – 8 M) and guanidine hydrochloride (1 M – 6 M) for 20 - 30 minutes at 20°C. The tertiary structure stability of the recombinant proteins was also monitored at increasing temperatures (25°C - 100°C) to observe any structural changes.

## **2.5 Surface plasmon resonance (SPR) analyses**

### **2.5.1 Investigating protein-protein interactions**

SPR can be used to validate protein-protein interactions. SPR can also be used to study the capability of the protein to self-associate (Zininga *et al*, 2015). SPR spectroscopy enables measurement of real-time quantification of ligand-binding affinities and kinetics using relatively small amounts of protein. The receptor molecule/protein is immobilised on a metal surface, and binding of the analyte is monitored using an optical method that measures the change in the refractive index of the medium in close vicinity of the metal surface (Patching, 2013). PfHsp70-1 was immobilized as a ligand on a GLC sensor chip (Appendix A10, Zininga *et al*, 2017). To investigate the chaperone co-chaperone interaction between PfHsp40s (PfHsp40, PfHsp40-SVN, PFF1010c, PFF1010c-HPD) with PfHsp70-1, a previously described protocol was followed (Zininga *et al*, 2016).

### **2.5.2 Investigating drug-protein interactions**

Amidst the emergence of resistance towards antimalarials and especially artemisinins in *Plasmodium falciparum*, the discovery of new antimalarial drugs is needed to treat infection and eliminate transmission of malaria (Ashley *et al*, 2014). Besides bioprospecting for antimalarial compounds of natural origin, synthesis of novel compound inhibitors is a key alternative. The combination of small synthetic molecule inhibitors (hybrids) is a viable option to combat resistance to antimalarials. In the current study, quinoline-pyrimidine hybrids obtained from Kayamba *et al* (2021), were

screened for PfHsp70-1 interaction using SPR. Pyrimidine-quinoline was used for PfHsp70-1 antimalarial screening

**Table 2.2** Formulas of the pyrimidine-quinoline hybrids

Pyrimidine-quinoline hybrid formula	Hybrid annotation
C <sub>31</sub> H <sub>28</sub> N <sub>5</sub> O <sub>2</sub>	PQH1
C <sub>29</sub> H <sub>26</sub> N <sub>5</sub> O <sub>3</sub>	PQH2
C <sub>33</sub> H <sub>32</sub> N <sub>5</sub> O <sub>4</sub>	PQH3
C <sub>29</sub> H <sub>26</sub> N <sub>5</sub> O <sub>2</sub>	PQH4

The effect of the proposed antimalarials on Hsp70-Hsp40 interaction was investigated following a protocol previously described in Zininga *et al* (2017).

## 2.6 ATPase assay

As an ATPase, PfHsp70-1 uses the energy from ATP hydrolysis to power and carry out its functions such as protein folding and trafficking (Rule *et al*, 2016). ATPases hydrolyze ATP into inorganic phosphate producing reaction and therefore, ATPase activity is determined by quantifying the amount of inorganic phosphate released *in vitro* (Rule *et al*, 2016; Mabate *et al*, 2018). In this experiment, the ATPase activity assay was being used to investigate the functional capability of PFF1010c and mutants to stimulate the ATPase activity of PfHsp70-1. For 5 minutes, 0.4 μM PfHsp70-1 was incubated in buffer HKMD (10 mM HEPES-KOH pH 7.5, 100 mM KCl, 2 mM MgCl<sub>2</sub>, 0.5 mM DTT). Thereafter, 0.4 μM the co-chaperones (PfHsp40, PfHsp40-SVN, PFF1010c, PFF1010c-HPD) were added to the mixture. The reaction was started by adding increasing concentrations (0 - 5 mM) of ATP and the reaction was incubated at 37°C for 4-6 hours.

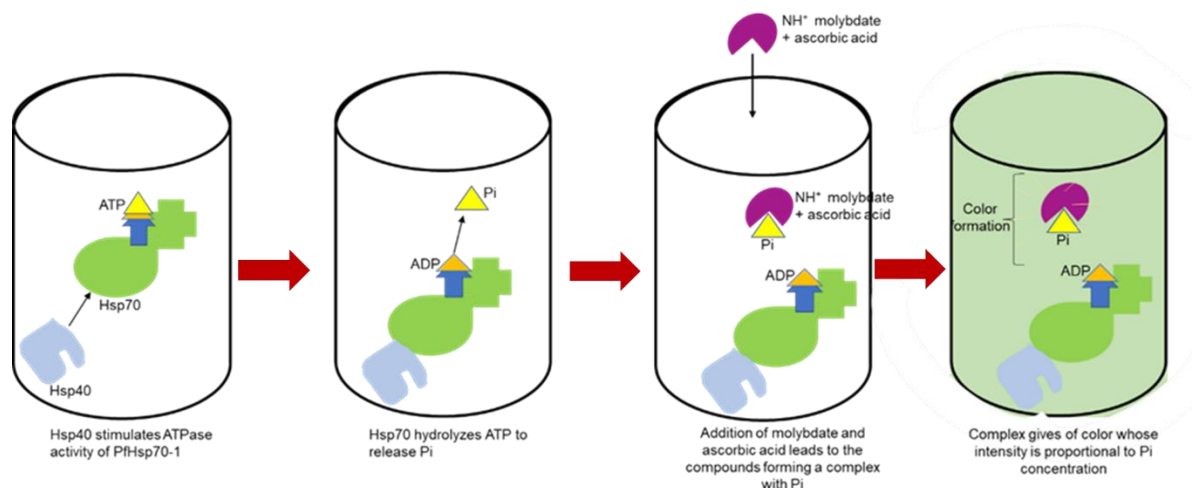


**Figure 2.2 Step by step process of ATPase assay.** Hsp40 stimulates Hsp70 to hydrolyze ATP. The Hydrolysis reaction results in ADP and inorganic phosphate (Pi). The formation of Pi is measured through the addition of  $\text{NH}_4^+$  molybdate and ascorbic acid, where the complex that forms can be measured at 660 nm.

To stop the reaction, 10% SDS was used and 1.25%  $\text{NH}_4^+$  molybdate and 9% ascorbic acid, incubated for 30 minutes to quantitate the released phosphate. Molybdate forms a complex with inorganic phosphate, a complex whose level of formation can be measured at 660 nm (Rule et al, 2016). Kinetics plots for the ATPase activity of PfHsp70-1 in the presence of the co-chaperones was determined by generating Michaelis-Menten plots using GraphPad prism 9 (Mabate *et al*, 2018). At least three independent ATPase activity assays were conducted.

## Chapter 3: Results

### 3.1 *In silico studies*

Bioinformatics provides opportunities to explore structure-function features of proteins prior to conducting wet lab assays. PFF1010c was aligned with canonical Hsp40s (Figure 3.1.A and Appendix B1). The data show that PFF1010c does not possess any of the functional/characteristic domains contained in other species except for its possession of a corrupted J-domain (Figure 3.1.A). Within the J-domain, PFF1010c does not contain the highly conserved HPD motif highlighted in green but rather has a SVN motif in its place. A conservational alignment of some type IV Hsp40s from *P. falciparum* (Figure 3.1.B and Appendix B2) shows that these proteins J-domain does not possess the HPD motif and rather has variable amino acid residues. The conservational alignment in Figure 3.1.C (Appendix B3) revealed that the Apicomplexa *Babesia bovis* had a conserved HPD motif while *Taxoplasma gondii* appears to be void of a J-domain. The *Plasmodium* species, *P. falciparum* (PFF1010c), *P. ovale* (SCP05061.1) and *P. malariae* (SBT 79714.1) have a highly conserved J-domain with a variable SVN/TVN motif in place of the canonical HPD motif.

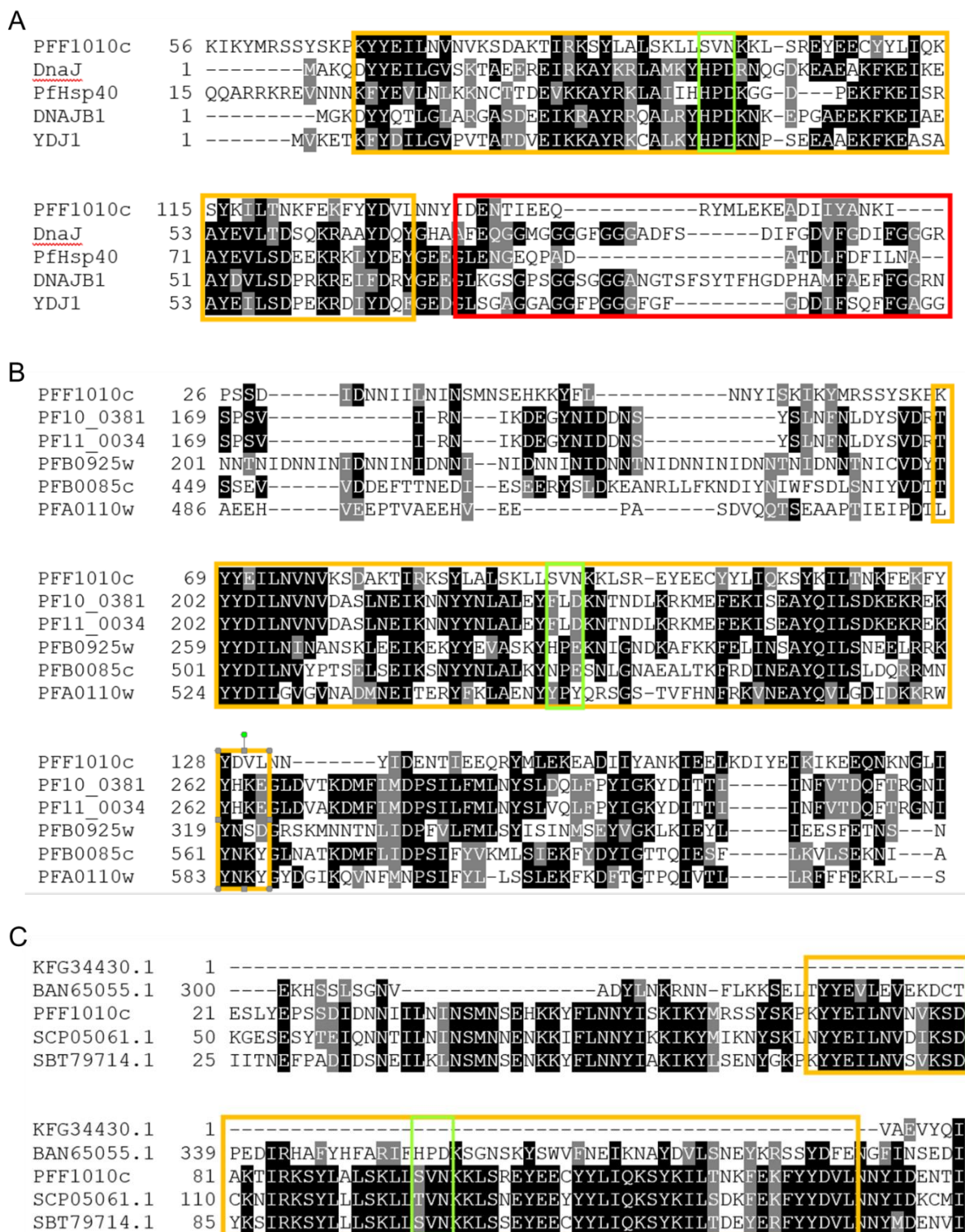


**Figure 3.1.1 Protein sequence alignments of J domain of Hsp40s.** (A) Alignment of PFF1010c with canonical Hsp40s from *E. coli*, *P. falciparum*, *H. sapiens* and *S. cerevisiae* showing the conservation of the J-domain and HPD motif across canonical Hsp40s in different species and deviation of PFF1010c, type IV *P. falciparum* Hsp40, from these Hsp40s. (B) Alignment of PFF1010c with other *P. falciparum* type IV Hsp40s. (C) Alignment of PFF1010c with other Apicomplexa Hsp40s.

Protein-protein interactions can be determined experimentally or predicted by text-mining, co-expression patterns, protein homology to name a few. Most of the predicted interactors are putative uncharacterized proteins with proposed/predicted functions. Eukaryotic actin-like proteins (PFE1105c) function in coordinating cell division machinery, aligning organelles and segregating DNA (Dhara and Sinai, 2016). Phosphoenolpyruvate carboxylase (PF14\_0246) is an enzyme that catalyzes the fixation of carbon dioxide with phosphoenolpyruvate to produce oxaloacetate and inorganic phosphate (Izui *et al*, 2003). SET domain containing proteins (PFD0190w) have been shown to methylate lysine residues in histones and other proteins (Yeates, 2002). Transport proteins (PFB0435C) transport substances across biological membranes occur within the membrane itself (Saier, 2003).

**Table 3.1: Proteins predicted to be co-express and to interact with PFF1010c**

Predicted functional partners	Gene ID	Size (aa)	Score
PFE1105c (putative uncharacterized protein)	PF3D7_0522100	763	0.741
PFD0487c (actin-like protein, putative)	PF3D7_0409900	416	0.683
PF11_0243 (leucine rich repeat protein)	PF3D7_1123200	814	0.674
PF14_0246 (phosphoenolpyruvate carboxylase, putative)	PF3D7_1426700	1148	0.673
PFD0190w (SET domain protein, putative)	PF3D7_0403900	1186	0.654
MAL13P1.228 (putative uncharacterized protein)	PF3D7_1345600	370	0.648
PFB0435C (Transporter, putative)	PF3D7_0209600	1132	0.638
PF10_0308 (OTU-like cysteine protease, putative)	PF3D7_1031400	938	0.638
PFD0530c (Ribosome biogenesis GTPase A, putative)	PF3D7_0410700	904	0.632

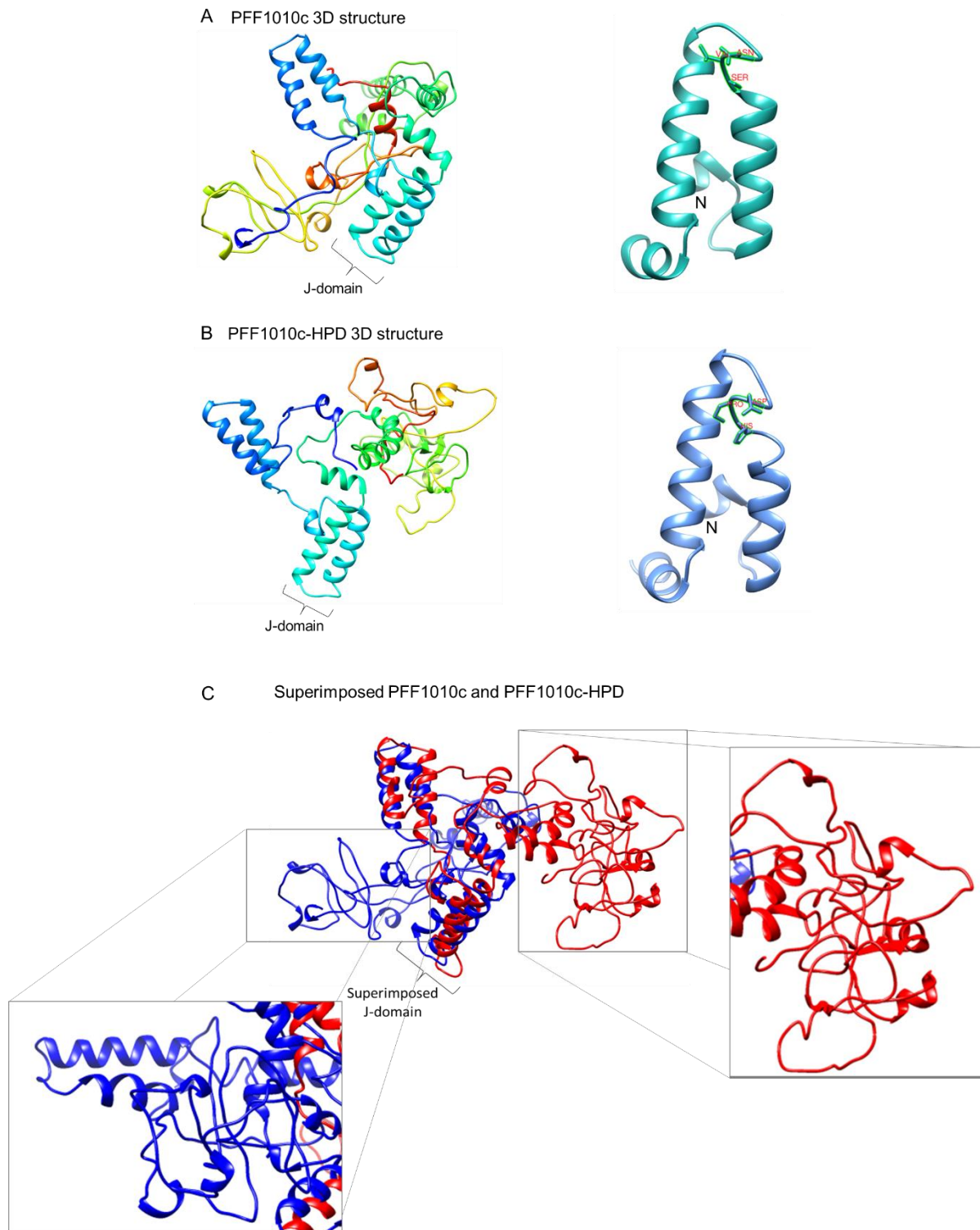


**Figure 3.2 Predicted tertiary structures of PFF1010c and its mutant PFF1010c-HPD.** (A) Predicted 3D model of PFF1010c appearing as a rainbow ribbon structure coloured with the N-terminus appearing in blue and the C-terminus in red, and alongside it is the enlarged structure of the J-domain with the SVN motif (B) The predicted 3D model of the mutant PFF1010c-HPD and its enlarged J-domain structure with the HPD motif. (C) PFF1010c-HPD was superposed onto PFF1010c with zoom-in regions that depict structural variations. The models were generated by Phyre2 ([www.sbg.bio.ic.ac.uk/phyre2](http://www.sbg.bio.ic.ac.uk/phyre2)) and visualized using Chimera ([www.cgl.ucsf.edu/chimera](http://www.cgl.ucsf.edu/chimera)).



The 3D model obtained from Phyre2 is generated from homologs whose structure has been elucidated either by x-ray diffraction or nuclear magnetic resonance spectroscopy and also by predicting the behaviour of the amino acid residues. The PFF1010c model (Figure 3.2A) was generated using the *Thermus thermophilus* DnaJ as a template. Generally, 23% of the protein was modelled with 99.9% confidence. Overall, 41% of the final model of PFF1010c was modelled at about 90% confidence. The structure of PFF1010c is predicted to be composed of 44% alpha helices, 31% disordered regions and 15% beta strands. Introducing the mutation on the SVN motif of PFF1010c results in a mutant, PFF1010c-HPD (Figure 3.2B), that is predicted to be composed of 43% alpha helices, 38% disordered region and 10% beta strands. The mutant protein significantly has more disordered regions and less beta strands and alpha helices. The J-domains of PFF1010c (Figure 3.2.A) and PFF1010c-HPD (Figure 3.2.B), respectively, do not appear to have any structural differences despite the HPD/SVN motif switch. However, superposition of PFF1010c-HPD (red) onto PFF1010c (blue) reveals major structural differences caused by the HPD/SVN motif switch in other regions of the proteins (Figure 3.2C). These differences can be seen in the N-terminus of the protein and well beyond the N-terminal helices which appear to be the only stretch of amino acids that remained unaltered after the motif switch in PFF1010c-HPD. The zoomed area (Figure 3.2.C) of PFF1010c and PFF1010c-HPD show how the proteins are structurally distinct.

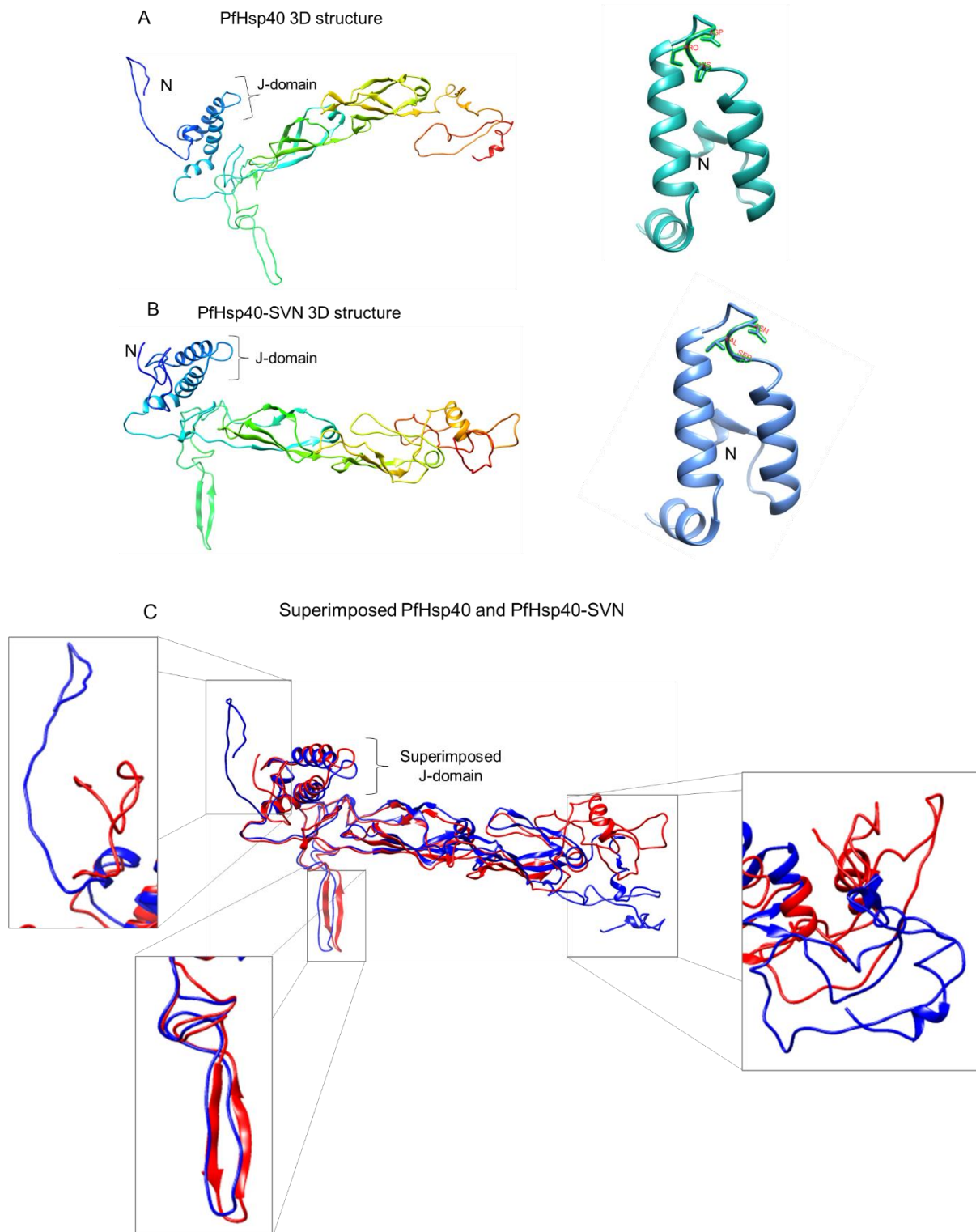


**Figure 3.3 Predicted tertiary structure of PfHsp40 and PfHsp40-SVN.** (A) Predicted 3D model of Hsp40 appearing as a rainbow ribbon structure with the N-terminus appearing in blue and the C-terminus in red, and alongside it is the enlarged structure of the J-domain with the HPD motif. (B) The predicted 3D model of PfHsp40-SVN and its enlarged J-domain structure with the SVN motif. (C) PfHsp40-SVN was superposed onto PfHsp40 with zoom-in regions that also depict structural variations. The models were generated by Phyre2 ([www.sbg.bio.ic.ac.uk/phyre2](http://www.sbg.bio.ic.ac.uk/phyre2)) and visualized using Chimera ([www.cgl.ucsf.edu/chimera](http://www.cgl.ucsf.edu/chimera)).

The predicted structure of PfHsp40 was modelled from the crystal structure of Hsp40 ydj1 where 36% of the protein was modelled with 100% confidence. Also, 44% of the protein was modelled from *Thermus thermophilus* DnaJ with 100% confidence. The J- and G/F domains were modelled with 99.9% confidence. PfHsp40 is predicted to possess 48% disordered regions and 16% alpha helices and 25% beta strands (Figure 3.3A). The mutant, PfHsp40-SVN, is predicted to have 47% disordered regions and 16% alpha helices and 25% beta strands (Figure 3.3B). On the other hand, PfHsp40-SVN was superimposed onto the wildtype PfHsp40 to discern structural differences that may be brought on by the HPD/SVN motif switch (Figure 3.3C). Major structural changes can be seen on both the N-terminal and C-terminal of PfHsp40-SVN. The N-terminals and C-terminals of these proteins consists mainly of disordered regions that appear to fold differently from each other (Figure 3.3C).

### 3.1.2 Hydropathy profiles of PFF1010c, PfHsp40 and mutants

Hydropathy profile analysis was used to investigate whether the HPD/SVN motif switch increased or decreased the hydrophobicity of the mutant proteins. Hydrophobicity and hydrophilicity are properties that affect protein structure and fold (Damodharan and Pattabhi, 2004). The hydropathy profile of PFF1010c and its mutant (PFF1010c-HPD) shows very little variation between the proteins and the region that brings on this slight variation is the HPD/SVN motif (Figure 3.1.4a and a1; red circles). The HPD motif of PFF1010c-HPD exhibits less hydrophobicity as compared to the SVN motif of PFF1010c. The hydropathy profile of PfHsp40 and its mutant, PfHsp40-SVN, shows there is very little variation—between the proteins and the region responsible for this variation is largely the HPD/SVN motif (Figure 3.1.4b and b1; red circles). The SVN appears to have slightly increased the hydrophobicity of PfHsp40. This can also be observed in the predicted properties of proteins (Appendix table B2) that shows PfHsp40-SVN exhibits slightly increase in hydrophobicity. The decreased hydrophobicity of PFF1010c-HPD and the increased hydrophobicity of PfHsp40-SVN may account for the structural differences observed in the 3D modelling (Figure 3.2.C and Figure 3.3.C)

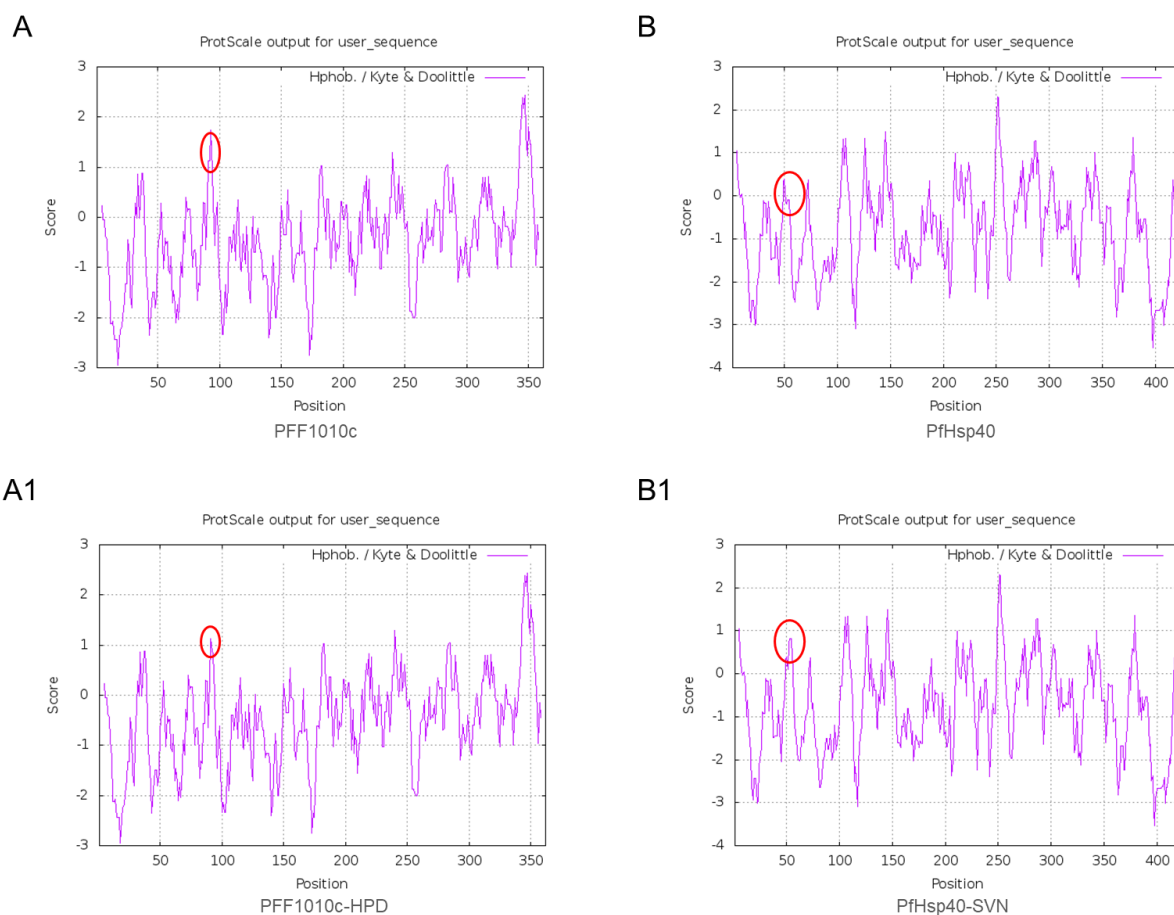


**Figure 3.4 Prediction of hydrophobicity in PFF1010c and Hsp40 versus their mutants.** The Kyte and Doolittle hydrophobic profile analysis for PFF1010c and PFF1010c-HPD reveals that the HPD amino acid residues decreased the hydrophobicity of PFF1010c (A and A1). The SVN motif substitution into PffHsp40 increased the proteins hydrophobicity (B and B1).

### 3.2 Confirmation of plasmid constructs used in this study

To verify the integrity of the plasmid constructs (pQE30/*PFF1010c*; pQE30/*PFF1010c-HPD*, pQE30/*PffHsp40*; pQE30/*PffHsp40-SVN* and pQE30/*PffHsp70-1*), restriction digests were carried out and the resulting DNA fragments were resolved using agarose gel electrophoresis. Double digest would result in the appearance of two linear DNA bands, a large band (in base pairs) is representative of the plasmid and a smaller band (in base pairs) is representative of the insert DNA. The restriction sites and thus the restriction of enzymes selected are those that flank the insert DNA from both ends (the 5' and 3' ends). The *Bam*HI and *Hind*III restriction sites of pQE30/*PFF1010c* plasmid were selected to confirm DNA integrity. The double digest of pQE30/*PFF1010c* resulted in two DNA fragments, a 1089 base pairs *PFF1010c* fragment and the plasmid vector with 3425 base pairs (figure 3.5). The *Bam*HI and *Pst*I restriction sites of pQE30/*PFF1010c-HPD* plasmid were selected to confirm DNA

integrity. The double digest of pQE30/PFF1010c-HPD resulted in a 1089 base pair fragment representative of PFF1010c-HPD DNA and the 3433 base pairs plasmid vector (figure 3.5).

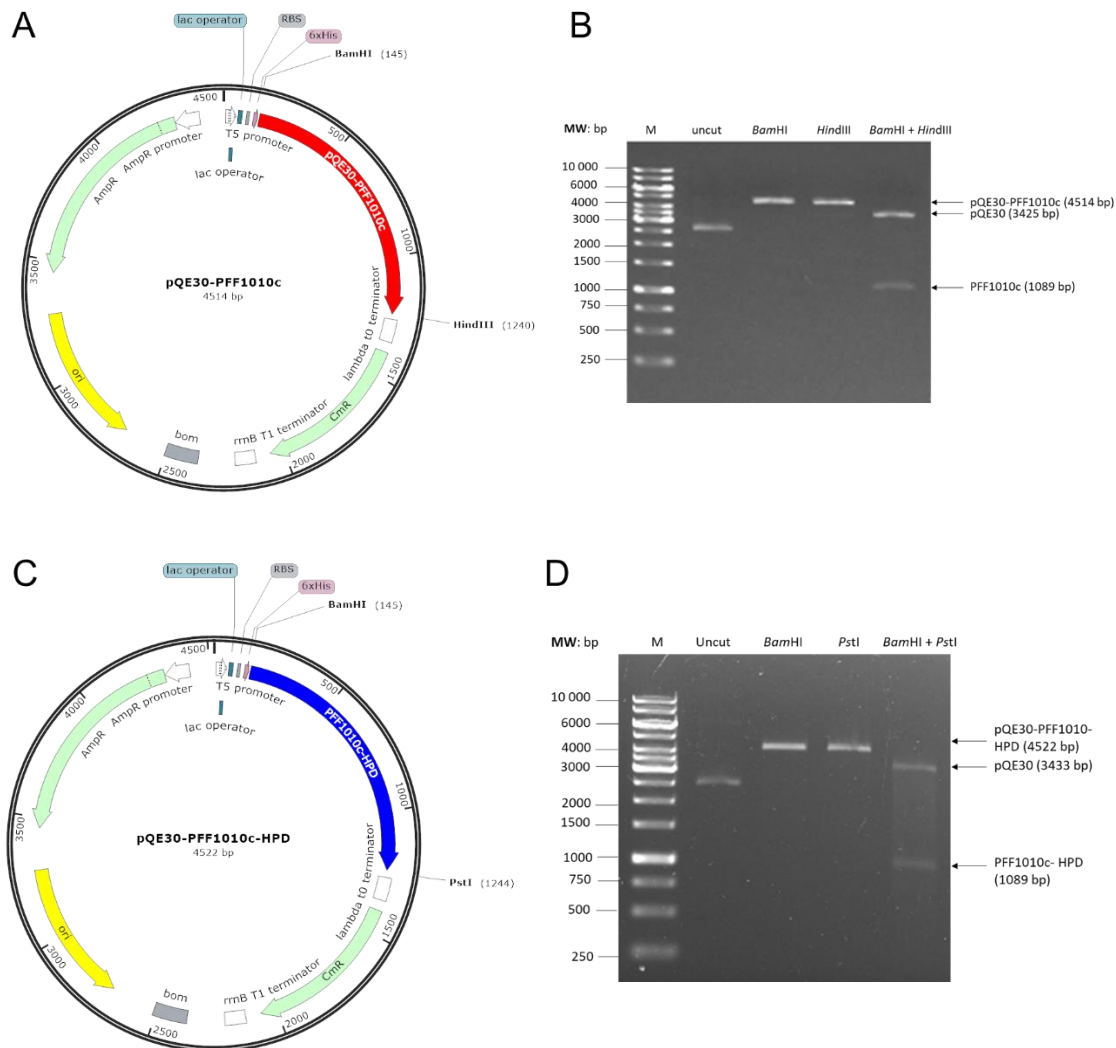


**Figure 3.5 Restriction digest of the pQE30/PFF1010c and pQE30/PFF1010c-HPD plasmid constructs.** (A) Plasmid map of pQE30/PFF1010c with the restriction sites of the enzymes *Bam*HI and *Hind*III, used for the restriction digest. (B) Agarose gel electrophoresis of pQE30/PFF1010c where the DNA sample was loaded onto the gel in the following order: M- molecular weight marker (lane 1); Uncut- undigested pQE30/PFF1010c DNA (lane 2); *Bam*HI- single digest of pQE30/PFF1010c with *Bam*HI (lane 3); *Hind*III- single digest of pQE30/PFF1010c with *Hind*III (lane 4); *Bam* HI + *Hind* III- double digest of pQE30/PFF1010c with both *Bam*HI and *Hind*III (lane 5). (C) Plasmid map of pQE30/PFF1010c-HPD with the restriction sites of the enzymes *Bam*HI and *Pst*I, used for the restriction digest. (D) Agarose gel electrophoresis of pQE30/PFF1010c-HPD where the DNA sample was loaded onto the gel in the following order: M- molecular weight marker (lane 1); Uncut- undigested pQE30/PFF1010c-HPD DNA (lane 2); *Bam*HI- single digest of pQE30/PFF1010c-HPD with *Bam*HI (lane 3); *Pst*I- single digest of pQE30/PFF1010c-HPD with *Pst*I (lane 4); *Bam* HI + *Hind* III- double digest of pQE30/PFF1010c-HPD with both *Bam*HI and *Pst*I (lane 5).

The *Bam*HI and *Hind*III restriction sites of pQE30/*PfHsp40* plasmid were also selected to confirm DNA integrity. The double digest of pQE30/*PfHsp40* resulted in a 1275 base pair fragment demonstrative of *PfHsp40* DNA and the 3425 base pairs plasmid vector (figure 3.6). The *Bam*HI and *Kpn*I restriction sites of pQE30/*PfHsp40-SVN* plasmid were selected to confirm DNA integrity. The double digest of pQE30/*PfHsp40-SVN* resulted in a 1275 base pair fragment representative of *PfHsp40-SVN* DNA and the 3449 base pairs plasmid vector (Figure 3.6).

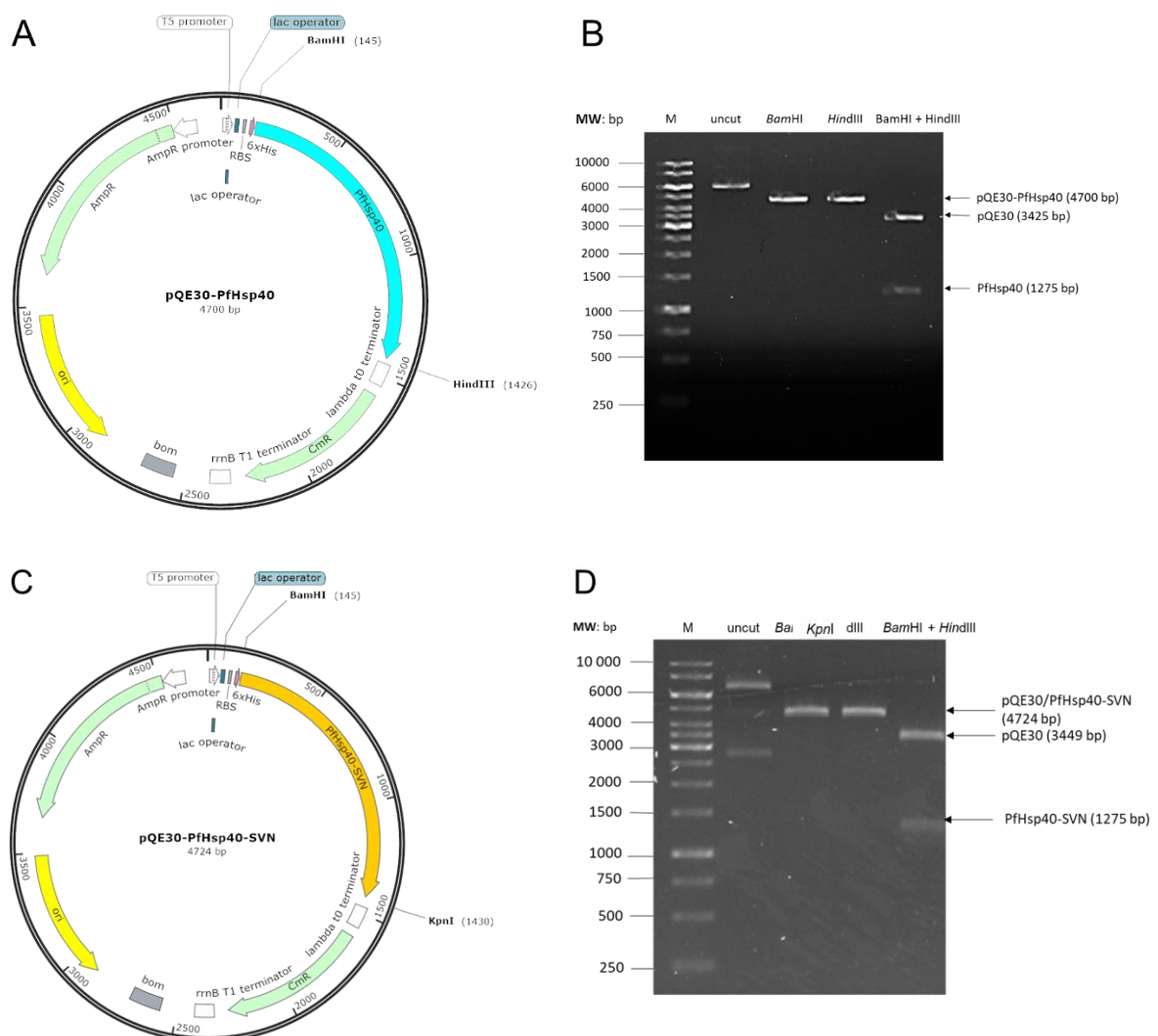


Figure 3.6 Restriction digest of the pQE30/*PfHsp40* and pQE30/*PfHsp40-SVN* plasmid constructs. (A) Plasmid map of pQE30/*PfHsp40* with the restriction sites of the enzymes *Bam*HI and *Hind*III, used for the restriction digest. (B) Agarose gel electrophoresis of pQE30/*PfHsp40* where the DNA sample was loaded onto the gel in the following order: M- molecular weight marker (lane 1); Uncut- undigested pQE30/*PfHsp40* DNA (lane 2); *Bam*HI- single digest of pQE30/*PfHsp40* with *Bam*HI (lane 3); *Hind*III- single digest of pQE30/*PfHsp40* with *Hind*III (lane 4);, *Bam* HI +

*Hind* III- double digest of pQE30/*PfHsp40* with both *Bam*HI and *Hind*III (lane 5). (C) Plasmid map of pQE30/*PfHsp40*-SVN with the restriction sites of the enzymes *Bam*HI and *Kpn*I, used for the restriction digest. (D) Agarose gel electrophoresis of pQE30/*PfHsp40*-SVN where the DNA sample was loaded onto the gel in the following order: M- molecular weight marker (lane 1); Uncut- undigested pQE30/*PfHso40*-SVN DNA (lane 2); *Bam*HI- single digest of pQE30/*PfHsp40*-SVN with *Bam*HI (lane 3); *Kpn*I- single digest of pQE30/*PfHsp40*-SVN with *Kpn*I (lane 4);, *Bam* HI + *Hind* III- double digest of pQE30/*PfHsp40*-SVN with both *Bam*HI and *Kpn*I (lane 5).

The *Bam*HI and *Hind*III restriction sites of pQE30/*PfHsp70-1* plasmid was also selected to confirm DNA integrity. The double digest of pQE30/*PfHsp70-1* resulted in a 2034 base pair fragment representative of *PfHsp70-1* DNA and the 3425 base pairs plasmid vector (figure 3.7).

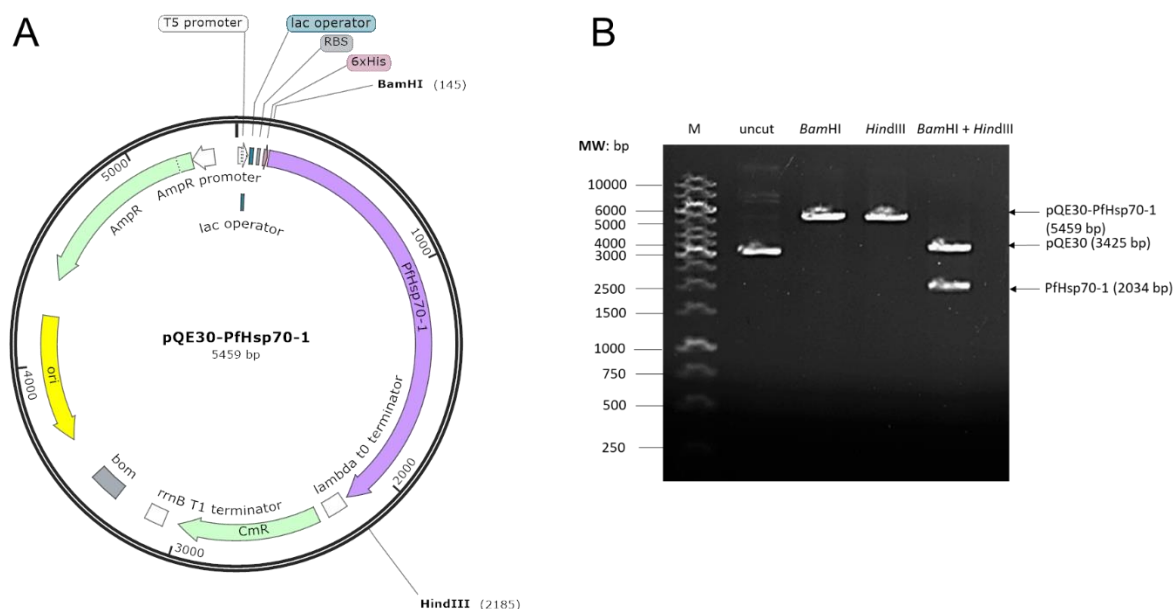
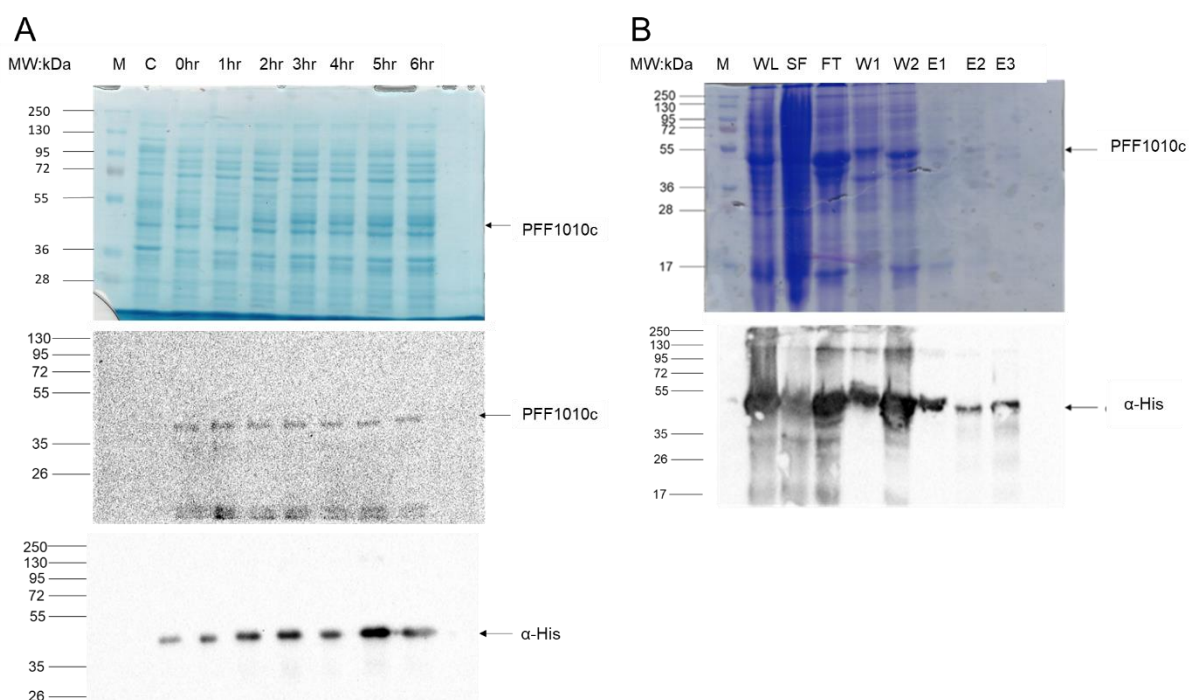


Figure 3.7 Restriction digest of the pQE30/*PfHsp70-1* plasmid construct. (A) Plasmid map of pQE30/*PfHsp70-1* with the restriction sites of the enzymes *Bam*HI and *Hind*III, used for the restriction digest. (B) Agarose gel electrophoresis of pQE30/*PfHsp70-1* where the DNA sample was loaded onto the gel as follows: M- molecular weight marker (lane 1); Uncut- undigested pQE30/*PfHsp70-1* DNA (lane 2); *Bam*HI- single digest of pQE30/*PfHsp70-1* with *Bam*HI (lane 3); *Hind*III- single digest of pQE30/*PfHsp70-1* with *Hind*III (lane 4); *Bam* HI + *Hind* III- double digest of pQE30/*PfHsp70-1* with both *Bam*HI and *Hind*III (lane 5).

### 3.3 Expression and purification of recombinant proteins

Chemically competent *E. coli* JM109/XL1 blue cells were transformed with each respective plasmid constructs to express the recombinant proteins (Appendix A1 and

A2). Recombinant PFF1010c and PfHsp40 and their mutant versions were successfully expressed at 37°C and purified under denaturing conditions using 8 M urea. Expression of the recombinant proteins was analysed using SDS-PAGE and Western blot. All the proteins were expressed as poly-histidine tagged proteins. PFF1010c (Figure 3.8.A) and its mutant version, PFF1010c-HPD (Figure 3.9.A), were expressed in *E. coli* XL1 blue and had the approximate size of 43 kDa. Expression of PFF1010c was confirmed by western blot analysis using  $\alpha$ -PFF1010c and  $\alpha$ -His antibodies (Figure 3.8.A; lower panels). After being treated with urea, a solubility analysis showed PFF1010c to be in the pellet/insoluble fraction (Figure 3.8.B), therefore PFF1010c was purified from the pellet/insoluble fraction using Ni-NTA affinity chromatography. Purification was analysed by Western blot analysis using  $\alpha$ -His antibodies (Figure 3.8.B; lower panel). The purified proteins were all quantified using Bradford's assay (Appendix A9).



**Figure 3.8 Expression and purification of PFF1010c.** (A) SDS-PAGE analysis of PFF1010c expressed in *E. coli* XL1 Blue cells and western blot analysis. Lane M: molecular weight marker (in kDa); Lane C: cell extract of cells transformed with pQE30 plasmid; Lane 0hr: represents pre-induction (with IPTG) cell extract from cells transformed with pQE30/PFF1010c plasmid; Lane 1hr – 6hr: post induction (with IPTG) cell extracts taken hourly for six hours. The western blot analysis of the expression (lower panels) was confirmed using  $\alpha$ -PFF1010c and  $\alpha$ -His antibodies. (B) SDS-PAGE and western blot analysis of PFF1010c solubility study and purification. Lane M: molecular weight marker; Lane WL: whole lysate/total lysate harvested for purification; Lane SF: soluble fraction of cell extract; Lane PF: pellet/insoluble fraction of cell extract; Lane FT: Flow through samples from Ni-NTA affinity chromatography,



Lane W1 - W2: wash steps; Lane E1 - E3: elution samples of proteins eluted using increasing concentrations of imidazole (250 mM – 500mM). Western blot analysis of the solubility study and purification (lower panel) using  $\alpha$ -His antibodies.

Expression of recombinant PFF1010c-HPD was confirmed by western blot analysis using  $\alpha$ -PFF1010c and  $\alpha$ -His antibodies (Figure 3.9.A; lower panels). After being treated with urea, a solubility analysis showed PFF1010c-HPD to be in the soluble fraction (Figure 3.9.B), therefore PFF1010c-HPD was purified from the soluble fraction using Ni-NTA affinity chromatography. Purification was analysed by Western blot analysis using  $\alpha$ -His antibodies (Figure 3.9.B; lower panel).

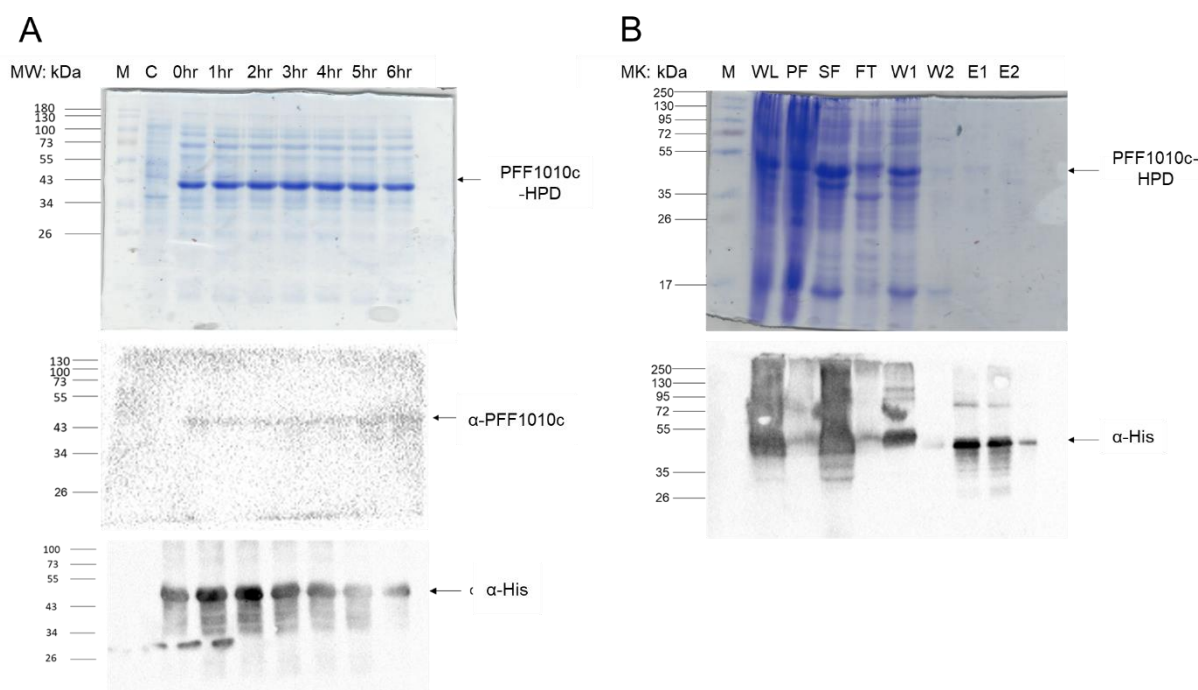


**Figure 3.9 Expression and purification of PFF1010c-HPD** (A) SDS-PAGE analysis of PFF1010c expressed in *E. coli* XL1 Blue cells and western blot analysis. Lane M: molecular weight marker (in kDa); Lane C: cell extract of cells transformed with pQE30 plasmid; Lane 0hr: represents pre-induction (with IPTG) cell extract from cells transformed with pQE30/PFF1010c-HPD plasmid; Lane 1hr – 6hr: post induction (with IPTG) cell extracts taken hourly for six hours. The western blot analysis of the expression (lower panels) was confirmed using  $\alpha$ -PFF1010c and  $\alpha$ -His antibodies. (B) SDS-PAGE and western blot analysis of PFF1010c-HPD solubility study and purification. Lane M: molecular weight marker; Lane WL: whole lysate/total lysate harvested for purification; Lane SF: soluble fraction of cell extract; Lane PF: pellet/insoluble fraction of cell extract; Lane FT: Flow through samples from Ni-NTA affinity chromatography, Lane W1 - W2: wash steps; Lane E1 – E2: elution samples of proteins eluted using increasing concentrations of imidazole (250 mM and 500mM). Western blot analysis of the solubility study and purification (lower panel) using  $\alpha$ -His antibodies.

PfHsp40 (Figure 3.10.A) and its mutant version, PfHsp40-SVN (Figure 3.11.A), were expressed in *E. coli* JM109 and had the approximate size of 48 kDa. Expression of PfHsp40 was confirmed by western blot analysis using  $\alpha$ -His antibody (Figure 3.10.A; lower panel). PfHsp40 was purified from the soluble fraction using Ni-NTA affinity chromatography (Figure 3.11.B), a procedure previously described in Lebepe *et al* (2020). Purification was analysed by Western blot analysis using  $\alpha$ -His antibodies (Figure 11.B; lower panel).

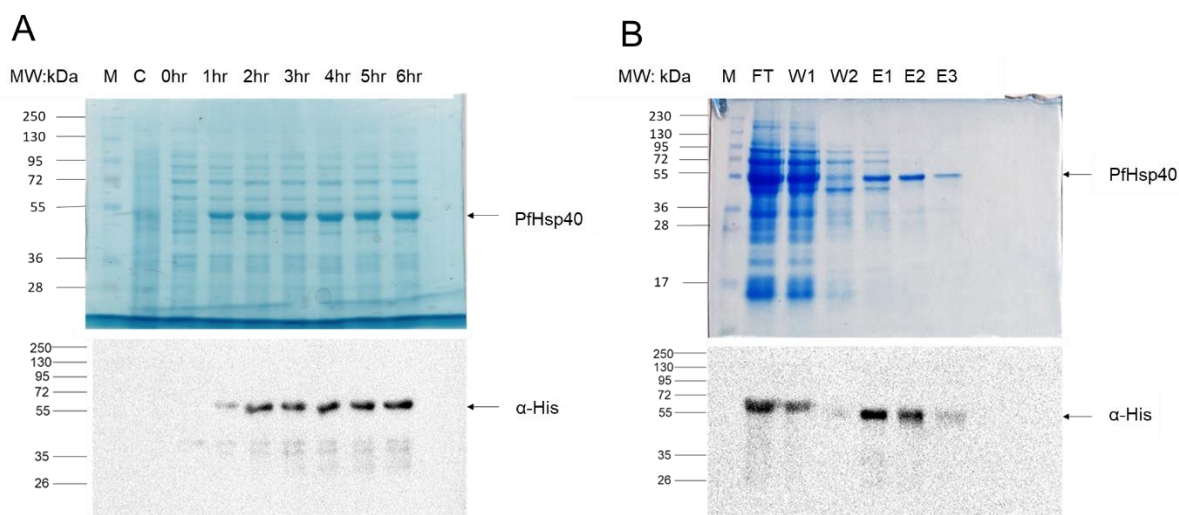


**Figure 3.10 Expression and purification of PfHsp40** (A) SDS-PAGE analysis of PfHsp40 expressed in *E. coli* JM109 cells and western blot analysis. Lane M: molecular weight marker (in kDa); Lane C: cell extract of cells transformed with pQE30 plasmid; Lane 0hr: represents pre-induction (with IPTG) cell extract from cells transformed with pQE30/PfHsp40 plasmid; Lane 1hr – 6hr: post induction (with IPTG) cell extracts taken hourly for six hours. The western blot analysis of the expression (lower panel) was confirmed using  $\alpha$ -His antibodies. (B) SDS-PAGE and western blot analysis of PfHsp40 purification. Lane M: molecular weight marker; Lane FT: Flow through samples from Ni-NTA affinity chromatography, Lane W1 - W2: wash steps; Lane E1 – E3: elution samples of proteins eluted using increasing concentrations of imidazole (250 mM - 500mM). Western blot analysis of the purification (lower panel) using  $\alpha$ -His antibodies.

Expression of PfHsp40-SVN was confirmed by western blot analysis using  $\alpha$ -His antibody (Figure 3.11.A; lower panel). After being treated with urea, a solubility analysis showed PfHsp40-SVN to be in the soluble fraction (Figure 3.11.B), therefore PFF1010c-HPD was purified from the soluble fraction using Ni-NTA affinity chromatography. Purification was analysed by SDS-PAGE and protein production confirmed by Western blot analyses using  $\alpha$ -His antibodies (Figure 3.11.B; lower panel).

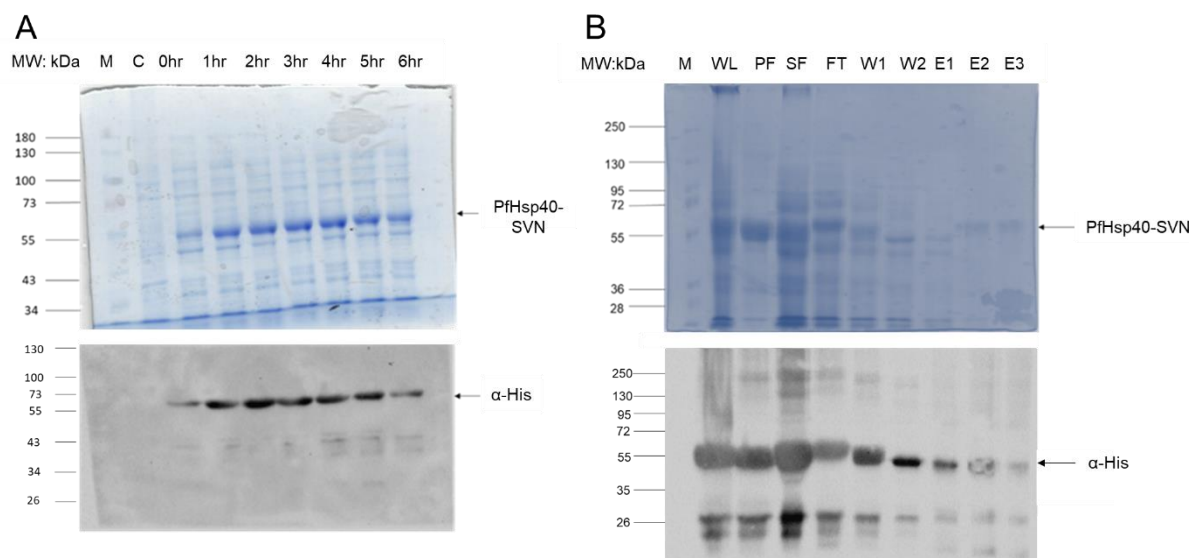


**Figure 3.11 Expression and purification of PfHsp40-SVN** (A) SDS-PAGE analysis of PfHsp40-SVN expressed in *E. coli* JM109 cells and western blot analysis. Lane M: molecular weight marker (in kDa); Lane C: cell extract of cells transformed with pQE30 plasmid; Lane 0hr: represents pre-induction (with IPTG) cell extract from cells transformed with pQE30/PfHsp40-SVN plasmid; Lane 1hr – 6hr: post induction (with IPTG) cell extracts taken hourly for six hours. The western blot analysis of the expression (lower panel) was confirmed using  $\alpha$ -His antibodies. (B) SDS-PAGE and western blot analysis of PfHsp40-SVN solubility study and purification. Lane M: molecular weight marker; Lane WL: whole lysate/total lysate harvested for purification; Lane SF: soluble fraction of cell extract; Lane PF: pellet/insoluble fraction of cell extract; Lane FT: Flow through samples from Ni-NTA affinity chromatography, Lane W1 - W2: wash steps; Lane E1 – E2: elution samples of proteins eluted using increasing concentrations of imidazole (250 - 500mM). Western blot analysis of the solubility study and purification (lower panel) using  $\alpha$ -His antibodies.

PfHsp70-1 (Figure 3.12.A) was expressed in *E. coli* XL1 Blue and migrated at approximately 73 kDa. Expression of PfHsp70-1 was confirmed by Western blot analysis using  $\alpha$ -PfHsp70-1 and  $\alpha$ -His antibody (Figure 3.12.A; lower panels). To help better solubilize the recombinant protein, 0.1% Triton X-100 was added into the whole lysate prior to separating the soluble fraction from the pellet/insoluble fraction. Then, using a previously described procedure (Lebepe *et al*, 2020), PfHsp70-1 was purified from the soluble fraction using Ni-NTA affinity chromatography (Figure 3.12.B). Purification was analysed by SDS-PAGE and Western blot analysis using  $\alpha$ -PfHsp70-1 and  $\alpha$ -His antibodies, and also confirming that DnaK (*E. coli* Hsp70 that has approximately the same size as PfHsp70-1) was not purified along with PfHsp70-1 using  $\alpha$ -DnaK (Figure 12.B; lower panels).

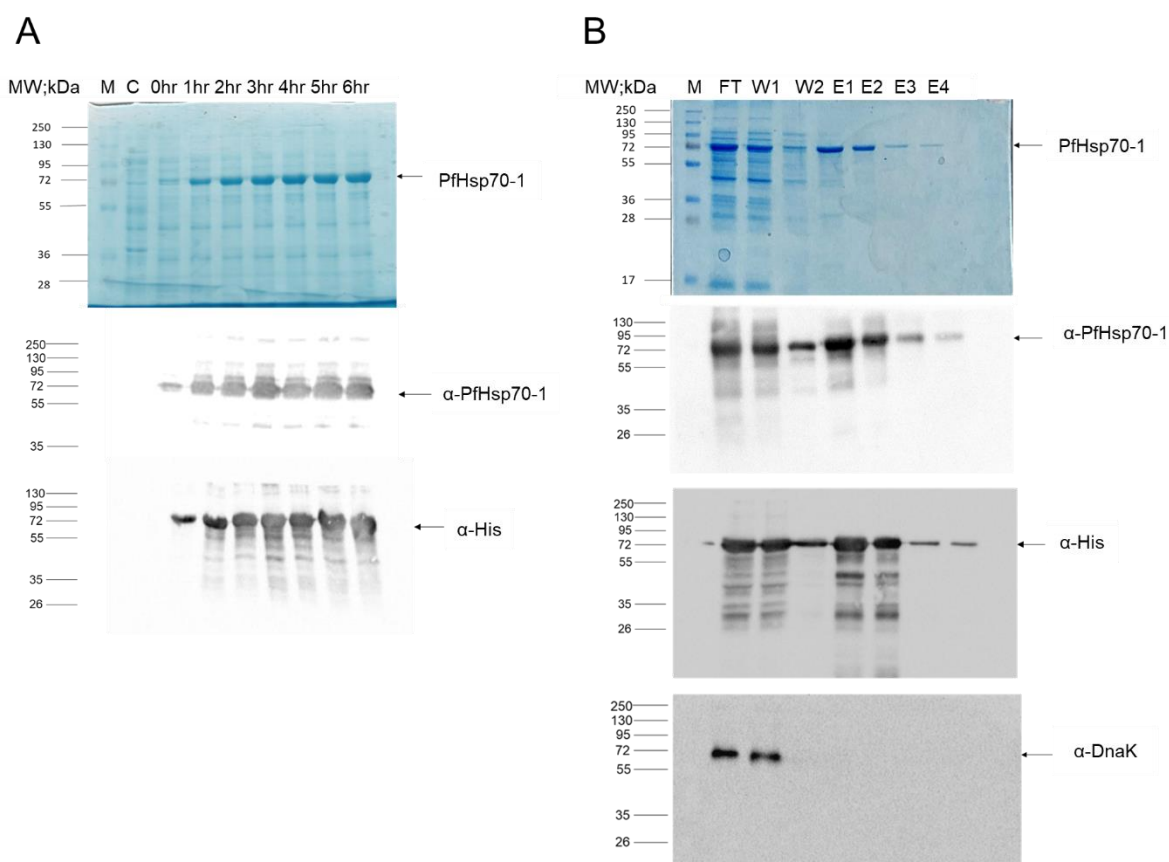


**Figure 3.12 Expression and purification of PfHsp70-1** (A) SDS-PAGE analysis of PfHsp70-1 expressed in *E. coli* XL1 Blue cells and western blot analysis. Lane M: molecular weight marker (in kDa); Lane C: cell extract of cells transformed with pQE30 plasmid; Lane 0hr: represents pre-induction (with IPTG) cell extract from cells transformed with pQE30/*PfHsp70-1* plasmid; Lane 1hr – 6hr: post induction (with IPTG) cell extracts taken hourly for six hours. The western blot analysis of the expression (lower panels) was confirmed using  $\alpha$ -PfHsp70-1 and  $\alpha$ -His antibodies. (B) SDS-PAGE and western blot analysis of PfHsp70-1 purification. Lane M: molecular weight marker; Lane FT: Flow through samples from Ni-NTA affinity chromatography, Lane W1 - W2: wash steps; Lane E1 – E4: elution samples of proteins eluted using increasing concentrations of imidazole (250 mM – 500mM). Western blot analysis of the solubility study and purification (lower panels) using  $\alpha$ -PfHsp70-1 and  $\alpha$ -His antibodies, and  $\alpha$ -DnaK to show that the *E. coli* Hsp70 was not purified along with PfHsp70-1.

### 3.4 Biophysical characterisation of Hsp40 proteins

#### 3.4.1 Hydrophobicity of proteins

For *in vitro* biophysical characterization, ANS fluorescence and tyrosine fluorescence were used to analyse the effects of the HPD/SVN motif switch on protein structure. To evaluate the impact the HPD/SVN motif switch might have had on protein

hydrophobicity, ANS fluorescence was monitored in the presence of the proteins (Figure 3.13). ANS is a fluorescence probe that binds to hydrophobic patches on proteins (Schonbrunn *et al*, 2000; Achilonu *et al*, 2014). Increase in protein hydrophobicity is represented by the emission spectrum shifts to shorter wavelengths, blue shift (Lakowicz, 1983). The fluorescence increased slightly upon excitation at 390 nm. A red shift in emission maxima was exhibited for PFF1010c-HPD, from 539 nm which is the emission maxima of the wildtype PFF1010c to 547 nm (Figure 3.13.A.). This is consistent with the predicted hydropathy profile in section 3.1 where PFF1010c is more hydrophobic than PFF1010c-HPD. In the presence of ANS, no shift in emission maxima was observed between PfHsp40 and PfHsp40-SVN (Figure 3.13.B). The hydropathy plots had predicted that PfHsp40-SVN was slightly more hydrophobic than PfHsp40. A difference in hydrophobicity can alter the binding/interaction capacity of the protein.

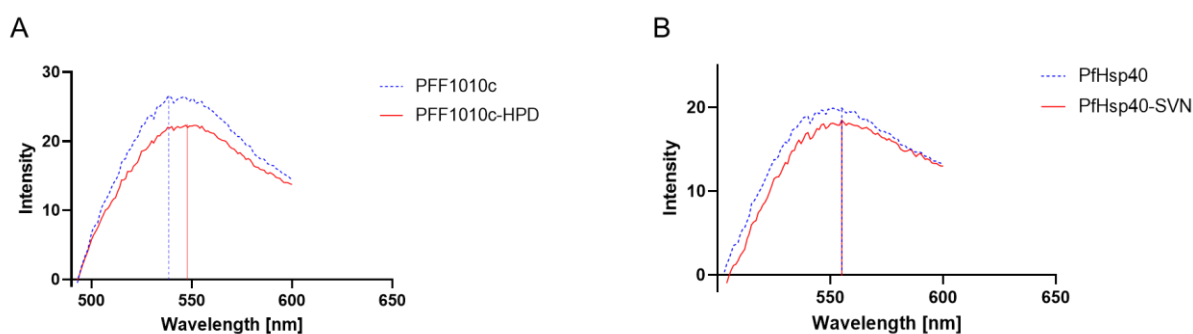


**Figure 3.13 Analysis of the tertiary structure of wildtype Hsp40s and mutants using ANS fluorescence.** (B) Emission spectra comparison of PfHs40 and PfHsp40-SVN. (A) PFF1010c and PFF1010c-HPD. ANS at 100 mM was mixed with 2  $\mu$ M proteins. Excitation was at 390 nm and the emission spectra was recorded between 400 and 600 nm.

### 3.4.2. Effects of denaturants on tertiary structure stability

PFF1010c is a protein that possesses 28 tyrosine residues and PfHsp40 possesses 17 tyrosine residues. Both proteins do not possess any tryptophan residues. Therefore, the proteins were analysed using tyrosine fluorescence in the presence of varying concentrations of urea and guanidine hydrochloride. All the proteins were incubated for 20-30 min in denaturants prior to the samples being read at an excitation wavelength of 280 nm. The fluorescence intensity was observed to increase with an

increase in denaturant concentrations (Appendix B8-B11). A blue shift in emission spectra was observed with increasing urea concentrations for PFF1010c (Figure 3.14.A. where the emission maxima gradually decreased from 330 to 326 nm. This is consistent with PFF1010c being purified from the pellet fraction after treatment with urea as the protein aggregates. With PFF1010c-HPD, a red shift in the maximum emission spectra was observed with increasing urea concentrations (Figure 3.14.A). PfHsp40 and PfHsp40-SVN both exhibited a red shift in the maximum emission spectra with increasing concentrations of urea (Figure 3.14.B). Urea weakens the hydrophobic effects of proteins leading to denaturation (Stumpe and Grubmuller, 2009).

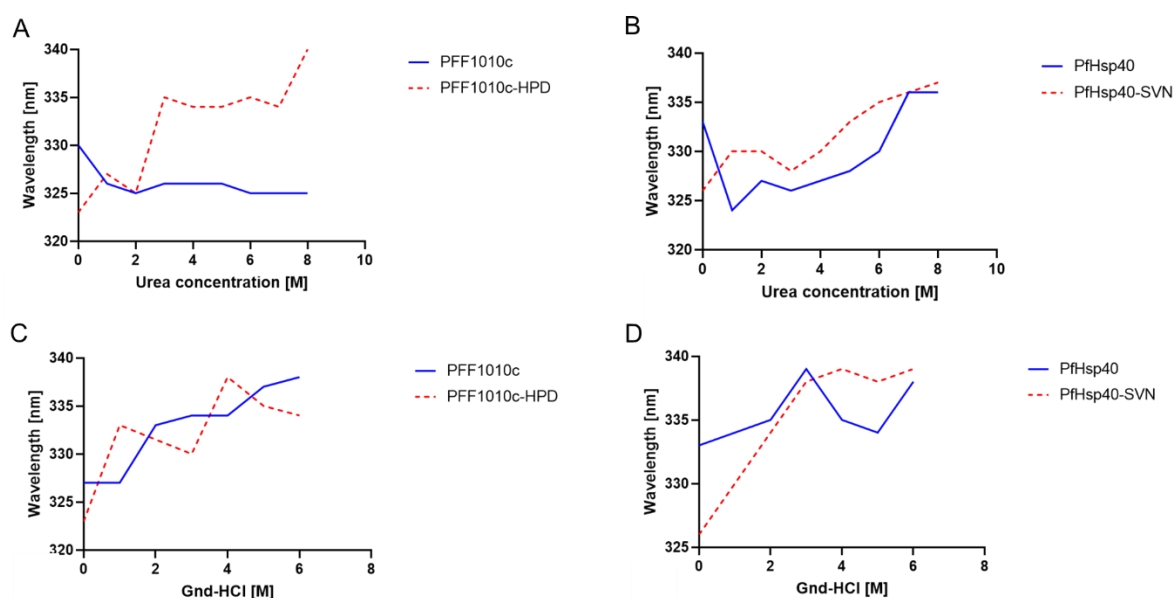


**Figure 3.14 Effect of denaturants, urea and guanidine hydrochloride, on the tertiary structure of Hsp40s.**

(A) Comparison of the effects urea has on PFF1010c and PFF1010c-HPD, (B) urea effects on PfHsp40 and PfHsp40-SVN. (C) Comparison of the effects of guanidine hydrochloride on PFF1010c and PFF1010c-HPD and, (D) PfHsp40 and PfHsp40-SVN. The tyrosine residues in the proteins were excited at 280 nm and the emission recorded between 300 to 500 nm.

All the proteins exhibited a red shift in the maximum emission spectra when treated with increasing concentrations of guanidine hydrochloride (Figure 3.14.C and D). The proteins showed sensitivity to the denaturants, with PFF1010c-HPD, PfHsp40 and PfHsp40-SVN gradually unfolding with increasing concentrations of urea and guanidine hydrochloride. Hydrophobic amino acids are prone to forming hydrophobic core that stabilizes protein structure while some hydrophobic amino acids can be

distributed on the surface of proteins. These hydrophobic surface amino acids, under unstable physiochemical and biological conditions brought upon by temperature, pH or denaturants, can interact to form protein aggregates (Lan et al, 2020). PFF1010c also showed sensitivity to the denaturants as the protein appeared to aggregate when treated with urea and unfolded when treated with guanidine hydrochloride. This validates the proteins having been in their native (folded) state prior to treatment with the denaturants.

### 3.4.3 Thermostability of the proteins

The thermal stability of the wildtype proteins was compared to that of mutants using tyrosine fluorescence (Figure 3.15). The fluorescence intensity decreased with an increase in temperature (Appendix B12 and B13). PFF1010c red shifted slightly before blue shifting at temperatures higher than 60 °C (Figure 3.15.A). PFF1010c-HPD remained stable before eventually exhibiting a blue shift at temperatures above 80 °C (Figure 3.15.B). PfHsp40 also remained stable before eventually exhibiting a red shift at temperatures above 80 °C (Figure 3.15.B). PfHsp40-SVN exhibited a red shift at temperatures exceeding 40 °C (Figure 3.15.B). The HPD motif appears to be responsible for the thermostability of both PFF1010c-HPD and PfHsp40 as these were the proteins whose tertiary structure remained stable at temperatures as high as 80 °C.

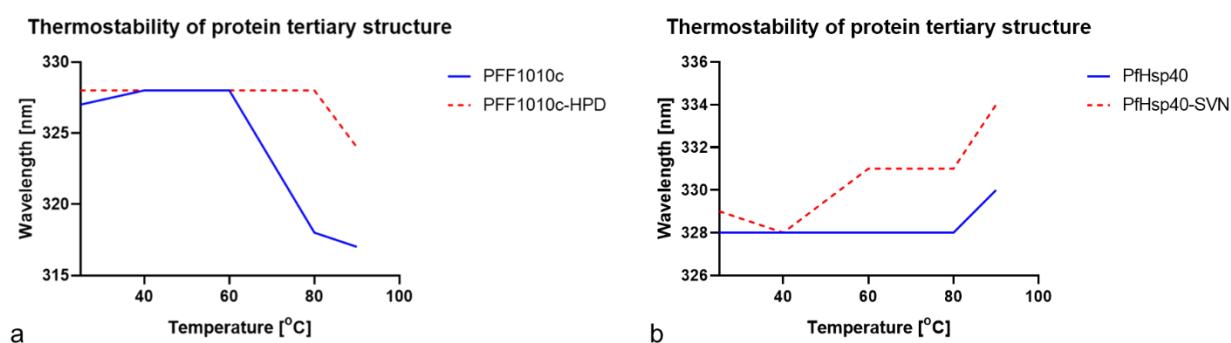


**Figure 3.15 Investigating the thermostability of Hsp40s.** (A.) Comparison of protein tertiary structure stability under increasing temperatures (20, 40, 60, 80 and 90°C) for PFF1010c (blue solid line) and PFF1010c-HPD (red dotted line) and (B.) PfHsp40 (blue solid line) and PfHsp40-SVN (red dotted line). Excitation was at 280 nm and the emission recorded between 300 to 500 nm.

### 3.5 Hsp70-Hsp40 interaction

#### 3.5.1 ATPase activity

To evaluate the effect of the HPD/SVN motif switch on PfHsp40 and PFF1010c function, an ATPase activity assay was conducted. The HPD motif of PfHsp40 is known to stimulate the ATPase activity of PfHsp70-1 (Fan *et al*, 2003). The Michaelis-Menten plots (Figure 3.5.1) show that in the presence of the proteins with the SVN motif (PFF1010c and PfHsp40-SVN), the ATPase activity of PfHsp70-1 is reduced.

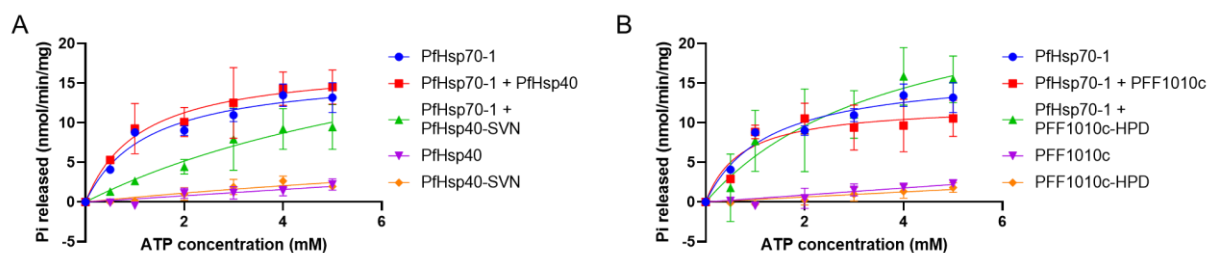


**Figure 3.16 Comparative analysis of ATPase activity stimulation by wildtype vs mutant Hsp40s.** Michaelis-Menten plots of the ATPase activity were plotted based on the amount of  $P_i$  released using a direct colorimetric assay. A.) Analysis of the basal activity of PfHsp70-1 and the ATPase activity in the presence of PfHsp40 and PfHsp40-SVN. B.) Analysis of the basal activity of PfHsp70-1 and the ATPase activity in the presence of PFF1010c and PFF1010c-HPD.

PfHsp70-1 in an ATPase chaperone whose ATPase activity is enhanced by its co-chaperone, PfHsp40 (Botha *et al*, 2011; Lebepe *et al*, 2020). The kinetics for the ATP hydrolysis are depicted in table 3.2. Basal PfHsp70-1 ATPase activity was found to exhibit a  $V_{max}$  value of 16.5 nmol/min/mg with a  $K_m$  value of 1.3 mM. In the Presence of PfHsp40, PfHsp70-1 had an increased  $V_{max}$  value of 17.6 nmol/min/mg with a  $K_m$  value of 1.1 mM. A similar trend was observed in Lebepe *et al* (2020), where PfHsp40 enhanced the ATPase activity of PfHsp70-1. A small  $K_m$  indicates high affinity of the substrate for the enzyme (Bosdriesz *et al*, 2017). Lower concentrations of substrate (ATP) were required to reach the  $V_{max}$  of the enzymatic activity in the presence of PfHsp40 as compared to PfHsp70-1 without PfHsp40. PFF1010c-HPD had a much higher  $V_{max}$  value (28.5 nmol/min/mg), although requiring much more substrate. PfHsp40-SVN requires a lot more substrate for the reaction to reach the reactions  $V_{max}$  ( $K_m$  value of 8.7). PFF1010c appeared to reduce the efficiency with which PfHsp70-1 hydrolyses ATP. The  $V_{max}$  of the enzymatic reaction depends on environmental conditions such as temperature and pH (Scopes, 1995). Hence enzymes have



optimum temperatures and pH, and this could account for the variable values obtained from different experiments with similar trends.

**Table 3.2 ATPase kinetics for PfHsp70-1 with Hsp40s**

Protein		$V_{max}$ (n/mol/min/mg)	$K_m$ ( $\mu$ M)	Reference
PfHsp70-1		16,52 (+/- 0,79)	1,26 (+/- 0,79)	This study
PfHsp70-1		11,57 (+/- 0,38)	37,08 (+/- 0,38)	Lebepe, 2019
PfHsp70-1 PfHsp40	+	17,59 (+/- 0,50)	1,12 (+/- 0,50)	This study
PfHsp70-1 PfHsp40	+	16,32 (+/- 0,32)	34,17 (+/- 0,32)	Lebepe, 2019
PfHsp70-1 PfHsp40-SVN	+	27,56 (+/- 2.21)	8,67 (+/- 2.21)	This study
PfHsp70-1 PFF1010c	+	13,31 (+/- 0,27)	0,73 (+/- 0,27)	This study
PfHsp70-1 PFF1010c-HPD	+	28,46 (+/- 1,11)	3,93 (+/- 1,11)	This study

The respective  $V_{max}$  and  $K_m$  values are shown.  $V_{max}$  is the maximum rate of reaction/the maximum rate at which the enzyme converts substrate to product.  $K_m$  is the concentration of substrate that gives the reaction rate that is halfway to  $V_{max}$ . Standard deviation of 3 independent repeats were shown.

### 3.3 SPR Analysis

PfHsp70-1 is known to interact with PfHsp40, where the HPD motif of PfHsp40 stimulates the ATPase activity of PfHsp70-1 and, also when PfHsp40 presents substrates to PfHsp70-1 (Botha *et al*, 2011). Therefore, the effect of the HPD/SVN motif switch on the interaction of Hsp40 with PfHsp70-1 was investigated using SPR analysis. SPR analysis was used to validate if a viable interaction exists between PFF1010c and PfHsp70-1. The sensograms obtained from the analysis demonstrated that the interactions occurred in a concentration dependent manner (Figure 3.17). In a previous study (Lebepe *et al*, 2020), the interaction between PfHsp70-1 and PfHsp40 was shown to be nucleotide dependent.

In the current study, no significant difference could be observed from the  $K_D$  for PfHsp70-1 – PfHsp40 interaction in the presence of ADP and absence of nucleotides. (Table 3.3). However, in the presence of ATP, PfHsp40 showed a higher affinity for PfHsp70-1. An observation also seen in Lebepe *et al* (2020). PfHsp40-SVN showed decreased affinity ( $K_D$ ) to interact with PfHsp70-1 in the presence of nucleotides.

PFF1010c-HPD showed the highest affinity for PfHsp70-1 in the absence of nucleotides in comparison to when nucleotides were present.

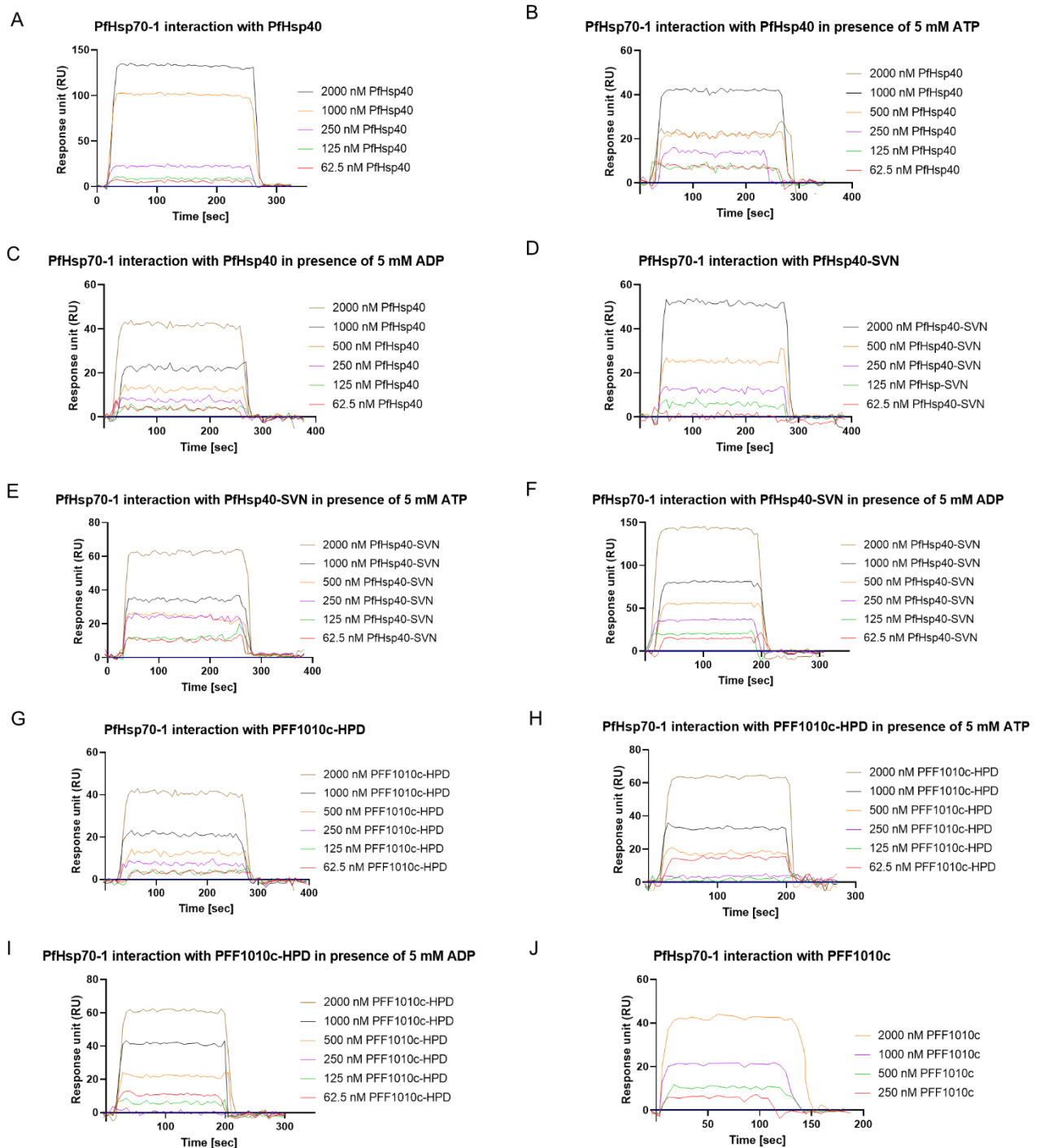


**Figure 3.17. Sensograms for PfHsp70-1 association with Hsp40s in presence and absence of nucleotides.** SPR analysis was used to analyse PfHsp70-1 and PfHsp40 interaction. (A) the interaction was monitored in the absence of nucleotides, (B) in the presence of 5 mM ADP and (C) in the presence of 5 mM ATP. Then to analyse PfHsp70-1 and PfHsp40-SVN interaction in the (D) absence of nucleotides (E) presence of ADP and (F) ATP. And to analyse PfHsp70-1 and PFF1010c-HPD interaction in the (G) absence of no nucleotide (H) presence of ADP and (I) ATP. Lastly, PfHsp70-1 and PFF1010c interaction was analysed in the absence of nucleotides. All the

interactions showed concentration dependence as the response units increased with increasing analyte concentrations.

**Table 3.3. Kinetics for the interaction of PfHsp70-1 with Hsp40s**

Ligand	Analyte	$K_a$ (M.s <sup>-1</sup> )	$K_d$ (s <sup>-1</sup> )	$K_D$ (M)	$\chi^2$	Reference
PfHsp70-1	PfHsp40 NN	8,23e <sup>+03</sup>	8,21e <sup>-02</sup>	9,98 e <sup>-06</sup>	0,01	This study
	PfHsp40 NN	1,33e <sup>+03</sup>	9,81e <sup>-02</sup>	1,88 e <sup>-05</sup>	7,80	Lebepe <i>et al</i> , 2020
	PfHsp40 ADP	1,35 e <sup>+04</sup>	9,07 e <sup>-02</sup>	6,71 e <sup>-06</sup>	0,14	This study
	PfHsp40 ADP	1,53e <sup>+03</sup>	8,66e <sup>-06</sup>	9.98 e <sup>-06</sup>	3,08	Lebepe <i>et al</i> , 2020
	PfHsp40 ATP	4,19 e <sup>+04</sup>	3,92 e <sup>-02</sup>	9,36 e <sup>-07</sup>	0,43	This study
	PfHsp40 ATP	1.81e <sup>+02</sup>	1.32e <sup>-04</sup>	2,08 e <sup>-07</sup>	2,12	Lebepe <i>et al</i> , 2020
	PfHsp40-SVN NN	7,12 e <sup>+03</sup>	6,07 e <sup>-02</sup>	8,52 e <sup>-06</sup>	0.02	This study
	PfHsp40-SVN ADP	9,54 e <sup>+03</sup>	8,85 e <sup>-02</sup>	9,28 e <sup>-05</sup>	0,32	
	PfHsp40-SVN ATP	8,70 e <sup>+03</sup>	1,11 e <sup>-01</sup>	1,28 e <sup>-05</sup>	0,13	
	PFF1010c-HPD NN	5,41e <sup>+05</sup>	8,07e <sup>-02</sup>	1,49 e <sup>-07</sup>	0,02	
	PFF1010c-HPD ADP	1,04 e <sup>+04</sup>	1,10 e <sup>-01</sup>	1,08 e <sup>-05</sup>	0,2	
	PFF1010-HPD ATP	1,34 e <sup>+04</sup>	1,04 e <sup>+01</sup>	7,75 e <sup>-06</sup>	0,24	
	PFF1010c	PfHsp70-1	1,71 e <sup>+04</sup>	7,03 e <sup>-02</sup>	4,11 e <sup>-06</sup>	0.02

SPR was conducted to investigate the interaction of PfHsp70-1 with wildtype vs mutant Hsp40s.  $\chi^2$  values indicate the score for the goodness of fit of the Langmuir fit model used to generate kinetics.

Typical binding affinity ( $K_D$ ) range is between  $10^{-03} - 10^{-12}$ . A  $K_D$  value in the micromolar and nanomolar range takes up to 40 seconds to reach equilibrium and the dissociation constant ( $K_d$ ) will be between  $1 - 0.001 \text{ s}^{-1}$  (Jarmoskaite *et al*, 2020). The affinity of PFF1010c for PfHsp70-1 occurred at the micromolar range ( $4.11 \mu\text{M}$ ).

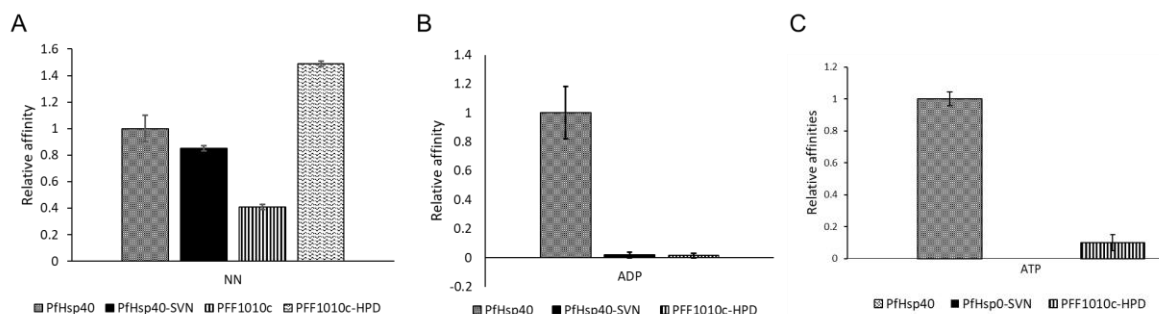


**Figure 3.18. Bar graphs representing relative affinities of Hsp40 for PfHsp70-1.** (A) Relative affinities of Hsp40s (PfHsp40, PfHsp40-SVN, PFF1010c and PFF1010c-HPD) in the absence of nucleotides (no nucleotides, NN). (B) Relative affinities of Hsp40s (PfHsp40, PfHsp40-SVN and PFF1010c-HPD) in the presence of ADP and (C) in the presence of ATP.

The relative affinities of the Hsp40s for PfHsp70-1 were investigated. In the absence of nucleotides, PFF1010c-HPD shows the highest affinity for PfHsp70-1 while PFF1010c showed the lowest affinity (Figure 3.18.A). PfHsp40-SVN interacted with PfHsp70-1 with relatively diminished affinity in comparison to PfHsp40 (Figure 3.18.A). In the presence of ADP, PFF1010c-HPD and PfHsp40-SVN show a very diminished affinity for PfHsp70-1 in comparison to PfHsp40 (Figure 3.18.B). In the presence of ATP, PfHsp40 shows the highest affinity for PfHsp70-1 and PfHsp40-SVN has the lowest affinity (Figure 3.18.C). In the presence of ATP, PfHsp70-1 assumes an open conformation where it interacts with Hsp40 and accepts substrate (Kytik *et al*, 2012). The HPD/SVN motif switch altered the affinities of the proteins to bind PfHsp70-1.

### 3.6 Screening of quinoline-pyrimidine hybrid compounds using SPR

Four quinoline-pyrimidine hybrids were screened for their binding affinity with PfHsp70-1 in the absence and presence of PfHsp40 (Figure 3.19; Table 3.4). The interaction exhibited concentration dependence as the response units increased with increasing analyte concentrations.

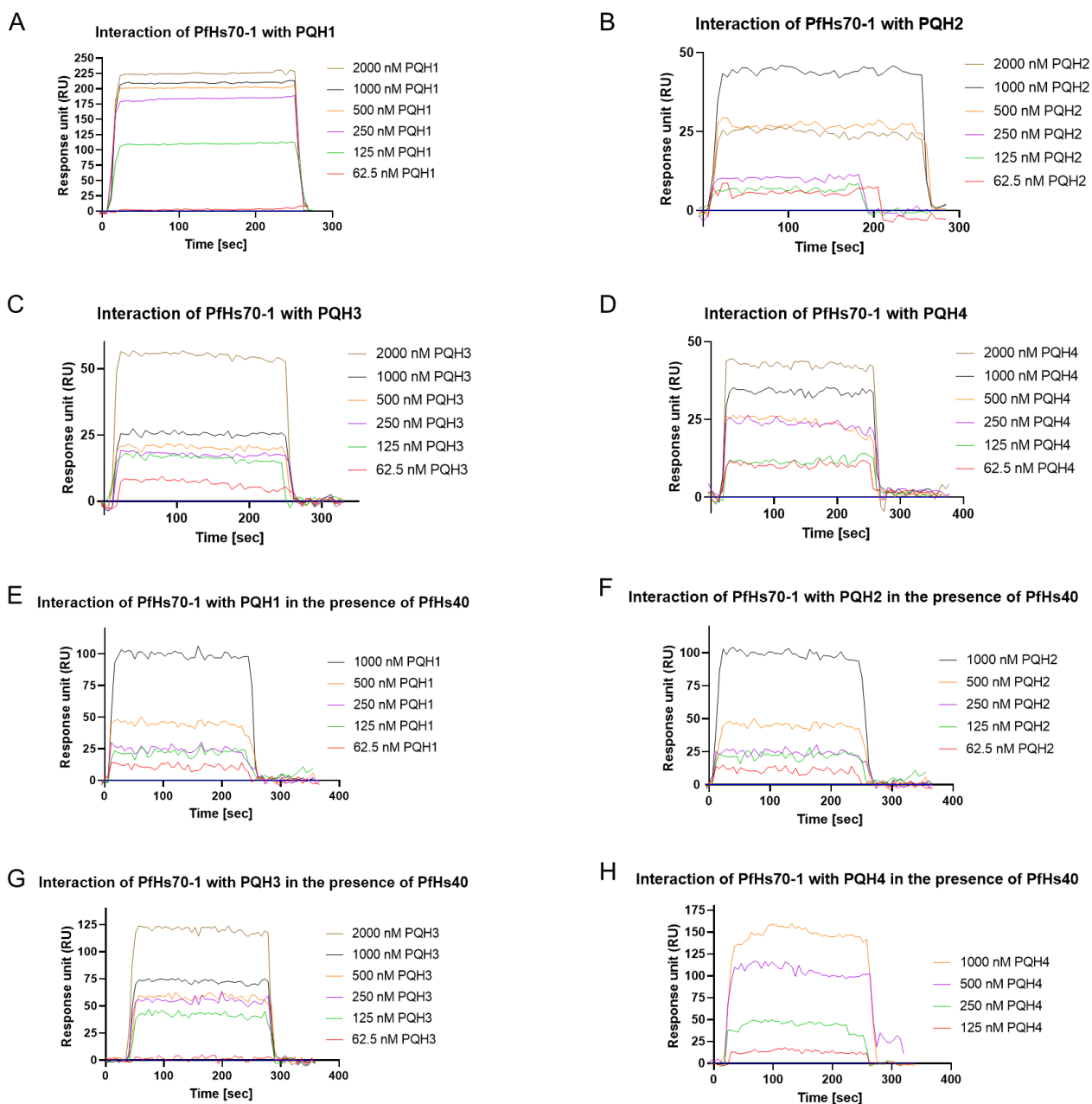


**Figure 3.19. Sensograms of PfHsp70-1 association with quinoline-pyrimidine hybrid compounds in the presence and absence of its co-chaperone, PfHsp40.** (A) Compound PQH1 interaction with PfHsp70-1 (B) Compound PQH2 interaction with PfHsp70-1 (C) Compound PQH3 interaction with PfHsp70-1 and (D) Compound PQH4 interaction with PfHsp70-1. (E) PQH1, (F) PQH2, (G) PQH3, (H) PQH4 interaction with PfHsp70-1 in the presence of PfHsp40.

Quinoline-pyrimidine compound PQH1 exhibited binding affinities very similar to one another in the nanomolar range in the presence and absence of PfHsp40. Compound, PQH2, exhibited a binding affinity above the nanomolar range for PfHsp70-1 in the absence of PfHsp40 and a binding affinity in the nanomolar range in the presence of

PfHsp40. Compound, PQH3, had the highest binding affinity in the absence of PfHsp40. The binding affinity of PQH4 was similar in the presence and absence of PfHsp40.

**Table 3.4.** Kinetics for the interaction of PfHsp70-1 and quinoline-pyrimidine hybrid compounds in the absence and presence of PfHsp40

Ligand	Analyte	Compound	$K_a$	$K_d$	$K_D$	$X^2$
PfHsp70-1		PQH1 (C <sub>31</sub> H <sub>28</sub> N <sub>5</sub> O <sub>2</sub> )	2,47e <sup>+07</sup>	5,73e <sup>-02</sup>	2,31e <sup>-09</sup>	1,46
		PQH2(C <sub>29</sub> H <sub>26</sub> N <sub>5</sub> O <sub>3</sub> )	8,31e <sup>+08</sup>	2,78e <sup>-02</sup>	3,34e <sup>-11</sup>	8,85
		PQH3(C <sub>33</sub> H <sub>32</sub> N <sub>5</sub> O <sub>4</sub> )	7,34e <sup>+06</sup>	9,64e <sup>-02</sup>	1,31e <sup>-08</sup>	3,82
		PQH4(C <sub>29</sub> H <sub>26</sub> N <sub>5</sub> O <sub>2</sub> )	7,2e <sup>+06</sup>	8,21e <sup>-02</sup>	1,14e <sup>-08</sup>	1,85
	PfHsp40	PQH1	1,02e <sup>+07</sup>	8,53e <sup>-02</sup>	8,35e <sup>-09</sup>	3,08
	PfHsp40	PQH2	9,46e <sup>+06</sup>	5,29e <sup>-02</sup>	5,59e <sup>-09</sup>	2,84
	PfHsp40	+ PQH3	6,93e <sup>+04</sup>	1,07e <sup>-01</sup>	1,55e <sup>-06</sup>	0,03
	PfHsp40	+ PQH4	3,92e <sup>+05</sup>	2,68e <sup>-02</sup>	6,85e <sup>-08</sup>	0,05

SPR was conducted to investigate the interaction of PfHsp70-1 the quinoline-pyrimidine hybrid compounds in the presence and absence PfHsp40. Chi<sup>2</sup> values indicate the score for the goodness of fit of the Langmuir fit model used to generate kinetics.

## Chapter 4: Discussion

The main findings of this study are that PFF1010c interacts with PfHsp70-1 and does not display any thermotolerance. The significance of this interaction could be of importance in the endeavour to find transmission blocking drug targets in the gametocytes. The HPD motif of PfHsp40 confers thermostability to the protein and the mutant protein, PFF1010c-HPD. The pyrimidine-quinoline hybrid compounds were effective in inhibiting PfHsp70-1 and PfHsp40 interaction, a chaperone complex responsible for maintaining proteostasis and evasion of the effects of some antimalarial treatments.

To fully characterize the structure of a protein involves the elucidation of its molecular and cellular functions, its three-dimensional features and understanding its interaction with other molecules (Koppensteiner *et al*, 2000). The first step in understanding proteins is computational characterization that detects sequence features, predicts three-dimensional protein structure, predicts protein interaction partners and cellular localization (Bienkowska, 2005). Bioinformatics showed that PFF1010c possesses a J-domain that does not lack the HPD motif. The HPD motif is typically present in type I – type III *Plasmodial* Hsp40s, as well as the canonical Hsp40s of other organisms (Figure 3.1; Botha *et al*, 2007). Sequence alignment of type IV *Plasmodial* Hsp40s reveals that none of the proteins have a conserved HPD motif (Figure 3.1). Prediction of protein interaction partners showed that PFF1010c interacts with proteins that are uncharacterized putative proteins (Table 3.1). Some of these interactors are proteins that through sequence feature predictions, have proposed functions. This includes proteins involved in methylating lysine residues in histones, coordinating cell division machinery as well as transport proteins (Dhara and Sinai, 2016; Saier, 2003). In a previous study by Mutavhatsindi (2016), PFF1010c was found to be expressed during the early and late gametocyte stages of the parasite development. The proteins expression at the gametocyte together with the predicted interactors suggest that PFF1010c works together with its interactors to assist in and coordinate gametocyte development.

In characterizing the structure of PFF1010c, both bioinformatics and biophysical techniques were employed. The HPD/SVN motif switch was introduced into the study in order to functionally characterize the SVN motif and evaluate whether it has the

same function as the HPD motif when introduced into PfHsp40. Furthermore, to also evaluate if the HPD motif retained its function in a non-canonical Hsp40 such as PFF1010c. Having introduced the motif switch, the effect on protein structure also had to be evaluated. Superimposing the wildtype proteins with the mutants is a way of comparing function similarity based on protein structure (Tian *et al*, 2018). If the mutant proteins retained structural similarities, then even function similarities would be retained. This was done comparing wildtype PFF1010c with PFF1010c-HPD and wildtype PfHsp40 with PfHsp40-SVN. The 3D protein structures obtained from Phyre2 were superimposed on Superpose. Superimposing the proteins revealed that the HPD/SVN motif switch introduces major structural changes on both PFF1010c-HPD (Figure 3.2) and PfHsp40-SVN (Figure 3.3). Knowing structure directly impacts on function, together with the HPD/SVN motif switch, it is expected that protein function will certainly be altered. The HPD motif in Hsp40s plays a critical role in regulating the ATPase activity of Hsp70 and mutations in this motif blocks this ability (Fan *et al*, 2003). Thus, it would be expected that this is a function that will be lost for PfHsp40-SVN and gained by PFF1010c-HPD. The Kyte and Doolittle hydrophobic profile analysis of PFF1010c and PFF1010c-HPD suggests that the motif switch makes PFF1010c-HPD slightly less hydrophobic (Figure 3.4). PfHsp40-SVN is predicted to be more hydrophobic than PfHsp40 (Figure 3.4).

In a previous study by Mutavhatsindi (2016), recombinant PFF1010c was successfully expressed in *E. coli* JM109 and *E. coli* BL21 Star, however, attempts to purify the recombinant protein were unsuccessful. In the current study, recombinant PFF1010c was successfully expressed in *E. coli* XL1 Blue. Western blot analysis of PFF1010c expression as confirmed using  $\alpha$ -PFF1010c antibody reveals a protein band of approximately 17 kDa that does not appear when  $\alpha$ -His antibody is used (Figure 3.8). With  $\alpha$ -PFF1010c being a PFF1010c specific antibody, this suggests that the protein band is a C-terminus truncated version (breakdown product) of PFF1010c. This truncated PFF1010c is also the protein band seen co-eluted with the full size PFF1010c in the purification. Purification of the protein was problematic under native conditions and the denaturant urea was then employed to purify the protein. Most of the protein appeared to precipitate into the insoluble fraction and thus the protein was successfully purified from the insoluble fraction (Figure 3.8). PFF1010c does however bind poorly to the purification beads even after long incubation periods, hence a lot of



the protein is washed off in the flow through. PFF1010c-HPD (Figure 3.9), PfHsp40 (Figure 3.10) and PfHsp40-SVN (Figure 3.11) were successfully expressed and purified from the soluble fraction under denaturing conditions. PfHsp70-1 was successfully expressed and purified under native conditions. The recombinant protein was then used in biophysical assays to study the structural characteristics of the protein and in interaction studies.

ANS fluorescence was used to probe for conformational changes that may have arisen from the motif switch (Schonbrunn *et al*, 2000). ANS fluorescence increases drastically when exposure to water is lessened, therefore, the more hydrophobic patches a protein has, the more intense the fluorescence emission (Hawe *et al*, 2008). When proteins transition from unfolded to fully or partially folded, the fluorescence also increases (Hawe *et al*, 2008). The mutant protein PFF1010c-HPD exhibited a slight red shift from the wildtype protein, PFF1010c in the presence of ANS (Figure 3.13). The red shift observed represents a decrease in hydrophobicity in the mutant protein. Under denaturing conditions, all the proteins, except PFF1010c, gradually unfolded (red shift) when subjected to increasing concentrations of urea (Figure 3.14). Similarly, all the proteins, including PFF1010c, gradually unfolded when subjected to increasing concentrations of guanidine hydrochloride. PFF1010c aggregated (blue shifted) when exposed to urea. Urea is a chaotropic denaturant that unravels the tertiary structure of proteins through the destabilization of internal, non-covalent bonds between atoms (Zou *et al*, 1998). But some proteins tend to aggregate due to the formation of disulfide bonds between sulfhydryl groups made by the unfolding of proteins or through hydrophobic surface amino acids that interact as in the case of PFF1010c (Ahmed and Saunders, 2012; Lan *et al*, 2020). PfHsp40-SVN was found to be a less stable protein than PfHsp40. While PFF1010c-HPD was found to be more stable than PFF1010c, suggesting that the HPD motif conferred stability to the mutant protein while the SVN motif reduced the protein stability of PfHsp40-SVN. Therefore, the increased stability would confer improved function for PFF1010c-HPD and the reduced stability of PfHsp40-SVN would have impaired its function.

The thermotolerance of a cell is accompanied by a temporary increase in the expression of heat shock proteins that protect against heat. Hsp40 has been found to work in partnership with Hsp70 to protect luciferase from heat induced aggregation *in vitro* (Michels *et al*, 1997). For Hsp40 to maintain such function, some structural

integrity has to be maintained and as such the structure of PfHsp40 should remain stable under increasing temperatures. To investigate the thermostability of PFF1010c and the effect of the HPD/SVN motif switch on protein thermostability, proteins were subjected to increasing temperatures and the tertiary structure monitored using tyrosine fluorescence (Figure 3.15). Wildtype PfHsp40 and mutant PFF1010c-HPD were more stable than when subject to increasing temperatures as compared to wildtype PFF1010c and mutant PfHsp40-SVN. The HPD motif appears to contribute towards the thermostability of a protein. PfHsp40s thermotolerance is required as it is a protein that functions even during febrile conditions where temperatures can reach 41°C (Marinkovic *et al*, 2008). Gametocytes appear 8-10 days after the first fever, where the fever that develops is lower during gametocytemia than during parasitemia (McKenzie *et al*, 2007). Therefore, PFF1010c would never have the need to withstand high temperatures. Furthermore, gametocytes are transmitted to the Anopheles mosquito where a drop in temperature and rise in pH stimulates gametocyte differentiation into gametes (Bousema and Drakeley, 2011).

Next, the interaction of PFF1010c with PfHsp70-1 and the effect of the HPD/SVN motif switch on interaction with PfHsp70-1 was investigated. In a previous study by Mutavhatsindi (2016), PfHsp70-1 was found to be expressed in both early and late-stage gametocytes, making an interaction between PfHsp70-1 and PFF1010c possible. The ATPase activity of PfHsp70-1 was enhanced with addition of PfHsp40 as reported in previous studies (Lebepe *et al*, 2020). PFF1010c-HPD reduces the efficiency with which PfHsp70-1 hydrolyzes ATP as more substrate is required to reach the maximum velocity ( $V_{max}$ ). One possible explanation would be that PFF1010c-HPD has another PfHsp70-1 binding/interacting domain besides the HPD motif, and that this domain may bring about allosteric regulation of PfHsp70-1 that interferes with efficient ATP hydrolysis. Chakafana *et al* (2019) postulated the possibility of co-chaperone binding with PfHsp70-1 through the GGMP repeat motifs. The GGMP repeat motifs of PfHsp70-1 have been shown to have an essential role in the chaperone function of the protein (Makumire *et al*, 2021). Apicomplexa parasites possess type IV Hsp40s (Hsp40 proteins with J-like domain with variations in the HPD motif) and six GGMP repeats (Morahan *et al*, 2011; Makumire *et al*, 2021). In this study the postulation is that the GGMP repeats may allow binding of non-canonical/type IV

Hsp40s. The proteins with the SVN motif, PFF1010c and PfHsp40-SVN appear to reduce ATP hydrolysis by PfHsp70-1.

PFF1010c having a binding affinity in the absence of nucleotides (Table 3.3), that is comparable to that of PfHsp40 reinforces the idea that PfHsp70-1 may have a binding domain that accommodates interaction with non-canonical Hsp40s. Introduction of the HPD/SVN motif switch to PFF1010c and PfHsp40 resulted in changes in the binding affinities of the mutant proteins, where PFF1010c-HPD exhibited slightly enhanced binding affinity to PfHsp70-1 and PfHsp40-SVN showed diminished binding affinity. PFF1010c-HPD binds better to PfHsp70-1 in its opened conformation (ATP bound) than the closed conformation (ADP bound) but binds best in the absence of nucleotide. The lower binding affinity of PfHsp40-SVN come with having lost its ability to stimulate the ATPase activity of PfHsp70-1.

In a study by Singh et al (2013), a series of 4-aminoquinoline-pyrimidine hybrids were reported as having antimalarial activity in the nanomolar range in a *in vitro* antimalarial activity assay. In the current study, with PfHsp70-1 being the target protein, the quinoline-pyrimidine hybrids screened were observed as have binding affinities ( $K_D$ ) mostly in the nanomolar range in the absence PfHsp40 except for PQH2 (Table 3.4). To reach a  $K_D$  value in the picomolar range, 10-hour incubation would be required (Jarmoskaite *et al*, 2020). Since compounds were passed through PfHsp70-1 for an average of 4 minutes (240 sec), a  $K_D$  reading above the nanomolar range would be inaccurate. In the presence of PfHsp40, PQH3 was observed as having the weakest binding affinity to PfHsp70-1 while the other compounds maintained binding affinities in the nanomolar range. The reduced binding affinity of PQH3 would imply that this is the least effective compound for blocking PfHsp70-1 PfHsp40 interaction. Compound PQH1 and PQH4 were not affected by PfHsp40 as their affinity for PfHsp70-1 binding remains the same.

### **Conclusions and future perspectives**

PFF1010c is a type IV Hsp40 expressed during the gametocyte stage that through string analysis is thought to be involved in the development and maturation processes of the gametocytes. PFF1010c does not observe the same thermostability as PfHsp40, but this may be a non-essential function for a protein that ultimately gets transmitted into the mosquito which is a cold-blooded insect. Also, PFF1010c is a

protein that rather aggregates when exposed to urea instead of unfolding, a phenomenon of great advantage in the purification process of the recombinant protein. Through the ATPase assay and SPR analysis, PFF1010c was found to interact with PfHsp70-1. Although this interaction would occur in a non-conventional way as with canonical Hsp40s because PFF1010c lacks the HPD motif. PfHsp70-1 and PFF1010c could therefore be a druggable complex that can be targeted for blocking the transmission of malaria from humans to mosquitoes. The possibility is that PFF1010c interacts with PfHsp70-1 on its GGMP repeats motif. But to ascertain how exactly this interaction takes place and at which protein domain, further SPR analysis is needed with the SBD, NBD and PfHsp70- $\Delta$ G (a PfHsp70-1 mutant that does not have the GGMP repeats motif).

Screening of the quinoline-pyrimidine hybrid compounds opened the door to the next step in the fight against *P. falciparum* drug resistance in re-designing known antimalarial drugs. These drugs would not only inhibit PfHsp70-1 protein folding but also protein trafficking. Compounds PQH and PQH4 were found to exhibit high binding affinity for PfHsp70-1 and inhibiting PfHsp40 interaction with PfHsp70-1. Further screening and evaluation of compounds PQH1 and PQH4 can be done with a protein refolding assay, this will show if the compounds are effective in blocking the chaperone activity of PfHsp70-1. Furthermore, a cell viability assay can be conducted to assess if the compounds have an effect on cell proliferation or if they can show direct cytotoxic effects.

## References

- Alano, P. 2007. *Plasmodium falciparum* gametocytes still many secrets of a hidden life, *Molecular Microbiology*, 66(2), 291-302
- Acharya, P., Kumar, R. and Tatu, U. 2009. Chaperoning a cellular upheaval in malaria: Heat shock proteins in *Plasmodium falciparum*, *Molecular & Biochemical Parasitology*, 153, 85-94
- Achilonu, I., Siganunu, T.P. and Dirr, H.W. 2014. Purification and characterisation of recombinant human eukaryotic elongation factor 1 gamma. *Protein Expression and Purification Journal*, 99, 70-77
- Ahmed, U. and Saunders, G. 2012. Progressive denaturation of globular proteins in urea, *Agilent technologies Inc*, 1-2
- Anderson, K.L., Leksa, N.C. and Schwartz, T.U. 2013 Optimized E. coli expression strain LOBSTR eliminates common contaminants from His-tag purification, *Proteins: Structure, Function, and Bioinformatics*, 81(11), 1857-1861
- Ashley, E.A. and Phyto, A.P. 2018. Drugs in development for malaria, *Drugs*, 78, 861-879
- Altieri D.C., Stein G.S., Lian J.B. and Languino L.R. 2012. TRAP-1, the mitochondrial Hsp90, *Molecular Cell Research*, 1823 (3), 767-773
- Aurrecochea, C., Brestelli, J., Brunk, B.P., Dommer, J., Fische, r S. and Gajria, B. 2009. PlasmoDB: a functional genomic database for malaria parasites, *Nucleic Acids Research*, 37, 539-543
- Baker, D.A. (2010) Malaria gametocytogenesis, *Molecular and Biochemical Parasitology*, 172(2), 57-65
- Baneyx, F. (2008) Molecular chaperones, viewed 08 March 2017 from <https://faculty.washington.edu/baneyx/Chaperones/Chaperones.html>
- Banumathy, G., Singh, V., Pavithra, S.R. and Tatu, U. 2003. Heat shock protein 90 function is essential for *Plasmodium falciparum* growth in human erythrocytes, *The Journal of Biological Chemistry*, 278(20), 18336-18345
- Begeman, A., Son, A., Litberg, T.J., Wroblewski, T.H., Gehring, T., Cabral, V.H., Bourne, J., Xuan, Z. and Horowitz, S. 2020. G-Quadruplexes act as sequence-dependent protein chaperones, *EMBO reports*, 21. 1-15
- Biebl, M.M. and Buchner, J. 2019. Structure, function and regulation of the Hsp90 machinery, *Cold Spring Harbor Perspectives in Biology*, 11, 1-33
- Bienkowska, J. 2005. Computational characterization of proteins, *Expert Review of Proteomics*, 2(1), 129-138
- Bloiland, P.B. 2001. Drug resistance in malaria, WHO, Geneva, Chapter 1.
- Botha, M., Pesce, E.R. and Blatch, G.L. 2007. The Hsp40 proteins of *Plasmodium falciparum* and other apicomplexa: Regulating chaperone power in the parasite and the host, *The International Journal of Biochemistry and Cell Biology*, 39, 1781-1803

- Botha, M., Chiang, A.N., Needham, P.G., Stevens, L.L. and Hoppe, H.C. 2010 *Plasmodium falciparum* encodes a single cytosolic type I Hsp40 that functionally interacts with Hsp70 and is upregulated by heat shock, *Cell Stress and Chaperones*, 16, 389-411
- Bosdriesz, E., Wortel, M.T., Haanstra, J.R., Wagner, M.J., de la Torre Cortes, P. and Teusink, B. 2017. Low affinity membrane transport can increase net substrate uptake rate by reducing efflux, *BioRxiv*, 1-27
- Bousema, T. and Drakeley, C. 2011. Epidemiology and infectivity of *Plasmodium falciparum* and *Plasmodium vivax* gametocytes in relation to malaria control and elimination, *Clinical Microbiology Reviews*, 24(2), 377-410
- Carra, S., Alberti, S., Arrigo, P.A., Benesch, J.L. and Benjamin, I.J. 2017. The growing world of small heat shock proteins: from structure to functions, *Cell Stress and Chaperones*, 20, 601-611
- CDC. 2013. Treatment of malaria, 22 February 2017. [Online]. Available at: <http://www.cdc.gov/malaria/treatmentguidelines>
- Chakafana, G., Zininga, T. and Shonhai, A. 2019. Comparative structure-function features of Hsp70s of *Plasmodium falciparum* and human origins, *Biophysical Reviews*, 11, 591-602
- Chang, C.C.H., Li C., Webb, G.I., Tey, B.T., Song, J. and Ramanan, R.N. 2016. Periscope: quantitative prediction of soluble protein expression in the periplasm of *Escherichia coli*, *Scientific Reports*, 6921844), 1-11
- Charnaud, S.C., Dixon, M.W.A., Nie, C.Q., Chappell, L., Sanders, P.R., Nebl, T., Hanssen, E., Berriman, M., Chan, J., Blanch, A.J., Beeson, J.G., Rayner, J.C., Przyborski, J.M., Tilley, L., Crabb, B.S. and Gilson, P.R. 2017. The exported chaperone Hsp7-x supports virulence functions for *Plasmodium falciparum* blood stage parasites, *Plos one*, 12(7), 1-22
- Chiang, A.N., Valderramos, J.C., Balachandran, R., Chovatiya, R.J., Mead, B.P., Schneider, C., Bell, S.L., Klein, M.G., Huryn, D.M., Chen, X.S., Day, B.W., Fidock, D.A., Wipf P. and Brodsky J.L. (2009) Select pyrimidinones inhibit the propagation of the malarial parasite *Plasmodium falciparum*. *Bioorganic and Medicinal Chemistry*, 17,1527–1533
- Chen, H., Chang, J.T., Chien, K., Lee, Y., You, G. and Cheng, A. 2018. The endogenous Grp78 interactome in human head and neck cancers: a deterministic role of cell surface Grp78 in cancer stemness, *Scientific Reports*, 8(536), 1-13
- Chisholm, S.A., Kalanon, M., Nebl, T., Sanders, P.R., Matthews, K.M., Dickerman, B.K., Gilson, P.R. and de Koning-Ward, T. 2018. The malaria PTEX component PTEX88 interacts most closely with HSP101 at the host–parasite interface, *The FEBS Journal*, 285, 2037-2056
- Chou, A.C. and Fitch, C.D. 1992. Heme polymerase: modulation by chloroquine treatment of a rodent malaria, *Life Science*, 51(26), 2073-2080
- Cohen, S.N., Chang, A.C. and Hsu, L. 1972. Non-chromosomal antibiotic resistance in bacteria: genetic transformation of *Escherichia coli* by R-factor DNA. Proc., *National Academy of Sciences*, 69, 2110-2114

- Cortez, M.H. and Weitz, J.S. (2013) Distinguishing between indirect and direct modes of transmission using epidemiological time series, *The American Naturalist*, 181 (2)
- Cui, L. and SU, X. 2009. Discovery, mechanism of actions and combination therapy of artemisinin, *Expert Review Anti-Infective Therapy*, 7(8), 999-1013
- Dahlstrom, S., Veiga, M.I., Ferreira, P., Martensson, A., kaneko, A., Andersson, B., Bjorkman, A. Gil J.P. 2008. Diversity of the sarco/endoplasmic reticulum Ca<sup>2+</sup>-ATPase orthologue of *Plasmodium falciparum*, *Infection, Genetics and Evolution*, 8(3), 340-345
- Damodharan, L. and Pattabhi, V. (2004) Hydropathy analysis to correlate structure and functions of proteins, *Biochemical and Biophysical Research Communications*, 323, 996-1002
- Daniyan, M.O., Boshoff, A., Prinsloo, E., Pesce, E. and Blatch, G.L. 2016. The malarial exported PFA0660w is an Hsp40 co-chaperone of PfHsp70-x, *PLoS one*, 11(2), 1-13
- Daniyan, M.O., Przyborski, J.M. and Shonhai, A. 2019. Partners in mischief: functional networks of heat shock proteins of *Plasmodium falciparum* and their influence on parasite virulence, *Biomolecules*, 9(295), 1-17
- de Jong, R., Tebeja, S.K., Meerstein-Kessel, L., Tadesse, F.G., Jore, M.M., Stone, W. and Bousema, T. 2020. Immunity against sexual stage *Plasmodium falciparum* and *Plasmodium vivax* parasites, *Immunological Reviews*, 293, 190-215
- Delves, M.J., Ruecker, A., Straschil, U., Lelièvre, J., Marques, S., López-Barragán, M.J., Herreros, E. and Sinden, R.E. 2013. Male and female *Plasmodium falciparum* mature gametocytes show different responses to antimalarial drugs, *Antimicrobial Agents and Chemotherapy*, 57(7), 1-7
- De Marco, A. 2009. Strategies for successful recombinant expression of disulphide bond-dependent proteins in *Escherichia coli*, *Microbial cell factories*, 8(26), 1-18
- Dhara, A. and Sinai, A.P. 2016. A cell cycle-regulated *Toxoplasma* deubiquitinase, TgOTUD3A, targets polyubiquitins with specific lysine linkages, *mSphere*, 1(3), 1-21
- Dixon, M.W.A., Dearnley, M.K., Hanssen, E., Gillberger, T. and Tilley, L. 2012 Shape-shifting gametocytes: how and why *P. falciparum* go banana shaped, *Trends in Parasitology*, 28(11), 471-478
- D'Urzo, N., Martinelli, M., Nenci, C., Brettoni, C, Telford, J.L. and Maione, D. 2013. High SP3 under the control of xylose inducible promoter, *Microbial Cell Factories*, 12 (12), 1-11
- Edkins, A.L. and Boshoff, A. 2014. General structural and functional features of molecular chaperones, A, Shonhai and G.L. Blatch (eds), *Heat Shock Proteins of Malaria*, Chapter 2, Springer, New York
- El Bakkouri, M., Pow, A., Mulichak, A., Cheung, K.L., Artz, J.D., Amani M. et al 2010. The Clp chaperones and proteases of the human malaria parasite *Plasmodium falciparum*. *J Mol Biol*, 404(3), 456–477
- Enslin, M. 2015. Malaria: An overview, *Lancet Laboratories*, 1-4

- Fakruddin, M.D., Mazumdar, R.M., Mannan, K.S.B., Chowdhury, A. and Hossain, M. N. 2012. Critical factors affecting the success of cloning, expression, and mass production of enzymes by recombinant *E. coli*, *ISRN Biotechnology*, 1-8
- Fan, C., Lee, S. and Cyr, D.M. 2003. Mechanisms for regulation of Hsp70 function by Hsp40, *Cell Stress and Chaperones*, 8(4), 309-316
- Flick, K., Ahuja, S., Chene, Arnaud., Bejarano, M.T. and Chen, Q. 2004. Optimized expression of *Plasmodium Falciparum* erythrocyte membrane protein 1 domains in *Escherichia coli*, *Malaria Journal*, 3(50), 1-8
- Gardiner, D.L. and Trenholme, K.R. 2015. *Plasmodium falciparum* gametocytes: playing hide and seek, *Annals of Translational Medicine*, 3(4), 1-3
- Gitau, G.W., Mandal, P., Batch, G.L., Przyborski, J. and Shonhai, A. 2012. Characterization of the *Plasmodium falciparum* Hsp70-Hsp90 organising protein, *Malaria Journal*, 9(2), 1-11
- Gong, W., Hu, W., Xu, L., Wu, S., Zhang, H., Wang, J., Jones, G.W. and Perrett, S. 2018. The C-terminal GGAP motif of Hsp70 mediates substrate recognition and stress response in yeast, *The Journal of Biological Chemistry*, 293(46), 17663-17675
- Grover, M., Chaubey, S. and Tatu, U. 2014. Heat shock proteins as targets for novel anti-malarial drugs, A, Shonhai and G.L. Blatch (eds), *Heat Shock Proteins of Malaria*, Chapter 10, Springer, New York
- Hall, D. 2019. On the nature of the optimal form of the holdase-type chaperone stress response, *FEBS Letters*, 594(1), 43-66
- Hall, G.M. 1996. *Methods of testing protein functionality*, Springer Science and Business Media, USA, Chapter 2
- Hartl, U.F., Bracher, A. and Hayer-Hartl, M. 2011. Molecular chaperones in protein folding and proteostasis, *Nature*, 475, 324-332
- Hawe, A., Sutter, M. and Jiskoot, W. 2008. Extrinsic fluorescent dyes as tools for protein characterization, *Pharmaceutical Research*, 25(7), 1487-1499
- Henry, N.B., Serme, S.S., Siciliano, G., Sombie, S., Diarra, A., Sagnon, N., Traore, A.S., Sirima, S.B., Soulama, I. and Alano, P. 2019. Biology of *Plasmodium falciparum* gametocyte sex ratio and implications in malaria parasite transmission, *Malaria Journal*, 18(70), 1-8
- Ho, C., Beck, J.R., Lai, M., Cui, Y., Goldberg, D.E., Egea, P.F. and Hong Zhou, Z. 2018. Malaria parasite translocon structure and mechanism of effector export, *Nature*, 561(7721), 70-75
- Irene, A.A., Enekembe, M.A., Meriki, H.D., Fritz-Fonkeng, N. F. and Nkuo-akenji, T. The Effect of Malaria/HIV/TB Triple Infection on Malaria Parasitaemia, Haemoglobin Levels, CD4+ Cell and AcidFast Bacilli Counts in the South West Region of Cameroon, *Journal of infectious Pulmonary Diseases*, 2(1), 1-4
- Izui, K., Matsumura, H., Furumoto, T. and Kai, Y. 2003. Phosphoenolpyruvate carboxylase: a new era of structural biology, *Annual Review of Plant Biology*, 55(1), 69-84



- Jang, D., Chae, G. and Shin, S. 2015. Analysis of surface plasmon resonance with a novel sigmoid-asymmetric fitting algorithm, *Sensors*, 15, 25385-25398
- Jarmoskaite, I., AlSadhan, I., Vaidyanathan, P.P. and Herschlag, D. 2020. How to measure and evaluate binding affinities, *eLife*, 9, 1-34
- Jolly, C. and Morimoto, R.I. 2000. Role of the shock response and molecular chaperones in oncogenesis and cell death, *Journal of the National Cancer Institute*, 92(19), 1564-1572
- Kayamba, K., Malimabe, T., Ademola, I.K., Pooe O.J., Kushwaha, N.D., Mahlalela, M., van Zyl, R.L., Gordan, M., Mudau, P.T., Zininga, T., Shonhai, A. and Nyamori, V.O. 2021, Design and synthesis of quinoline-pyrimidine inspired hybrids as potential *Plasmodium* inhibitors, *European Journal of Medicinal Chemistry*, 217, 1-20
- Kelley, L.A., Mezulis, S., Yates, M.N. and Sternberg, M.J.E. 2015. The Phyre2 web portal for protein modelling, prediction and analysis, *Nature Protocol*, 10(6), 845-858
- Kiyk, R., Vogel, M., Schiecht, R., Bukau, B. and Mayer, M.P. 2015. Pathways of allosteric regulation in Hsp70 chaperone, *Nature Communications*, 6(1), 8308-8319
- Koppensteiner, W.A., Lackner, P., Weiderstein, M. and Sippl, M.J. 2000. Characterization of novel proteins based on known protein structures, *Journal of Molecular Biology*, 296, 1139-1152
- Kudyba, H.M., Cobb, D.W., Fierro, M.A., Florentin, A., Ljolje, D., Singh, B., Lucchi, N.W. and Muralidharan, V. 2019. The endoplasmic reticulum chaperone PfGRP170 is essential for asexual development and is linked to stress response in malaria parasites, *Cellular Microbiology*, 21(9), 1-18
- Kyte, J. and Doolittle, R.F. (1982) A simple method for displaying the hydrophobic character of a protein, *Journal of Molecular Biology*, 157, 105-132
- Lakowicz, J.R. 1983. Principle of fluorescence spectroscopy, Chapter 7, Plenum Press, New York
- Lakowicz, J.R. 2006. Principles of fluorescence spectroscopy, Chapter 7, Springer, Boston
- Lan, H., Liu, H., Ye, Y. and Yin, Z. (2020) The role of surface properties on protein aggregation behaviour in aqueous, *AAPS PharmSciTech*, 21(122), 1-13
- Lebepe, C.M., 2019, Comparative analysis of a chimeric Hsp70 of *E. coli* and *Plasmodium falciparum* origin relative to its wildtype forms, University of Venda, 1-77
- Lebepe, C.M., Matambanadzo, P.R., Makhoba X.H., Achilonu, I., Zininga, T. and Shonhai, A. 2020. Comparative characterisation of *Plasmodium falciparum* Hsp70-1 relative to *E. coli* DnaK reveals functional specificity of the parasite chaperone, *bioRxiv*, 1-30
- Lin-Cereghino, J., Wong, W.W., Xiong, S., Giang, W., Luong, L.T., Vu, J., Johnson, S.D. and Lin-Cereghino, G.P. 2005. Condensed protocol for competent cell preparation and transformation of the methylotrophic yeast *Pichia pastoris*, *BioTechniques*, 38(1), 44-48

- Liou, S. 2010. The heat shock response, 09 March 2017. [Online]. Available at: [http://web.stanford.edu/group/hopes/cgi-bin/hopes\\_test/the-heat-shock-reponse/](http://web.stanford.edu/group/hopes/cgi-bin/hopes_test/the-heat-shock-reponse/)
- Liu, K. and Houry, W.A. 2014. Chaperones and proteases of *Plasmodium falciparum*, A, Shonhai and G.L. Blatch (eds), *Heat Shock Proteins of Malaria*, Chapter 9, Springer, New York
- Mabate, B., Zininga, T., Ramatsui, L., Makumire, S., Achilonu, I., Dirr, H.W. and Shonhai, A. 2018. Structural and biochemical characterization of *Plasmodium falciparum* Hsp70-x reveals functional versatility of its c-terminal EEVN motif, *Proteins: Structure, Function, and Bioinformatics*, 1189-2001
- Makhnevych, T. and Houry, W.A. 2012. The role of Hsp90 in protein complex assembly, *Biochimica et Biophysica Acta*, 1823, 674-682
- Makhoba, X.H., Burger, A., Coertzen, D., Zininga, T., Birkholtz, L. and Shonhai, A. 2016. Use of chimeric Hsp70 to enhance the quality of recombinant *Plasmodium falciparum* S-Adenosylmethionine decarboxylase protein produced in *Escherichia coli*, *PLOS one*, 11(3), 1-21
- Makumire, S., Dongola, T.H., Chakafana, G., Tshikonwane, L., Chauke, C.T., Maharaj, T., Zininga, T. and Shonhai, A. 2021. Mutation of GGMP repeat segments of *Plasmodium falciparum* Hsp70-1 compromise chaperone function and Hop co-chaperone binding, *International Journal of Molecular Sciences*, 22 (2226), 1-22
- Mandal, A. (2013) Malaria symptoms, 22 February 2017. [Online]. Available at: <http://www.news-medical.net/health/Malaria-Symptoms.aspx>
- Marinkovic, M., Diez-Silva, M., Pantic, I., Fredberg, J.J., Suresh, S. and Butler, J.P. 2009. Febrile temperature leads to significant stiffening of *Plasmodium falciparum* parasitized erythrocytes, *American Journal of Physiology Cell Physiology*, 296, 59-64
- Matteelli, A. and Castelli, F. 2015. Life cycle of malaria parasites, Research Gate, Chapter 2
- Mayer, M.P. and Bukau, B. 2005. Hsp70 chaperones: Cellular functions and molecular mechanism, *Cellular and Molecular Life Sciences*, 62, 670-684
- Mbengue, A. Y. and Braun-Breton, C. 2012. Human erythrocyte remodelling during *Plasmodium falciparum* malaria parasite growth and egress, *British Journal of Hematology*, 157, 171-179
- McKenzie, F.E., Jeffery, G.M. and Collins, W.E. 2007. Gametocytemia and fever in human malaria infections, *Journal of Parasitology*, 93(3), 627-633
- Miao, J., Wang, Z., Liu, M., Parker, D., Li X., Chen, X. and Cui, L. 2013. *Plasmodium falciparum*: Generation of pure gametocyte culture by heparin treatment, *Exp Parasitol.*, 135(3), 1-12
- Michels, A.A., Kanon, B., Konings, A.W., Ohtsuka, K., Bensaude, O. and Kampinga, H.H. 1997. Hsp70 and Hsp40 chaperone activities in the cytoplasm and the nucleus of mammalian cells, *Journal of Biological Chemistry*, 272(52), 33283-33289
- Miyata, Y., Koren, J., Kiray, J., Dickey, C.A. and Gestwicki, J.E. 2011. Molecular chaperones and regulation of tau quality control: Strategies for drug discovery in tauopathies, *NIH Public Access, Future Med Chem*, 3(12), 1523-1537.

- Mogk, A., Kummer, E. and Bukau, B. 2015. Cooperation of Hsp70 and Hsp100 chaperone machines in protein disaggregation, *Frontiers in Molecular Biosciences*, 2(22), 1-11
- Morahan, B.J., Strobel, C., Hasan, U., Czesny, B., Mantel, P., Marti, M., Eski, S. and Williamson, K.C. 2011. Functional analysis of the exported type IV Hsp40 protein PfGECO in *Plasmodium falciparum* gametocytes, *Eukaryotic Cell*, 10, 1492-1503
- Morky, D.Z., Abrahao, J. and Ramos, C.H.I. 2015. Disaggregates, molecular chaperone that resolubilize protein aggregates, *Annal of the Brazilian Academy of Sciences*, 872(2), 1273-1292
- Mudeppa, D.G. and Rathod, P.K. 2013. Expression of functional *Plasmodium falciparum* enzymes using wheat germ cell-free system, *American Society for Microbiology*, 12(12), 1653-1663
- Munishkina, L.A. and Fink, A.L. 2007. Fluorescence as a method to reveal structures and membrane-interactions of amyloidogenic proteins, *Biochimica et Biophysica Acta*, 1768, 1862-1885
- Muregi, F.W. and Ishih, A. 2010. Next-generation antimalarial drugs: hybrid molecules as a new strategy in drug design, *Drug Development Research*, 71, 20-32
- Mutavhatsindi, H. 2016. Characterization of PFF1010c, a type IV *Plasmodium falciparum* heat shock protein 40, University of Venda, 1-107
- Neckers, L. and Tatu, U. 2008. Molecular chaperones in pathogen virulence: emerging new Targets for therapy, *NIH Public Access, Cell Host Microbe*, 4(6), 519-527
- Neha, D.W. and Priyanka, Y. 2017. Protein folding using fluorescence spectroscopy, *Imperial Journal of Interdisciplinary Research*, 3(2), 785-788
- Ngwa, C.J., Rosa, T.F. and Pradel, G. 2016. The biology of malaria, Rodriguez-Morales, A.J. (eds), *Current Topics in Malaria*, 117-144, IntechOpen, London
- Njunge, J.M., Ludewig, M.H., Boshoff, A., Pesce, E.R., Blatch, G.L. 2013. Hsp70s and J proteins of *Plasmodium* parasites infecting rodents and primates: Structure, function, clinical relevance, and drug targets. *Current Pharmaceutical Design*, 19, 387-403.
- Nqoro, X., Tobeka, N. and Aderibigbe, B.A. 2017. Quinoline-based hybrid compounds with antimalarial activity, *Molecules*, 22(12), 2268-2290
- Nyakundi, D.O., Vuko, L.A.M., Bentley S.J., Hoppe, H., Blatch, G.L. and Boshoff, A. 2016. *Plasmodium falciparum* Hep1 is required to prevent the self-aggregation of PfHsp70-3, *Plos one*, 11(6), 1-13
- Okello, D. and Kang, Y. 2019. Exploring antimalarial herbal plants across communities in Uganda based on electronic data, *Hindawi*, 2019, 1-27
- Pace, N.C., Trevino, S., Prabhakaran, E. and Scholtz, M.J. 2004. Protein structure, stability and solubility in water and other solvents, *The Royal Society*, 359, 1225-1235
- Park, C. and Seo, Y. 2015. Heat shock proteins: a review of the molecular chaperones for plant immunity, *The Plant Pathology Journal*, 31(4), 323-333

- Panda, A.K., Bisht, S.S., DeMondal, S., Kumar, N.S., Gurusubramanian, G., and Panigrahi, A.K. 2014. *Brevibacillus* as a biological tool: A short review, *Antonie van Leeuwenhoek*, 105, 623-639
- Patching, S.G. 2013. Surface plasmon resonance spectroscopy for characterization of membrane protein-ligand interaction and its potential for drug discovery, *Biochimica et Biophysica Acta*, 1834, 43-55
- Patterson, C. and Höhfeld, J. 2006. Molecular chaperones and the ubiquitin-proteasome system, *Protein degradation*, 2, 1-30
- Pesce, E., Cockburn, I.L., Goble, J. and Blatch, Malaria heat shock proteins: drug targets that chaperone other drug targets, *Infect Disord Drug Targets*, 10(3), 147-155
- Pesce, E., Maier A.G. and Blatch, G.L. 2014. Role of the Hsp40 family of proteins in the survival and pathogenesis of the malaria parasite, A, Shonhai and G.L. Blatch (eds), *Heat Shock Proteins of Malaria*, Chapter 5, Springer, New York
- Poe, O.J., Köllsch, G., Heine, H. and Shonhai, A. 2017. Plasmodium falciparum heat shock protein 70 lacks immune modulatory activity, *Protein and peptide letters*, 24, 503-510
- Portugaliza, H.P., Miyazaki, S., Geurten F.J.A., Pell, C. Rosanas-Urgell, A., Janse, C.J. and Cortes, A. 2020. Artemisinin exposure at the ring or trophozoite stage impacts Plasmodium falciparum sexual conversion differently, *Cell Biology, Microbiology, and Infectious Disease*, 1-22
- Pretorius, S.I., Breytenbach, W.J., de Kock, C., Smith P.J. and N'Da, D.D. 2012. Synthesis, characterization and antimalarial activity of quinoline-pyrimidine hybrids, *Bioorganic and Medicinal Chemistry*, 21, 269-277
- Przyborski, J.M., Miller, S.K., Pfahler, J. M., Henrich, P.P., Rohrbach, P., Crabb, B.S. and Lanzer, M. 2005. Trafficking of STREXOR to the Maurer's clefts in *Plasmodium falciparum*-infected erythrocytes, *The EMBO Journal*, 24, 2306-2317
- Przyborski J.M., Diehl M. and Blatch G.L. 2015. Plasmodial Hsp70s are functionally adapted to the malaria parasite life cycle, *Frontiers in Molecular Biosciences*, 2(34), 1-7
- Roth, T.L., Milenkovic, L. and Scott, M.P. 2014. Rapid and simple method for DNA engineering using cyclized ligation assembly, *Plos One*, 9(9), 1-9
- Rug, M. and Maier, A.G. .2011. The heat shock protein 40 family of the malaria parasite *Plasmodium falciparum*, *Critical Review*, 63(12), 1081-1086.
- Rug, M., Cyrklaff, M., Mikkonen, A., Lemgruber, L., and Kuelzer, S. 2014. Export of virulence proteins by malaria-infected erythrocytes involves remodeling of host actin cytoskeleton, *Blood*, 124(23), 3459-3468
- Rule C.S., Patrick M. and Sandkvist M. 2016. Measuring *in vitro* ATPase activity for enzymatic characterization, *Journal of Visualized Experiments*, 114, 1-5
- Saibil, H. 2013. Chaperone machines for protein folding, unfolding and disaggregation, *Macmillan Publishers Limited*, 14, 630-672

- Saier, M.H. 2003. Tracing pathways of transport of protein evolution, *Molecular Microbiology*, 48(5), 1145-1156
- Schirmer E.C., Glover J.R., Singer M.A. and Lindquist S. 1996. HSP100/Clp proteins: a common mechanism explains diverse functions, *Trends in Biochemical Sciences*, 21, 289-296
- Schmidt, J. and Vakonakis, I.2020. Structure of the substrate-binding domain of *Plasmodium falciparum* heat-shock protein 70-x, *Acta Crystallographica*, 76,495-500
- Schumacher, R. and Spinelli, E. 2012 Malaria in children, *a*, 4(1), 1-12
- Schonbrunn, E., Escheburg, S., Luger, K., Kabsch, W. and Amrhein, N. 2000. Structural basis for the interaction of the fluorescence probe 8-anilino-1naphthalene sulfonate (ANS) with the antibiotic target MurA, *PNAS*, 97(12), 6345-6349
- Scopes, R.K. 1995. The effect of temperature on enzymes used in diagnostics, *Clinica Chimica Acta*, 237, 17-23
- Shahinas, D. and Pillai, D.R. 2014. Role of Hsp90 in *Plasmodium falciparum* Malaria, A., Shonhai and G.L. Blatch (eds), Heat Shock Proteins of Malaria, Chapter 5, Springer, New York
- Shivanand, P. and Noopur, S. 2010. Recombinant DNA technology and genetic engineering: A safe and effective meaning for production valuable biologicals, *International Journal of Pharmaceuticals Sciences Review and Research*, 1(1), 14-20
- Shonhai, A., Boshoff, A. and Blatch, G.L. 2007. The structural and functional diversity of Hsp70 proteins from *Plasmodium falciparum*, *Protein Science*, 16(9), 1803-1818
- Shonhai, A. 2014. The role of Hsp70s in the Development and Pathogenicity of *Plasmodium* species, A, Shonhai and G.L. Blatch (eds), Heat Shock Proteins of Malaria, Chapter 3, Springer, New York
- Shonhai, A. 2010. *Plasmodial* heat shock proteins: targets for chemotherapy, *Immunology and Medical Microbiology*, 58, 61-74
- Siciliano, G. and Alano, P. 2015. Enlightening the malaria parasite life cycle: bioluminescent *Plasmodium* in fundamental and applied research, *Frontiers in Microbiology*, 6(391), 1-8
- Singh, K., Kaur, H., Chibale, K. and Balzarini, J. 2013. Synthesis of 4-aminoquinoline-pyrimidine hybrids as potent antimalarials and their mode of action studies, *European Journal of Medicinal Chemistry*, 66, 314-323
- Slater, A.F.G. 1993. Chloroquine: Mechanism of drug action and resistance in *Plasmodium falciparum*, *Pharmacology and therapeutics*, 57(2-3), 203-235
- Sojourner, S.J., Graham, W.M., Whitmore, A.M. Miles, J.S., Freeny, D. and Flores-Rozas, H. 2018. The role of Hsp40 conserved motifs in the response to cytotoxic stress, *Journal of Natural Science*, 4(4), 1-19
- Spjeldnaes, A.O., Kitua, A.Y. and Blomberg, B. 2014. Education and knowledge helps combating malaria, but not degedege: a cross-sectioned study in Rufiji, Tanzania, *Malaria Journal*, 13(200), 1-20

Soulard, V., Bosson-Vanga, H., Lorthiois, A., Roucher, C., Franetich, J., Zanghi, G. 2015. Plasmodium falciparum full life cycle and Plasmodium ovale liver stages in humanized mice, *Nature Communications*, 1-9

Sousa, R. (2014). Structural mechanisms of chaperone mediated protein disaggregation, *Frontiers in Molecular Biosciences*, 1(12), 1-18

Srinivas. 2015. Malaria Parasites, 09 March 2019. [Online]. Available at: <http://www.malariasite.com/author/srinivas/page/5/>

Srinivas. 2015. Severe malaria, 15 March 2019. [Online] Available at: <http://www.malariasite.com/severe-malaria/> Prodromou, C, Roe, S.M., O'Brien, R., Ladbury, J.E., Piper, P.W. and Pearl, L.H. 1997, Identification and structural characterization of the ATP/ADP- binding site in the Hsp90 molecular chaperone, *Cell*, 90, 65-75

Szklarczyk, D., Franceschini, A., Wyder, S., Forslund, K. and Heller, D. 2014. STRING v10: protein-protein interaction networks, integrated over the tree of life, *Nucleic Acids Research*, 45, 447-452

Taldone, T., Kang, Y., Patel, H.J., Patel, M.R., Patel, P.D., Rodina, A., Patel, Y., Gozman, A., Maharaj, R., Clement, C.C., Lu, A., Young, J.C. and Chiosis, G. 2014. Heat shock protein 70 inhibitors. 2,2,5'-Thiodiprimidines, 5-(Phenylthio)pyrimidines, 2-(Pyridin-3-ylthio)pyrimidines, and 3-(Phenylthio)pyridines as reversible binders to an allosteric site on heat shock protein 70, *Journal of Medicinal Chemistry*, 57(4), 1208-1224

Talman, A.M., Domarle, O., McKenzie, F.E., Ariey, F. and Robert, V. 2004. Gametocytogenesis: the puberty of *Plasmodium falciparum*, *Malaria Journal*, 3(24), 1-14

Tian, K., Zhao, X., Zhang, Y. and Yau, S. 2018. Comparing protein structures and inferring functions with a novel three-dimensional Yau-Hausdorff method, *Journal of Biomolecular and Dynamics*, 1-10

Tibúrcio, M., Sauerwein, R., Lavazec, C. and Alano, P. 2015. Erythrocyte remodelling by *Plasmodium falciparum* gametocytes in the human host interplay, *Trends in Parasitology*, 31(6), 270-278

Tilley, L., Straimer, J., Gnädig, N.F., Ralph, S.A. and Fidock, D.A. 2016. Artemisinin action and resistance in *Plasmodium falciparum*, *Trends Parasitol*, 32(9), 682-696

Tonkin, C.J., van Dooren, G.G., Spurck, T.P., Struck, N.S., Good, R.T., Handman, E., Cowman, A.F. and McFadden, G.I. 2004. Localization of organellar proteins in *Plasmodium falciparum* using a novel set of transfection vectors and a new immunofluorescence fixation method, *Molecular and Biochemical Parasitology*, 137,13-21

Trevino, S.R., Scholtz, M.J. and Pace, N.C. 2006. Amino acid contribution to protein solubility: Asp, Glu, and Ser contribute more favorably than the other hydrophilic amino acids in RNase, *Journal of Molecular Biology*, 366(2), 449-460

Tse E.G., Korsik M. and Todd M.H. 2019. The past, present and future of anti-malarial medicines, *Malaria Journal*, 18(93), 1-21

- Vaughn, A.M. and Kappe S.H.I. 2017. Malaria parasite liver infection and exoerythrocyte biology, *Cold Spring Harbor Perspectives in Medicine*, 7, 1-21
- Vieira, W.A, and Coetzer, T. 2016. Localization and interactions of *Plasmodium falciparum* SWIB/MDM2 homologues, *Malaria Journal*, 15(32), 1-16
- Watermeyer, J.M., Hale, V.L., Hackett, F., Clare, D.K., Cutts, E.E., Vakonakis, I., Fleck, R.A., Blackman, M.J. and Saibil, H.R. 2015. A spiral scaffold underlies cytoadherent knobs *plasmodium falciparum*-infected erythrocytes, *American Society of Hematology*, 1-35
- Wellems, T.E. and Plowe, C.V. 2001, Chloroquine-resistant malaria, *The Journal of Infectious Diseases*, 184, 770-776
- Westra, D.F., Welling, G.W., Koedijk, D.G.A.M., Scheffer, A.J., The, T.H. and Welling-Wester, S. 2001. Immobilised metal-ion affinity chromatography purification of histidine-tagged recombinant proteins: a wash step with a low concentration of EDTA, *Journal of Chromatography B*, 760, 129-136
- WHO. 2008. World malaria report,
- WHO. 2015. Guidelines for the treatment of malaria, 3<sup>rd</sup> ed, Geneva, Chapter 11
- WHO. 2016. Giemsa staining of malaria blood films: Malaria microscopy standard operating procedure, Version 1
- WHO. 2016. Malaria, 20 February 2018. [Online]. Available at: <http://www.who.int/mediacentre/factsheets/fs094/en/>
- WHO. 2017. Global infectious disease surveillance, 14 January 2021. [Online] Available at: <http://www.who.int/mediacentre/factsheets/fs200/en/>
- WHO. 2017. Malaria, 22 April 2018. [Online] Available at: <http://www.who.int/mediacentre/factsheets/fs094/en/>
- WHO. 2019. World malaria report
- Willcox, M.L. and Bodeker, G. 2004. Traditional herbal medicines for malaria, *BMJ*, 529, 1156-1159
- Wiser, M.F. 2011. Plasmodium species infecting humans, 03 March 2018. [Online]. Available at: [http://www.tulane.edu/~wiser/protozoology/notes/pl\\_sp.html](http://www.tulane.edu/~wiser/protozoology/notes/pl_sp.html)
- Yang, Y., Liu, B., Dai, J., Srivastava, P.K., Zammit, D.J., Lefrancois, L. and Li. Z. 2007. Heat shock protein gp96 is a master chaperone for Toll-like receptors and is important in the innate function of macrophages, *Immunity*, 26, 215-226
- Yeates, T.O. 2002. Structure of the SET domain proteins: protein lysine methyltransferases make their mark. *Cell*, 111(1), 5-7
- Yeo, S., Liu, D. and Park, H. 2015. Potential interaction of *Plasmodium falciparum* Hsp60 and calpain, *Korean Journal of Parasitology*, 53(6), 665-673
- Zininga T. and Shonhai A. 2014. Are heat shock proteins druggable candidates?, *American Journal of Biochemistry and Biotechnology*, 10(4), 209-210

Zininga, T., Achilonu, I., Hoppe, H., Prinsloo, E., Dirr, H.W. and Shonhai, A. 2015. Overexpression, purification and characterization of the *Plasmodium falciparum* Hsp70-z (Pfhsp70-z) protein, *PLOS one*, 10(6), 1-13

Zininga, T., Makumire, S., Gitau, G.W., Njunge, J.M. and Pooe, O.J. 2015. *Plasmodium falciparum* Hop (PfHop) interacts with the Hsp70 chaperone in a nucleotide-dependent fashion and exhibits ligand selectivity, *PLOS one*, 10(8),1-15

Zininga T., Achilonu I., Hoppe H.C., Prinsloo E., Dirr H. and Shonhai A. 2016. *Plasmodium falciparum* Hsp70-z, an Hsp110 homologue, exhibits independent chaperone activity and interacts with Hsp70-1 in a nucleotide-dependent fashion, *Cell Stress and Chaperones*, 21(3), 1-16

Zou, Q., Habermann-Rottinghaus, S.M. and Murphy K.P. 1998. Urea effects on protein stability: Hydrogen bonding and the hydrophobic effect, *Proteins: Structure Function and Bioinformatics*, 31(2), 107-115



## Appendix A

### A1. Preparation of competent *E. coli* JM109 and *E. coli* XL1 Blue cells

Competent cells had to be prepared, in order to transform *E. coli* JM109 cells and XL1 Blue with pQE30 plasmids containing the gene of interest (PfHsp70-1, PfHsp40, PfHsp40-SVN, PFF1010c, PFF1010c-HPD). A colony of *E. coli* cells was inoculated in 5ml 2x YT broth (1.6 g tryptone, 1.0 g yeast, 1.5 g agar, 0.5 g NaCl per 100 ml preparation in distilled water) broth and grown overnight with shaking at 37 °C. The overnight culture was diluted 1:10 into 50 ml YT broth and thereafter grown with shaking for 2-3 hours and the optical density (of 0.3-0.6) was measured at 600 nm. The cells were harvested by centrifuging at 5000 xg for 10 minutes at 4 °C. The cells were kept on ice from this point onwards. The cells were resuspended in 10 ml 0.1 M MgCl<sub>2</sub> and left on ice for 30 minutes. The suspension was centrifuged for 10 minutes at 4000 xg at 4 °C. The cells were pelleted as before and gently resuspended in 10 ml ice cold 0.1 M CaCl<sub>2</sub> and then followed by incubation on ice for 4 hours. Centrifugation was carried out at 4000 xg at 4 °C for 10 minutes. The competent cells were aliquoted by adding 2 ml of sterile 30% glycerol and an equal volume of 0.1 M CaCl<sub>2</sub>. The competent cells were left to sit for 10 minutes. Thereafter 200 µl aliquots were added into Eppendorf tubes and stored at -80 °C.

### A2. Transformation of competent cells

A volume of 2 µl of plasmid DNA was added into an aliquot of 100 µl of competent cell. The cells were then incubated on ice for 30 minutes followed by heat shocking at 42°C for 45 seconds and immediately placed on ice for 10 minutes. Volume of 900 µl of 2x YT broth was added and then incubated at 37°C for 1 hour. Then 100 µl of the cells (diluted cell solution), were transferred onto the 2x YT plate containing the desired antibiotics ampicillin (100 µg/ml). The remaining cells were centrifuged at 15000 rpm for 2 minutes in a microcentrifuge. Thereafter, 800 µl of the supernatant was discarded and the pellet was resuspended by vortexing the cells. The remaining cells, concentrated cell solution, were transferred on 2x YT plates containing the desired antibiotics, ampicillin (100 µl/ml). The control plates contained cells with no plasmid DNA. Plates were incubated at 37°C overnight

### A3. Plasmid DNA extraction

The pQE30 plasmid DNA was extracted from JM109 *E. coli* cells that had been inoculated into YT media the night before for overnight growth. This was done using the GeneJET Plasmid Miniprep Kit from Thermo Scientific following the manufacturer's instructions

### A4. Restriction digest of plasmid DNA

Restriction endonucleases are enzymes that cut specific sequences on double stranded DNA to yield fragments of that particular DNA. The DNA cutting process is also referred to as DNA digestion (Weaver, 2012). When the plasmid is treated with restriction enzymes, a specific number of DNA is produced (Boyer, 2012). In order to confirm the integrity of the plasmid constructs (pQE30/PFF1010c, pQE30/PFF1010c-HPD, pQE30/PfHs40, pQE30/PfHsp40-SVN and pQE30/PfHsp70-1), fast digest restriction enzymes *Bam*HI, *Hind*III, *Kpn*I and *Pst*I were used. Four reactions in total were ran (Table 2), one with uncut DNA (enzyme free), two with single digestion of the DNA with each enzyme respectively and the last was a double digestion with both enzymes. The samples were incubated at 37°C for 1 hour.

**Table A1.** Reagents added per tube for digestion of plasmid DNA.

Reagents	Reaction Tube 1	Reaction Tube 2	Reaction Tube 3	Reaction Tube 4
NF water	16µl	15 µl	14 µl	13 µl
Green buffer	2 µl	2 µl	2 µl	2 µl
<i>Bam</i> HI	0 µl	1 µl	0 µl	1 µl
<i>Hind</i> III/ <i>Kpn</i> I/ <i>Pst</i> I	0 µl	0 µl	2 µl	2 µl
DNA	1-2µg (2 µl)	1-2µg (2 µl)	1-2µg (2 µl)	1-2µg (2 µl)
Total	20 µl	20 µl	20 µl	20 µl

### A5. Agarose gel electrophoresis

To characterize RNA and DNA in the range 200 to 50 000 base pairs, the standard method used is that of electrophoresis with agarose as the support medium (Boyer, 2012). To prepare a 0.8% agarose gel, 1.2 g of agarose was measured out and dissolved in 150 ml of a 1X TAE buffer in a microwavable flask. The flask was covered and microwaved for about 2 minutes or until the agarose was completely dissolved. The solution was left to cool for 5 minutes and then a final concentration of 5 µl/ml ethidium bromide was added to the flask. The solution was poured into the casting

tray. The comb was placed within the casting tray and the tray was left to sit for 20-30 minutes at room temperature to allow the gel to set. The gel electrophoresis unit was set up and the gel box was filled with 1X TAE buffer until it was completely covered. The 2  $\mu$ l of the molecular weight marker was added into the first lane. The digest samples were then also loaded onto the gel wells. The gel unit was plugged in and the gel ran at 100V for 1 hour.

#### **A6. Determination of protein solubility**

Protein solubility can be defined as an operational that can be determined by retention of protein in the supernatant after centrifugation (Hall, 1996). The solubility of a protein depends on the stability and structure of a protein (Pace et al, 2004). Competent *E. coli* XL1 Blue/JM109 cells were transformed with the recombinant plasmid and grown overnight in 10 ml 2x YT broth containing 100  $\mu$ g/ml ampicillin. Cultures grown overnight were diluted into fresh 90 ml 2x YT broth containing 100  $\mu$ g/ml ampicillin and allowed to grow at 37 °C with agitation at 160 rpm until mid-log phase (OD<sub>600</sub> 0.5–0.6) was reached. Protein expression was induced by the addition of 1 mM IPTG. The cells were harvested by centrifugation at 5000 g for 20 minutes at 4 °C 4 hours post induction and thereafter resuspended in 1 ml lysis buffer (10 mM Tris, pH 8.0, 300 mM NaCl and 10 mM imidazole, 1 mM PMSF and 1 mg/ml Lysozyme). Then the cells were mildly sonicated at an amplitude setting of 30 for 7 cycles with 15 seconds pulse and 30 seconds pause after each cycle. Cell lysates were subsequently centrifuged at 5000 xg for 20 minutes at 4 °C and the supernatant (soluble fraction) separated from the pellet (insoluble fraction). The pellet was resuspended in 1 ml PBS (pH 7.5). The samples were analysed by 12% SDS-PAGE and Western blot analysis to determine the solubility of recombinant proteins.

#### **A7. Sodium dodecyl sulphate-polyacrylamide gel electrophoresis (SDS-PAGE)**

In SDS-PAGE, proteins are treated so that they possess a uniform charge hence their electrophoretic mobility depends primarily on size so that larger protein molecules migrate slower than smaller protein molecules (Boyer, 2012). Proteins were treated by boiling in SDS sample loading buffer (0.25 % Coomassie Brilliant blue [R250]; 2 % SDS; 10 % glycerol [v/v]; 100 mM tris; 1 %  $\beta$ -mercaptoethanol) in a ratio of 4:1 for 10 minutes

and resolved using 12 % acrylamide resolving gel. The gel was then transferred into the electrophoresis tank and electrophoresis buffer (25 mM Tris, pH 8.3 250 mM Glycine and 0.1 % [w/v] SDS) was added. The boiled samples were loaded in respective wells and pre-stained protein molecular weight markers were also loaded. The electrophoresis gel was run at 120 volts for an hour.

**Table A2.** Preparation of 12% separating gel and of stacking gel

Reagents	1X Separating gel (ml)	1X Stacking gel (ml)
30 % Bis/acrylamide	2.08	0.235
1.5 M Tris pH 8.8	1.25	-
0.5 M Tris pH 6.8	-	0.438
10 % SDS	0.05	0.017
dH <sub>2</sub> O	1.58	1.05
10 % APS	0.025	0.085
TEMED	0.02	0.02

#### A8. Western blot analysis

Proteins were resolved in 12 % SDS-PAGE. SDS-PAGE gels were removed from the glass plates after completion of the electrophoresis process. The filter papers, gel, two scotch brite fibre pads and nitrocellulose were immersed in Western transfer buffer. Preparation of the gel for transfer was done as follows: filter paper was placed on a scotch brite pad. The gel was placed on the filter paper ensuring no air bubbles were trapped. Nitrocellulose membrane was placed over the gel; another filter paper was laid on top of the nitrocellulose, followed by another scotch brite pad. The transfer of the protein onto the nitrocellulose membrane was performed by running at 100 volts for 10 minutes using the TransBlotter. Upon completion, the membrane was removed and rinsed using transfer buffer using a cotton swab. The membrane was blocked in 10 ml of (5 % non-fat milk in TBS, pH 7.4) for 1 hour on a shaker set at 60 rpm. The membrane was washed 3 times in wash buffer (TBS-Tween pH 7.4) in 5-minute intervals followed by incubation of the membrane with primary antibody (anti-PFF1010c for PFF1010c and PFF1010c-HPD; anti-PfHsp70-1 for PfHsp70-1 and anti-Histidine for PfHsp40 and PfHsp40-SVN; 1:2000 dilution in 5% non-fat milk in TBS) in blocking solution at 4 °C on a shaker set at 60 rpm for 1 hour. Unbound antibodies were removed by washing the membrane 3 times using TBS-Tween for 15 minutes each wash. For the protein specific primary antibody, this was followed by incubation

in secondary antibody (anti-Rabbit) and subsequent washing under the same conditions as primary antibody. The bands were visualized using ECL.

### A9. Protein concentration determined using Bradford assay

The protein concentration of the purified recombinant protein was determined using Bradford's method. Bovine serum albumin (BSA) standards were prepared using concentration ranging from 0 to 1 mg/ml in 0.15 M NaCl. Bradford's reagent 200  $\mu$ l (Sigma Aldrich, USA) was added to the BSA protein preparations and to 10  $\mu$ l of recombinant protein prepared also prepared in 0.15 M NaCl. The reactions were incubated in the dark at room temperature for five minutes and the absorbance was read at 595 nm using a SpectraMax M3 (Molecular devices, USA). The series of BSA readings was used to draw up a standard curve as shown in (Figure A1) and the concentration of the recombinant protein was determined by extrapolation from the standard curve. All the readings were prepared in triplicate and the average obtained.

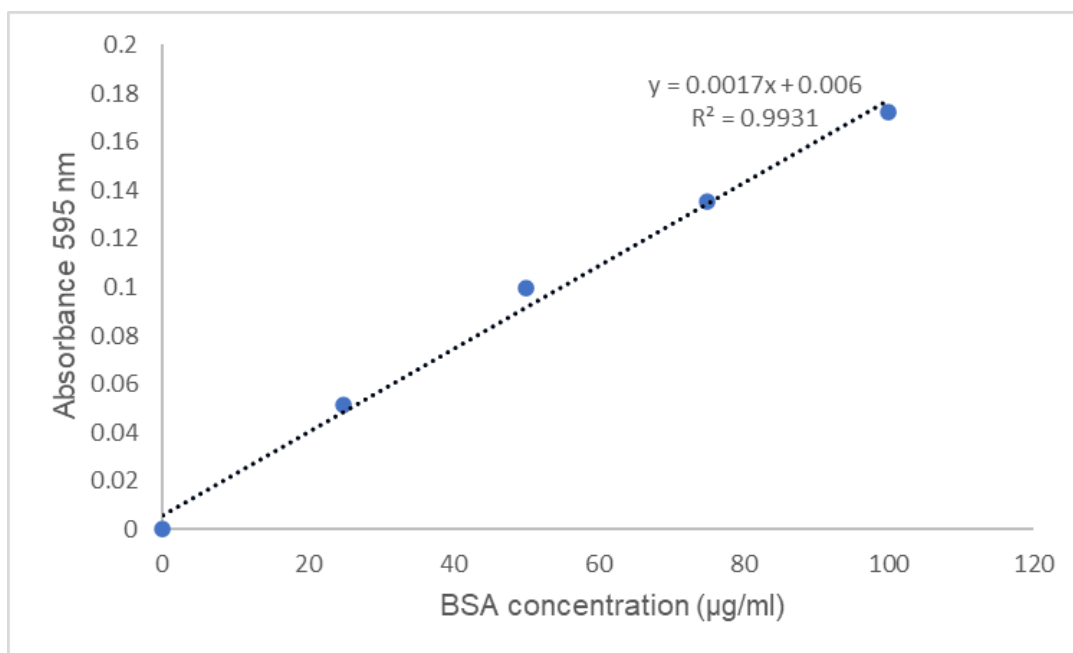


Figure A1. Protein standard curve.

### A10. Immobilization of ligand (PfHsp70s) on GLC sensor chip

The GLC sensor chip has four channels onto which ligand/protein can be immobilised on. Buffers are run through the channels using microfluidics. The chip was washed

with NaOH, which in continuation serves as a regeneration buffer. The second wash step is with EDC/NHS (this was prepared immediately before the washing as NHS has a short half-life). The protein, PfHsp70-1 (100 µg/ml), prepared in NaAc was immobilised onto the sensor chip. Ethanolamine was ran through the channels where PfHsp70-1 had now been immobilised with protein. The last step was a regeneration step using NaOH.

## Appendix B: Supplementary data

PFF1010c	1	MNTILTVNKTNELGKENEKNESELYEPSSDIDNNIILNINSMNSEHKKYFLNNY-----IS
DnaJ	1	-----
PfHsp40	1	-----MFFSSGFPFDSMGG
DNAJB1	1	-----
YDJ1	1	-----
PFF1010c	56	KIKYMRSSYSKPKYYEILNINVKSDAKTIRKSYLALSKLLSVNKKL-SREYEECYLIQK
DnaJ	1	-----MAKQDYEILGVSKTAEEREIRKAYKFLAMKYHPDINQGDKEAEAKFKEIKE
PfHsp40	15	QQARRKREVNNNKYYEVLNFKNCTTDEVKKAYRKLAIHHPDKGG-D---PEKFKIEISR
DNAJB1	1	-----MGKDYQTLGLARGASDEEIKRAYRQALRYHPDKNK-EPGAEEKFKIEIAE
YDJ1	1	-----MVKETKYYDILGVVPTADVEIKKAYRKCALKYHPDKNP-SEEAAEKFKIEASA
PFF1010c	115	SKILLNKFEKYYDVLNNYIDENTIEEQ-----RYMLEKEADIIYANKI----
DnaJ	53	AYEVLIDSQKRAAYDQYGHAFEGCGMGGGFGGGADFS-----DIFGDVFDIFGGGR
PfHsp40	71	AYEVLSDDEEKRKTYDEYGEELNCEQPAD-----ATDLDFILNA--
DNAJB1	51	AYVLSDPKRRELFDRYGEELKLGSGPSSGGSGGANGTSFSYTFHGDPHAMFEEFFGGRN
YDJ1	53	AYEVLSDPEKRDYDQEGEDLSEAGGAGGFPGGFGF-----GDDIFSQDFGAGG
PFF1010c	160	-----EELKDIYEKKEEQNKNGIIEKALYGDLSKKEECINNCFNIESIS
DnaJ	107	-----GRQRAARGADLRNMEELILEAVRGVT--KEIRIPTLEECDVCH---G---SG
PfHsp40	112	-----GKGGKRGEDIVSEYKVILEQLYNGAT--KKLAISKDICTNCE---G---HG
DNAJB1	111	PFDTFGQRNGEEGMDIDDPFSG---FPMGGGFTNVNFGRS-----RS
YDJ1	104	AORPR---GPORGDIKHEISASLEELYKGR--AKLAINKQITCKECE---G---RG
PFF1010c	207	EQLLQGPYIDLTKILQCKVENSSLIY---NDDFSFAYFCD--IPKPLIKISSKQTKKK
DnaJ	152	AKP---GTQPQTGPTCHGSGQV---QMRQGFFAVQQTCPHCQGRGTLLI--KDECNKCH
PfHsp40	157	GPK---DA-KVDCKQCNGRGTKTYMRYHSSVHQTEVTCNTRGKQKIFNEKDKQANK-
DNAJB1	152	AQE---PA-RKQD---PPVTHDLRVSEEI---YSCCTKKMKISHKRLNPD
YDJ1	151	GK---GA-VKCTSCNGQGIKIVTRQMGPMQRFQTECDVCHGTGDIIDPKDFCKSCN
PFF1010c	260	LYSIIHQDTEMYIYIKYKFLNVYHELIVVDR-----SNFSTIPQSS
DnaJ	202	G--HG-----RVERSKTLSVRLPAGVDTGDFIRLAGEGEAGEHGAPAGDLYVQVQVKQ
PfHsp40	211	G--MC-----VLKTRKILEVYIPKCAPNKHIVFNGEAGEKPNVIT--GNIVVILNEKQ
DNAJB1	194	G--KS-----LRNEDKILTEVKKGWKEGTITTEPKEGDQTSNNIP--ADIVFVILKDKP
YDJ1	206	G--KK-----VENERKILEVHEPFGMKDQRIIVFKGEADQAPDVIP--GDVVFVLSERP
PFF1010c	300	HRVFGDRISGPISPNVL-----KMTHESSSF-----K-----NI
DnaJ	253	HPVFEREGNNLCEVPIINFAMAALGGEIEVPTLDGRVVKL---VPGETQTGKLFMRCKG
PfHsp40	261	HPVFEREGIDLIMNYKISLYESITGFVAEVTHLDERKILVNCNMSGFTRHGDIIEVLDEG
DNAJB1	244	HNVFRKRDGSDVIYPARISLREALCGCTVNVPTLDGRT--IPVVFKVIRPGRMRKVPGE
YDJ1	256	HKSEFRDGDLLVYEAEDLLTLAGGEFALHEVSCDWLKVGI VPGVVIAPGMRVIEGKG
PFF1010c	331	LKF---FSKPKFYITLFTTI---VLCA-----
DnaJ	310	VKSVRGG-AQGDLLCRVVVETPVGINERQK--QILQELQESFGGPTGEHNSPRSKSFFDG
PfHsp40	321	MPTYKDPFKRGNLYITFEVEYPMDLIITNENKEVLIKILKKQNEVEKKYDLENSELEVVSC
DNAJB1	302	LPLPKTPEKRGDLIEFEVIFPERIPQTSRT---VLEQVLP-----
YDJ1	316	MPIPKYK-GYGNLLIKFTIKFENHFTSEENLKKLEEILPPRIVPAI----PKKATVDEC
PFF1010c	352	---QSIKIKMNLLE-----
DnaJ	367	VKKFFDDL---TR-----
PfHsp40	381	SPVDKKEYIKVRVTKQQQQQQEAYDDEDHQPEMEGGRVACAQQ
DNAJB1		
YDJ1	371	VLADFDPAK--YNSTRASRGGANYDSDE--EEQGGEGVQCASQ

- J-domain
  - HPD motif  
 - G/F rich region  
 - Zinc finger  
 - CAAX box

Figure B1. Full sequence alignment of PFF1010c with canonical Hsp40s. Highlighted in gold is the J-domain with the HPD motif in neon green, in red is the G/F rich region

and in purple is the zinc finger repeats. The Hsp40 proteins aligned with PFF1010c are from *E. coli* (DnaJ), *S. cerevisiae* (Ydj1), *Homo sapiens* (DNJB1) and *P. falciparum* (PF14\_0359).



```

KFG34430.1 1 -----
BAN65055.1 1 MGSVGI PRMEQSLPSDTAELSN TLE EYKQR RCKLQNGNDISLYGILELEPTCAQSDVRKS
PFF1010c 1 -----
SCP05061.1 1 -----
SBT79714.1 1 -----

KFG34430.1 1 -----
BAN65055.1 61 YYHFSRILHPDKCQDHS AASLLNDVQ MAYTILCDDYKRVLYDIKNGFSTGDQLQAQMSAL
PFF1010c 1 -----
SCP05061.1 1 -----
SBT79714.1 1 -----

KFG34430.1 1 -----
BAN65055.1 121 QQGLKERYMQFLNERQMN YIASVQEQYRLRGLVIQKAIYGDLSLKEPNKLVSMETITEQH
PFF1010c 1 -----
SCP05061.1 1 -----
SBT79714.1 1 -----

KFG34430.1 1 -----
BAN65055.1 181 LKGFIDVTVQLQLLCVRGTLN VNSGGPMSYAF LPGFYNP LEIATS DLMPCFEVDAQLYV
PFF1010c 1 -----
SCP05061.1 1 -----MS-----IPP-----
SBT79714.1 1 -----

KFG34430.1 1 -----
BAN65055.1 241 LYLFGKDVHEVTISDGT PFKLPMFTHR VYGSYIKG PYADGNLAVLVHCFSTHRXP-MEER
PFF1010c 1 -----MNTILT---VNKTNELGEKNEKN
SCP05061.1 6 ----HTDITTMKHND EETFQNGER-----EGERE GEGLR---EGERKGEGLRGER
SBT79714.1 1 -----MTH-----TSGQR-----ERTNGEAR---VGEESNKS-

KFG34430.1 1 -----
BAN65055.1 300 ----EKHSSLSGNV-----ADYLNKRNN-FLKKS ELTYEYEVLEVEKDCT
PFF1010c 21 ESLYEPSSDIDNNIILNINSMN SEHKKYFLN NYISKIKYR SSYSKPKYYEILNVNWKSD
SCP05061.1 50 KGESYETEIQNNTILNINSMN ENKKIFLN NYIKKIKYIKNYSKLNYYEILNVNWKSD
SBT79714.1 25 IITNEFPADIDSNEILKINSMN SENKKYFLN NYIAKIKYI SENYKPKYYEILNVNWKSD

KFG34430.1 1 -----VAEYVQI
BAN65055.1 339 PEDIRHAFYHFARIFHPDKSGNSKYSWVNEITKNAYDVL SNEYKRSSYDFENGFINSEDI
PFF1010c 81 AKTIRKSYLALS KLLSVNKKLSREYEECY YLIQKSYKILNKFEKFFYDVLN NYIDENTI
SCP05061.1 110 CKNIRKSYLLS KLLTVNKKLSNEYEEY YLIQKSYKILSDKFEKFFYDVLN NYIDKCMI
SBT79714.1 85 YKSIRKSYLLS KLLSVNKKLSSEYEECY YLIQKSYKILDEYERFYYDVLN NYIDENVI

KFG34430.1 8 QRE-----RAARDIENMRIDYQSKIEHEKKVGLIIRKALGNLR LRHSLIEEE-
BAN65055.1 399 QEKLTSIGDAMKQIYYTFINEKADAYINSYHEFTHKGLIKR ALFGDLSLVDPNLS--
PFF1010c 141 EEQRYLEKEADIT YANKIEELKDIYEIKKEEQNKNGLIIEKALFGDLSLKECINNCF
SCP05061.1 170 EKQRKYLEKEAD IYTNKIEELKDIYFKKIEENKNGLIIEKALFGNLLKDECINNCL
SBT79714.1 145 EEERKYLEKEAD IYTNKINELKNIYNKKIKKEEKNGLIIEKALFGNLLKDECINNCF

KFG34430.1 57 YSGPIREDCL EGPFLNVTIPLQ CQVDNSRFTFPGGSGS SMELNGFYNEAPC-----
BAN65055.1 457 STETINVKRLQGPYIDVTVQLQVLIQNGV LHLNSGNFSSFAYLPGFYNP-----
PFF1010c 201 NIESISEQHLOGP YIDTKILQCKVENSSLLNDD--FSFAYFC DIPKPLIKISKQTKK
SCP05061.1 230 NIEPIEDHVQGPFLDFTIILQARIENSSLLFNDD--FSFAHFC DIPKPLIKISSEK--K
SBT79714.1 205 NIEPIEDHIQGPFLDFTIILQSRVENSSLLFNDD--FSFAYFC DIPKPLIKIKSET-EK

KFG34430.1 109 -----VHEQDVCLYMLYDFRGLHEVTVCDRSYLAMP LKSHRVSPVTGCPGPEAFSNVR
BAN65055.1 507 -HFDQHRDSEAQLYMLYLFNDNVHEVTVSDNPIISLPMKSHMVYGA-YIKGYPPLANID
PFF1010c 259 KLYSHILQDTEMYLYIKYKFLNVYHELIVVDRSNFSLPQSSHRVFGD-RISGPFSPVNVL

```

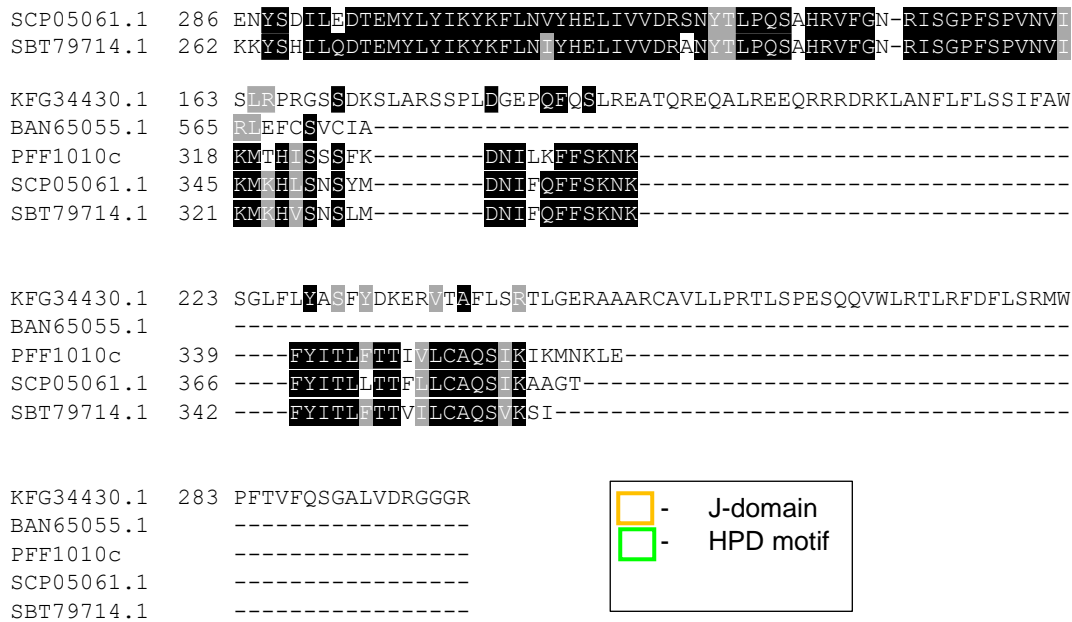


Figure B2. Full sequence alignment of PFF1010c with other parasitic Apicomplexa species. Highlighted in gold is the J-domain and in green the HPD/SVN/TVN motif of *P. falciparum* (PFF1010c), *P. ovale* (SCP05061.1), *P. malariae* (SBT79714.1), *Babesia bovis* (BAN65055.1) and *Toxoplasma gondii* (KFG34430.1) that does not possess a J-domain.

PFF1010c 1 -----  
 PF10\_0381 1 -----  
 PF11\_0034 1 -----  
 PFB0925w 1 -----  
 PFB0085c 1 -----MKCKRNVFFSKSLKFGHISVVFIFGIL  
 PFA0110w 1 MRPFHAYSWIFSQQYMDTKNVKEKNPTIYSFDDEEKRNENKSFLKVLCSKRGVLPITIGIL

PFF1010c 1 -----  
 PF10\_0381 1 -----  
 PF11\_0034 1 -----  
 PFB0925w 1 -----  
 PFB0085c 27 YGVINKLFISDVNSCYSVSNIIYERQLSEKDNLSNSLEQNGEPVVIGQFFSLPNGKSIS  
 PFA0110w 61 YIILNGLNGYNGSSSSGVQFTDRCSRNLGETLPVNPYADSENPIVVSQVFGLPFEKPTF

PFF1010c 1 -----  
 PF10\_0381 1 -----  
 PF11\_0034 1 -----  
 PFB0925w 1 -----  
 PFB0085c 87 ISDDIFIDEEQSIVNFIDNIEGLEQYMLWNNYMVIPHMKQYPPVFNNDKDIELNNKVDN  
 PFA0110w 121 TLESPPDIDHTNILGFNEKFMTPDVRNRYRSNNYEAIPHISEFNPLIVDKVLFDYNEKVDN

PFF1010c 1 -----  
 PF10\_0381 1 -----MLMFNLSN-----MNMS-----K  
 PF11\_0034 1 -----MLMFNLSN-----MNMS-----K  
 PFB0925w 1 -----  
 PFB0085c 147 LERNREDIIIETEKMLEIMKNEKNKFASLKCKLFNQYNKFKNKHNPKEQYKGCNLC  
 PFA0110w 181 LGRSGGDI IKMQTLMDEIMDINKRKYDSLKEKLQKTYSQYKVQYDMPKEAYESKWTCI

PFF1010c 1 -----  
 PF10\_0381 14 K-----RLNKN-NVNYMFEINLFDKNGKKNRKITSWKF-----CKSIIILT  
 PF11\_0034 14 K-----RLNKN-NVNYMFEINLFDKNGKKNRKITSWKF-----CKSIIILT  
 PFB0925w 1 -----MTLICGTPYMF-----MVV  
 PFB0085c 207 KLIEIGEKYLELKLNSVFYEWYDKKVICVEDFKRKIERCRTAKKALS NKIQYLCKNTIIN  
 PFA0110w 241 KLIDQGGENLEERLNSCFKNWYRQKYINLEFYRRLTVLNQTAKKALS NQIQYSCKIMNS

PFF1010c 1 -----  
 PF10\_0381 54 TLGMLYTF-LLKVDC--TI-----KNCTSKN-----  
 PF11\_0034 54 TLGMLYTF-LLKVDC--TI-----KNCTSKN-----  
 PFB0925w 16 CVNKLYAEFFAYT-----F-----  
 PFB0085c 267 CLDKIKYMNEKIMKAKKKAQKVVE---KPEPKKQEEENLSMVEGLNCFEENH-KIICI  
 PFA0110w 301 DISFFKHINELKSLHRAAKAAEAEMKKRAQPKKKK-----SRRGWLCCGGGDIETVPEP

PFF1010c 1 -----  
 PF10\_0381 78 -----FTHKRRLYENEFFNNY-NDEFSNENYNKVGEKYFHCIKTAKFIDDDSSDVL  
 PF11\_0034 78 -----FTHKRRLYENEFFNNY-NDEFSNENYNKVGEKYFHCIKTAKFIDDDSSDVL  
 PFB0925w 29 -----DERHQRNLYTAECLIKNKESYSLEKNDSSSIINYYKSTQNPYIDEIDVDNY  
 PFB0085c 322 KNDLIS---GCENWDTQGC-----PSNEIINSSSINYYEKMRDGLYHDDIYDAL  
 PFA0110w 356 QQEPEVQTVQEQVNEBYGDIL-----PSIRASITNSAINYYDTVKDCVYLDHETSAL

PFF1010c 1 -----  
 PF10\_0381 129 VKEHDNNIKELE-----NYNLFESDEINSNSN-----  
 PF11\_0034 129 VKEHDNNIKELE-----NYNLFESDEINSNSN-----  
 PFB0925w 81 KGELKEIKINKNDISNEINKNDTLNDLKRSDEFHNRNGLHNREGSESKYVSNISAKEMT  
 PFB0085c 371 VTDDDLIFEMFDENKEDDIEESENESD--EDDLIVESESNESDE---DDLIVEEYE  
 PFA0110w 409 YTDEDLIFDLEKQKYMD-MLDTSEESVKENEEHTVDDEHVEEHTA---DDEHVEEPT

PFF1010c 1 -----MN-----TILTVNKTNELGEK-----NEKNESIYE-  
 PF10\_0381 156 -----YKEGKEL-----NOIDE-T-----

```

PF11_0034 156 -----YKEGKLE-----NVIDE-T---
PFB0925w 141 NQDNCRKSSHNRKRCYSLEKELEKLYRIALNNSNLNNKKKKKHNKLNLDNTNIDNNIYID
PFB0085c 425 NNESEDEDESIIIEYGAQ-----EEVA--T--S
PFA0110w 464 ---VADDE-HVEEPTVAD-----EHVEEPT-V

PFF1010c 26 PSSD-----IDNNIIDNINSMNSEHKKYF-----NNYISKIKYMRSSYSKPK
PF10_0381 169 SPSV-----I-RN-----IKDEGYNIDDNS-----YSNENFLDYSVDRT
PF11_0034 169 SPSV-----I-RN-----IKDEGYNIDDNS-----YSNENFLDYSVDRT
PFB0925w 201 NNTNIDNNINIDNNINIDNNI--NIDNNINIDNNINIDNNINIDNNINIDNNINIDNNINICVDYT
PFB0085c 449 SSEV-----VDDEFTTNEI--ESEERYSLDKEANRLLFKNDIYNIWFSDLNIIYVDIT
PFA0110w 486 AEEH-----VEEPTVAEEHV--EE-----PA-----SDVQQTSEAAPTIEIPDTL

PFF1010c 69 YYEILNVNVKSDAKTIRKSYLAKSKLLSVNKLKR-EYEECYLIQKSYKILTNKFEKFFY
PF10_0381 202 YYDILNVNVDASLNEIKNNYYNLALEYFLDKNTNDLKRKMEFEKISEAYQILSDKEKREK
PF11_0034 202 YYDILNVNVDASLNEIKNNYYNLALEYFLDKNTNDLKRKMEFEKISEAYQILSDKEKREK
PFB0925w 259 YYDILNINANSKLEIKKYYEYASKYHPEKNIIGNDKAFKFFELINSAYQILSNEELERK
PFB0085c 501 YYDILNVYPTSELSKSNYYNLALKYNPENLGNAEALTKFERDINEAYQILSLDQERMN
PFA0110w 524 YYDILGVGVNADNNEITERYKLAENYRYORSQS-TVFHNERKNEAYQVLGDIIDKRW

PFF1010c 128 YDVLNN-----YIDENTEEQRYMLEKEADIIYANKIEELKDIYEIKIKEEQNKNCCLI
PF10_0381 262 YHKEGLDVTKDMFIMDPSILFMLNYSLDQLEPYIGKYDITTI-----INFVTDQFTRGNI
PF11_0034 262 YHKEGLDVAKDMFIMDPSILFMLNYSLVQLEPYIGKYDITTI-----INFVTDQFTRGNI
PFB0925w 319 YNSDERSKMNTNLDPEFVLFMLSYISINMSFYVQGLKIEYL-----TEESFETNS---N
PFB0085c 561 YNKYELNATKDMFLIDPSIFVYKMLSTEKFDYIGTTQIESF-----LKVLSKNI---A
PFA0110w 583 YNKYEVYGIKQVNFNPSIFYI--LSSLEKFRDITGTPQIVTL-----LRFFFEKRL---S

PFF1010c 181 IEKALYGDLSLKEECINNCFNIE-SISEQH-----LQGPYIDLT-KILQCKVE-NSSL
PF10_0381 317 FETLIGKSSLEKYGDLIRKMDKEEERKKNLVLFLKDRLOEYVDVDEDTWIKMENEIMG
PF11_0034 317 FETLIGKSSLEKYGDLIRKMDKEEERKKNLVLFLKDRLOEYVDVDEDTWIKMENEIMG
PFB0925w 371 FYDI-----LLSNKIMNYYLNVEOKIREVELALLRDRLETYEGD-ENCTVPTKNNIRA
PFB0085c 613 LHEL-----EHRLEDLMNLMYEQQEVROVKALMLRNKLQPYVDGD-DQWKKHMEBEVKK
PFA0110w 634 MNDL-----ENKSEHLKFMEOYQKEREAHSEYLLNLIQPCITAGD-SKWNVPTITKLEG

PFF1010c 231 LYNDDFSFAFYCD-----IPKPLIKISSKQT-----K-----K
PF10_0381 377 LLESKFSSYIIESVGVYENVAFAIGKEGKMSMDEKKARKOAKHREOMNRKEA---MI
PF11_0034 377 LLESKFSSYIIESVGVYENVAFAIGKEGKMSMDEKKARKOAKHREOMNRKEA---MI
PFB0925w 425 ILEYSFSSSIMNFVGNLYEYFSKLYMGYNIETLS-----L-MND-----NK---GIME
PFB0085c 667 LNKSIFGTEFLKSLGWYITNIQCYREDNCHSFGVNLKLANMEFENRNKKNQLKVSXSMR
PFA0110w 688 LKGSREFDIPILLESIRWLEKHKVAKTHIKKSSKSA-----KKLQQRTOANKQELANINN

PFF1010c 259 KLYSHL-----QDTEMYLYI-----KYKFLNMYHEIIVVDRSNFSPPSSHRVFGDRIS
PF10_0381 433 WSFRTVSSIGYIISGEPKNHLMHGVTCNYYNYE-----M-----
PF11_0034 434 WSFRTVSSIGYIISGEPKNHLMHGVTCNYYNYE-----M-----
PFB0925w 468 NLFERN-----VKKEMHKNL-----LN-KNN-----V--N-----ITKDS
PFB0085c 727 NLLSII--KEYIPRNEITGL-----VKKIEYKSEN--D-----ENNISNVNEKSSS
PFA0110w 740 NLMSTI--KEYVGSSEOMNSI-----TYNFENINSNV--D-----NGVQS

PFF1010c 309 GPFSPVN-----VL-----KMTHTI--SSFKDNILKFFSKNKFY--
PF10_0381 469 NNFYNYDD-----KLVC--HYPNGYSINKMFHRIHTFVKNTTVYF
PF11_0034 470 NNFYNYDD-----KLVC--HYPNGYSINKMFHRIHTFVKNTTVYF
PFB0925w 495 DDFIITDEKD-----HNNENIKNCTVLFNHIR--SNNENNINLEDMTRNVLII
PFB0085c 772 NDNSSDDENQENENENENQENENENENRDKL-----KLL--SDNEKRKVLHFMKKNKVV
PFA0110w 776 -----KNI-----SDL--SYTDQKELLEKIVSYVDS

```

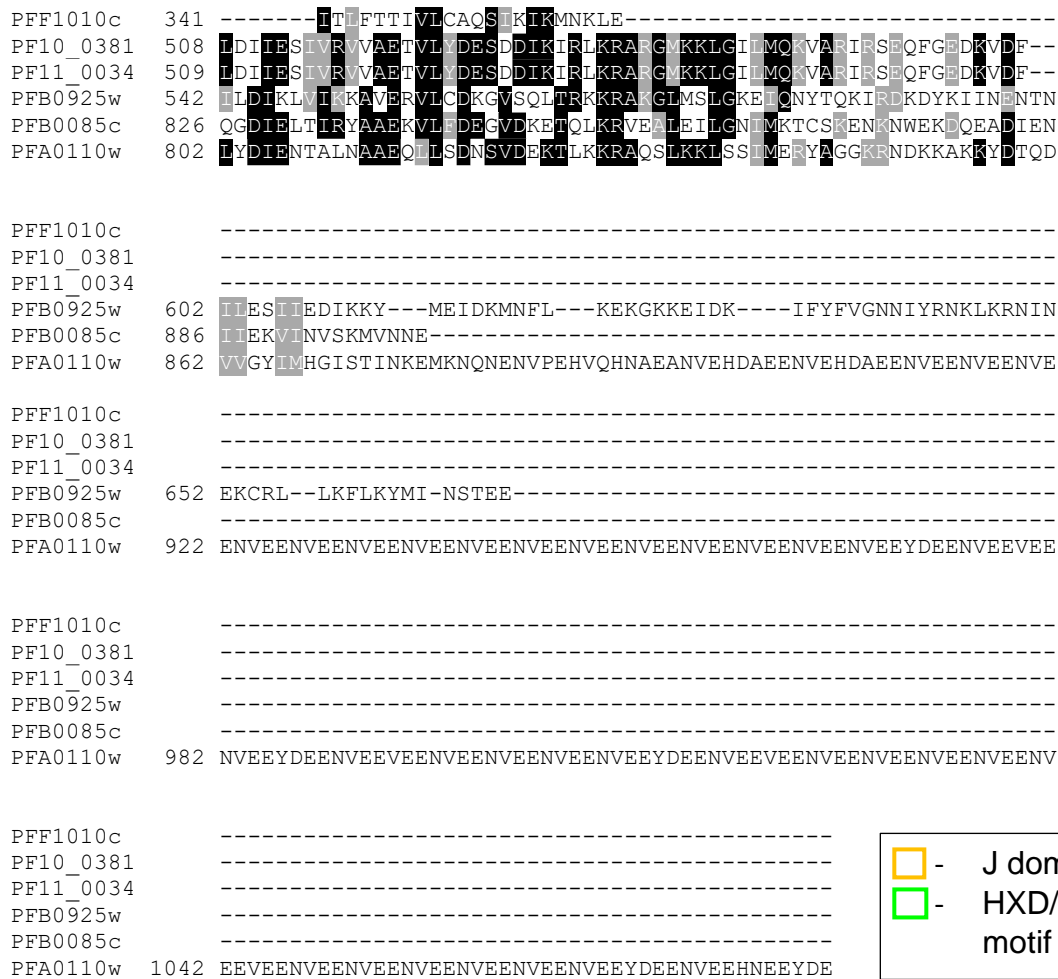
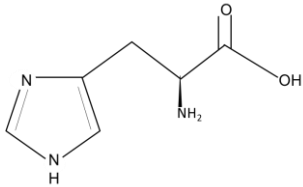
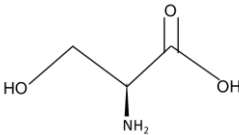
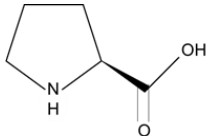
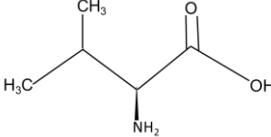
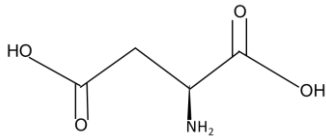
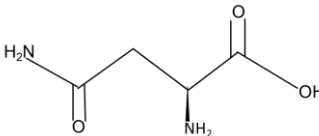
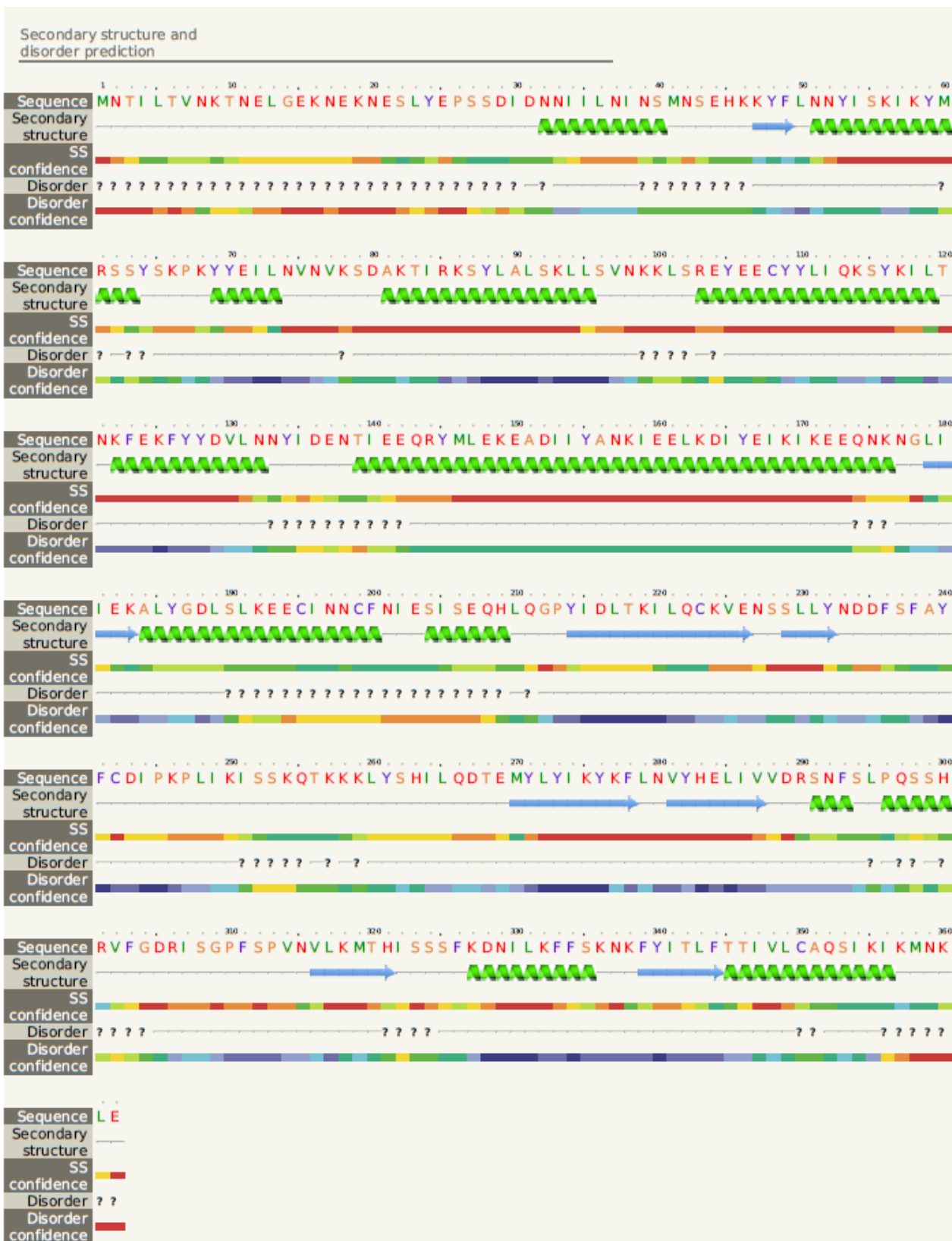


Figure B3. Full sequence alignment of PFF1010c with other *P. falciparum* type IV Hsp40s

**Table B1.** Properties of amino acid residues in HPD and SVN motif

HPD motif	SVN motif
 <p>Histidine, His, H MW: 155 pI: 7,59 Basic side chain</p>	 <p>Serine, Ser, S MW: 105,09 pI: 5,68 Neutral side chain</p>
 <p>Proline, Pro, P MW: 115,13 pI: 6,30</p>	 <p>Valine, Val, V MW: 117,15 pI: 5,96 Hydrophobic side chain</p>
 <p>Aspartic acid, Asp, D MW: 133,11 pI: 2,77 Acidic side chain</p>	 <p>Asparagine, Asn, N MW: 132,12 pI: 5,41 Neutral side chain</p>



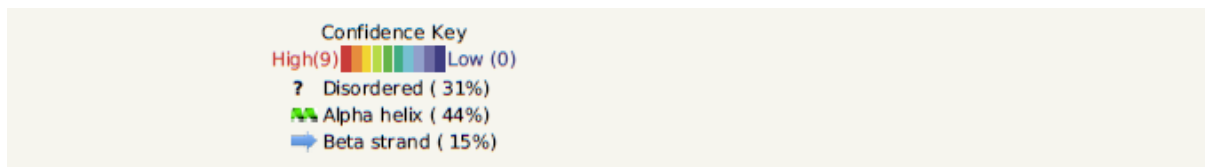
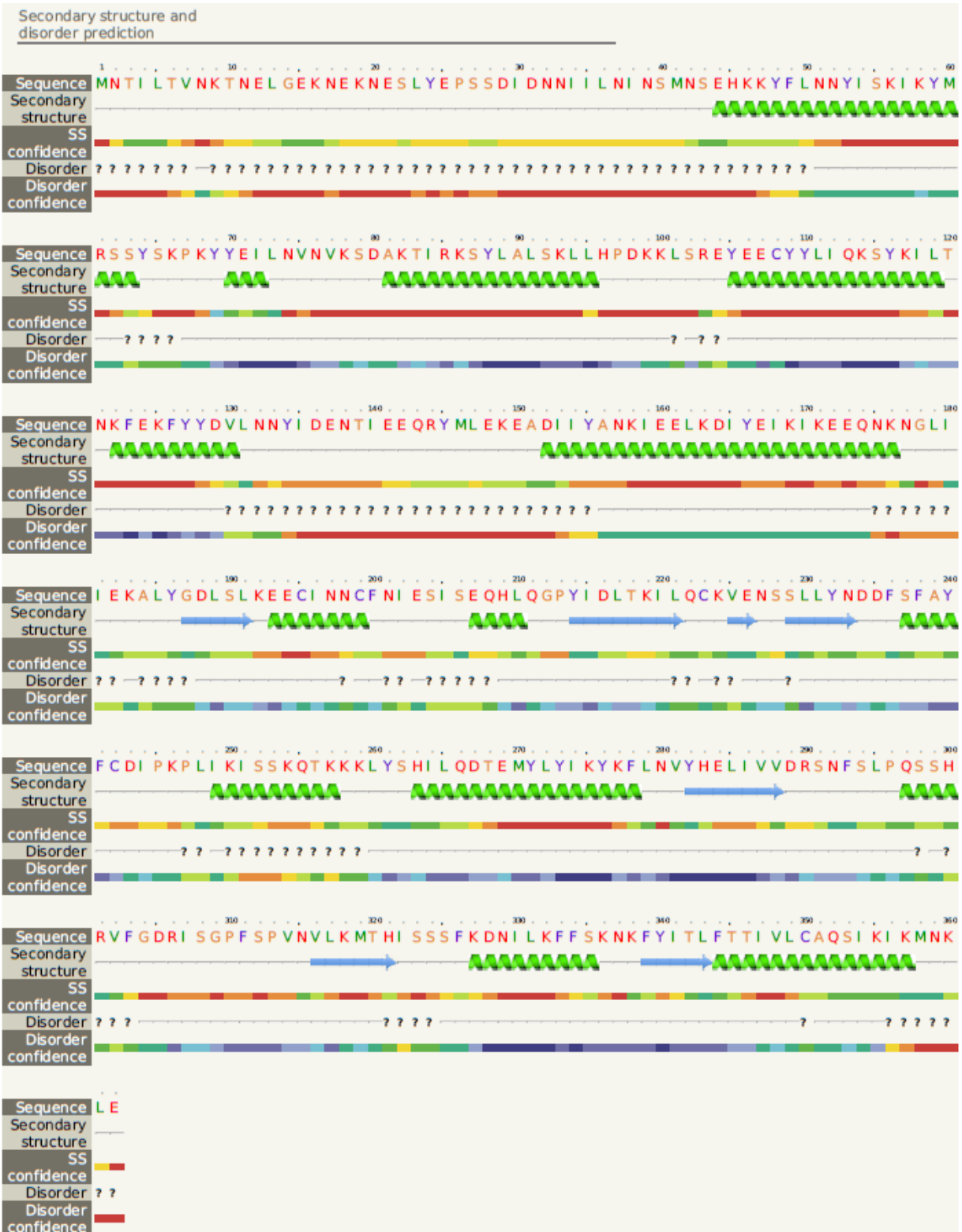


Figure B4. Secondary structure prediction of PFF1010c obtained from Phyre2 showing the position and percentage of alpha helices, beta strands and disordered regions.





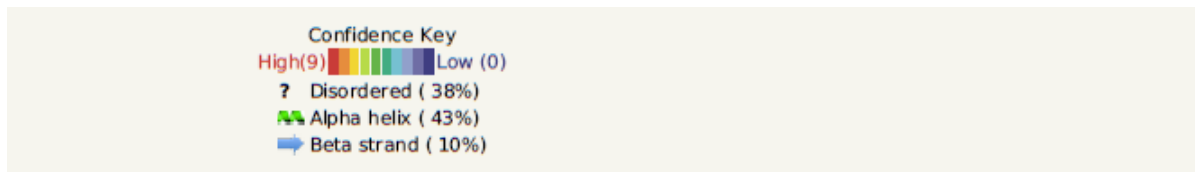
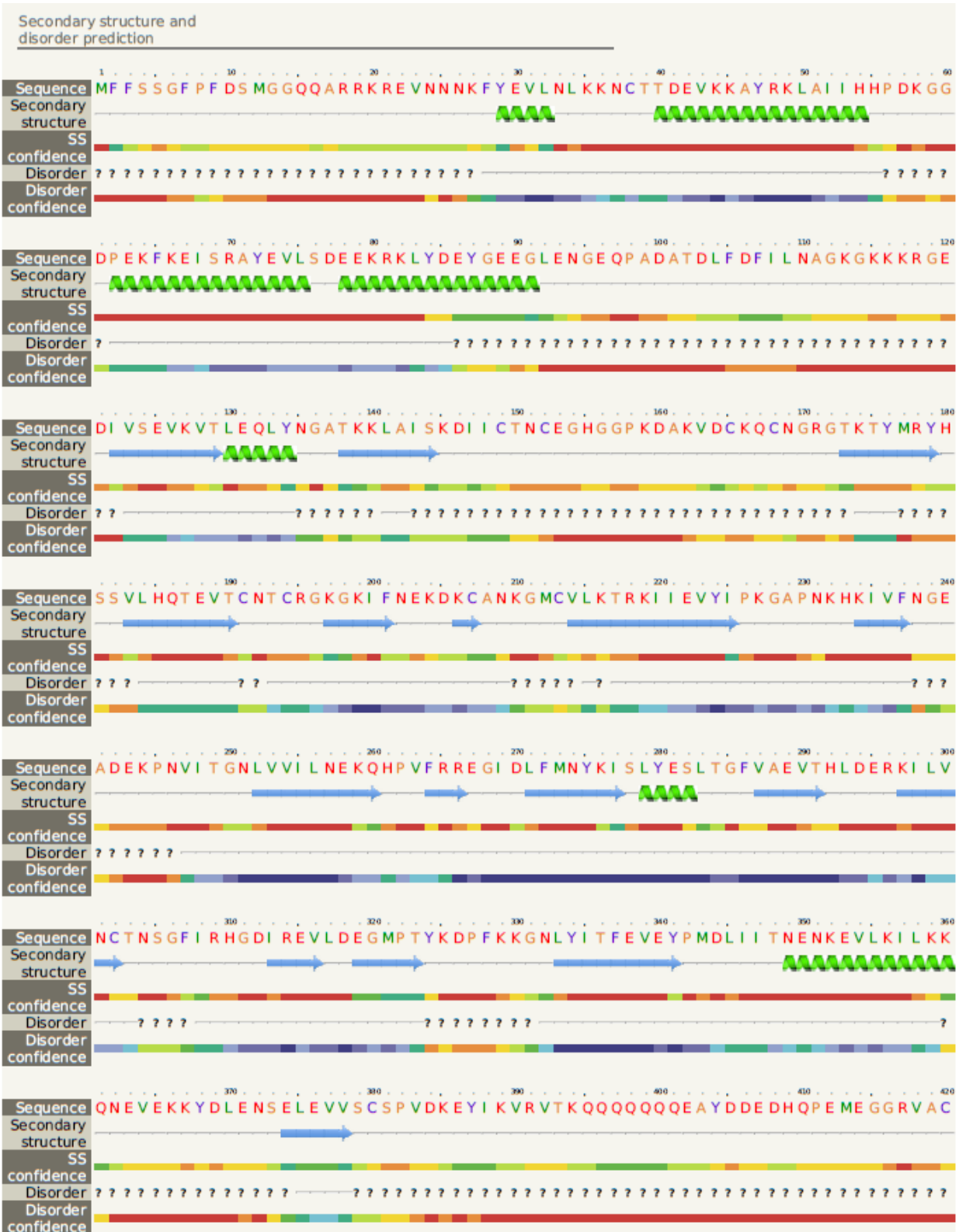


Figure B5. Secondary structure prediction of PFF1010c-HPD obtained from Phyre2 showing the position and percentage of alpha helices, beta strands and disordered regions.



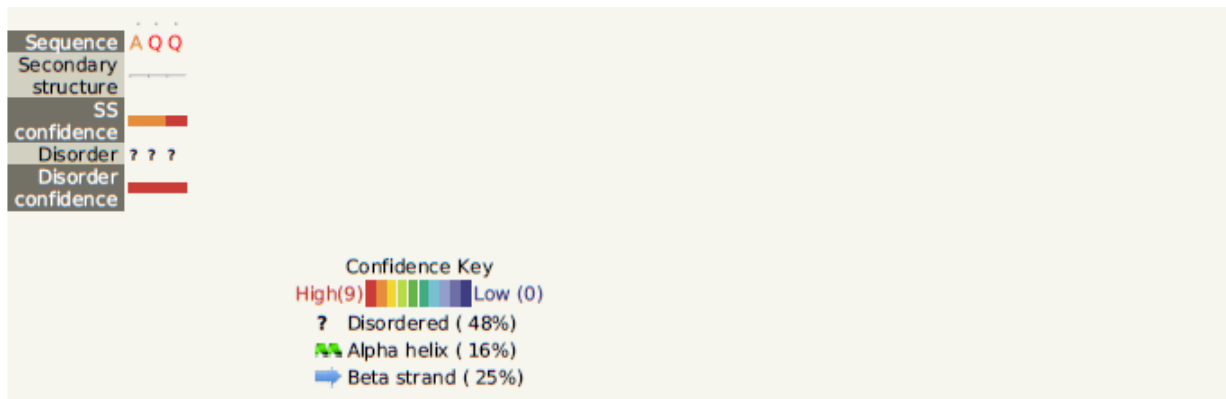
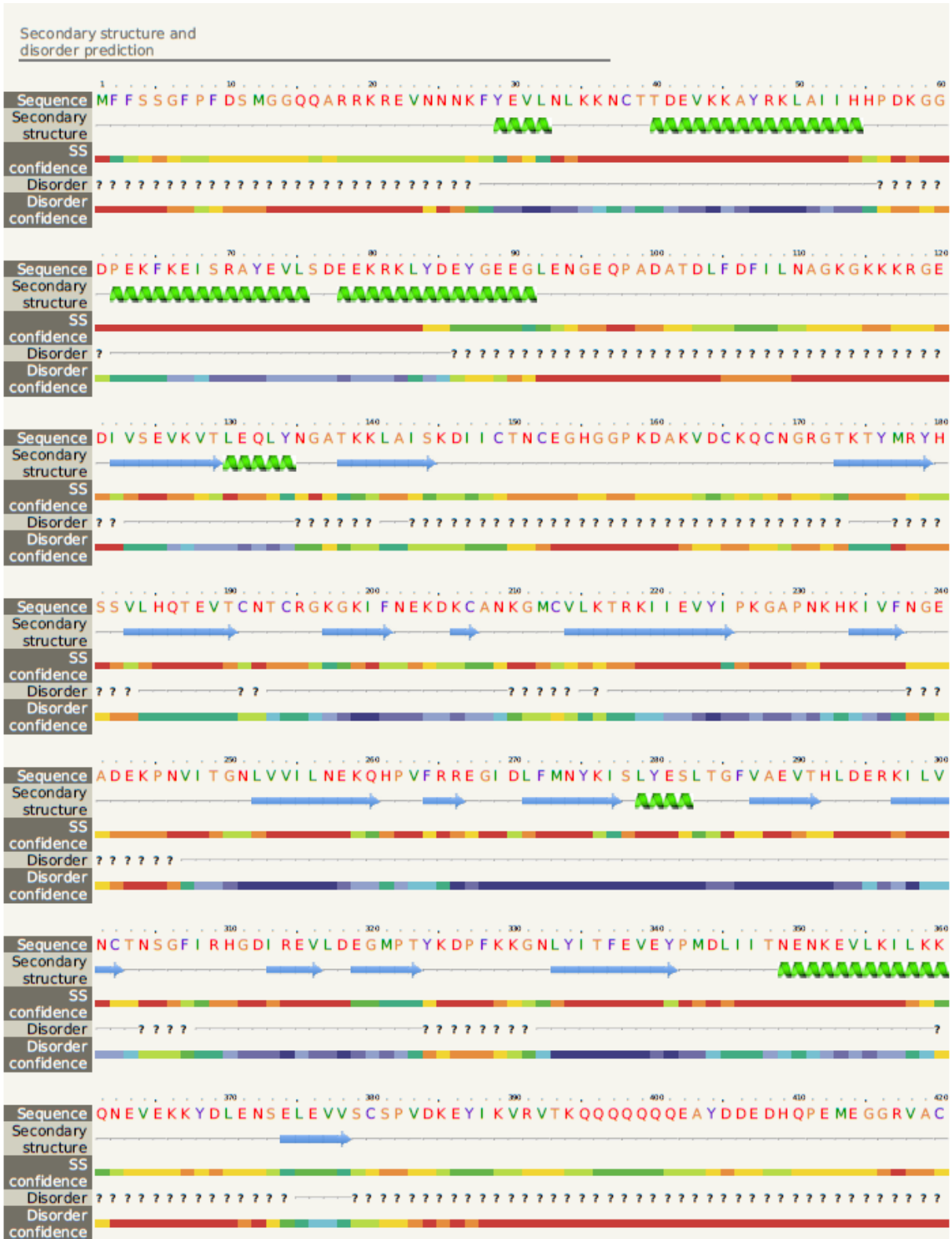


Figure B6. Secondary structure prediction of PfHsp40 obtained from Phyre2 showing the position and percentage of alpha helices, beta strands and disordered regions.



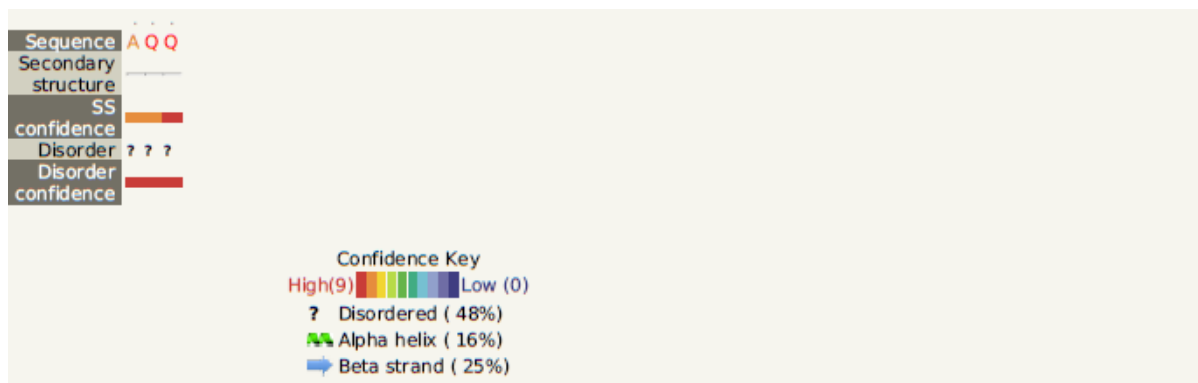
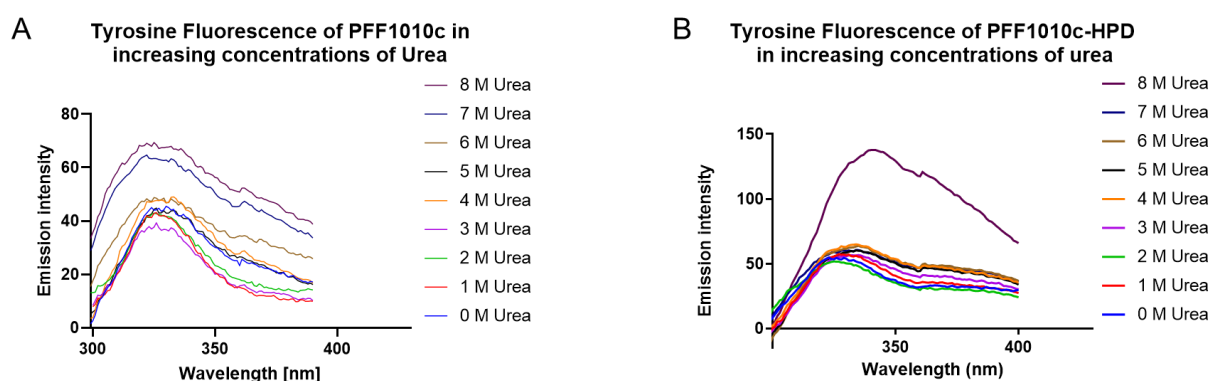


Figure B7. Secondary structure prediction of PfHsp40-SVN obtained from Phyre2 showing the position and percentage of alpha helices (green helices), beta strands (blue arrows) and disordered regions (black question marks).

**Table B2** Peptide properties of Hsp40s

Protein	Hydrophobic %	Acidic %	Basic %	Neutral %
PFF1010c	35.08	12.71	16.02	36.17
PFF1010c- HPD	35.08	12.98	16.3	35.64
PfHsp40	32.38	16.31	18.44	32.8
PfHsp40-SVN	32.39	16.08	18.2	33.33



**Figure B8. Effect of urea on PFF1010c and PFF1010c-HPD tertiary structures.** Increasing concentrations of urea (0 – 8 M) were used to investigate structure conformation changes on (A) PFF1010c and (B) PFF1010c-HPD. Tyrosine fluorescence was used to monitor shifts in wavelengths.

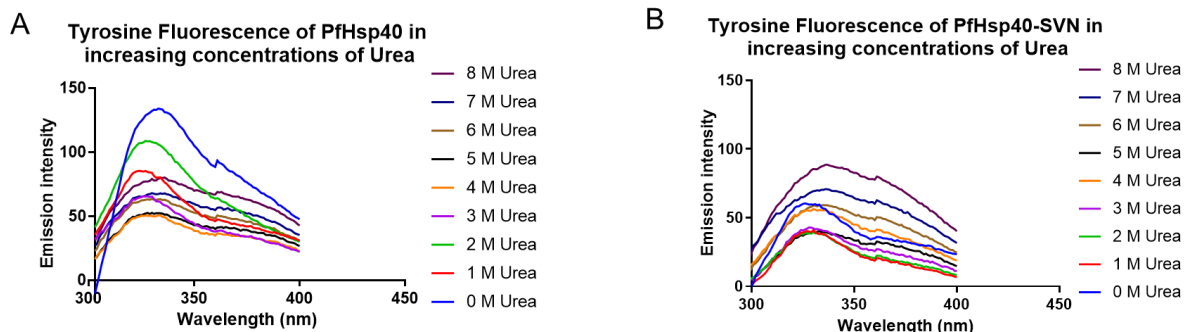


**Figure B9. Effect of urea on PfHsp40 and PfHsp40-SVN tertiary structures.** Increasing concentrations of urea (0 – 8 M) were used to investigate structure conformation changes on (A) PfHsp40 and (B) PfHsp40-SVN. Tyrosine fluorescence was used to monitor shifts in wavelengths.

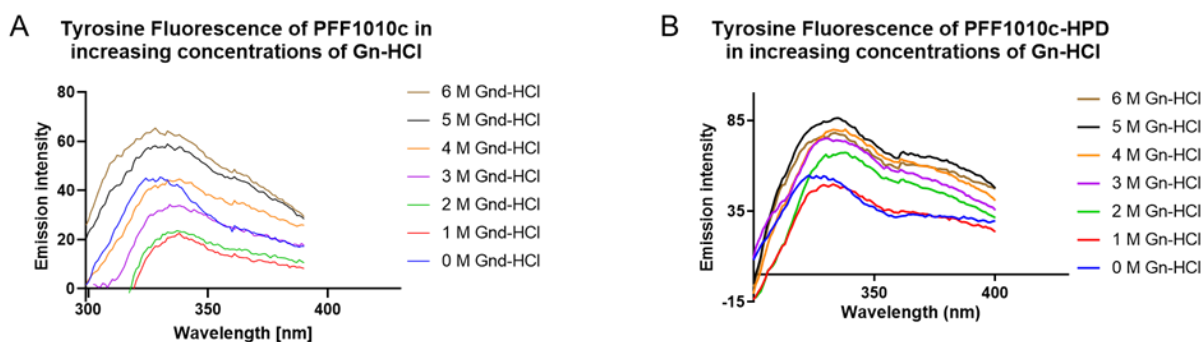


**Figure B10. Effect of guanidine hydrochloride on PFF1010c and PFF1010c-HPD tertiary structures.** Increasing concentrations of urea (0 – 6 M) were used to investigate structure conformation changes on a.) PFF1010c and b.) PFF1010c-HPD Tyrosine fluorescence was used to monitor shifts in wavelengths.

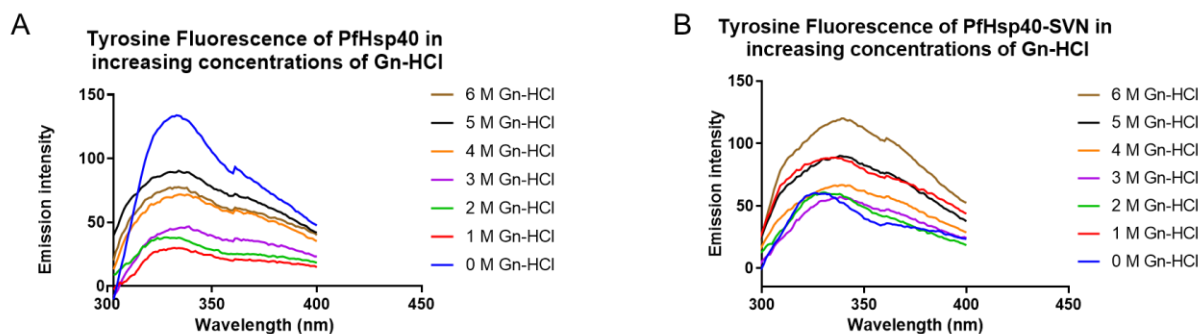


**Figure B11. Effect of guanidine hydrochloride on PfHsp40 and PfHsp40-SVN tertiary structures.** Increasing concentrations of urea (0 – 6 M) were used to investigate structure conformation changes on a.) PfHsp40 and b.) PfHsp40-SVN. Tyrosine fluorescence was used to monitor shifts in wavelengths.

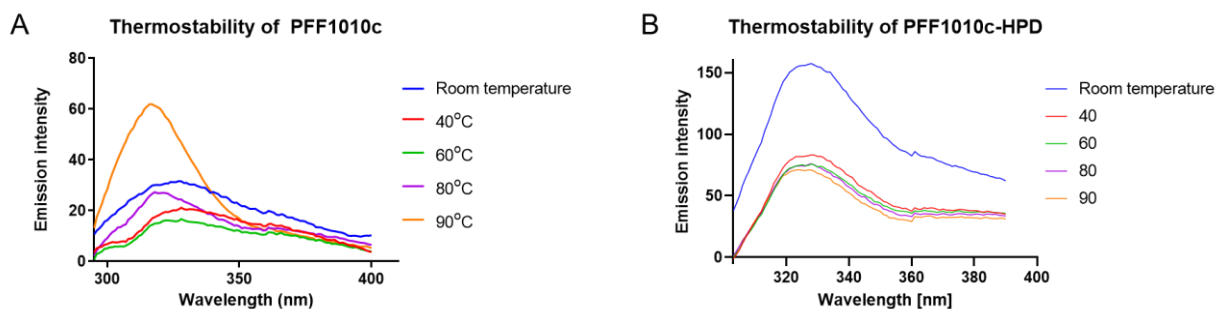


**Figure B12. Investigating the thermostability of PFF1010c and PFF1010c-HPD.** The proteins a.) PFF1010c and b.) PFF1010-HPD, were subjected to increasing temperatures to investigate the stability of their tertiary structures under heat stress.

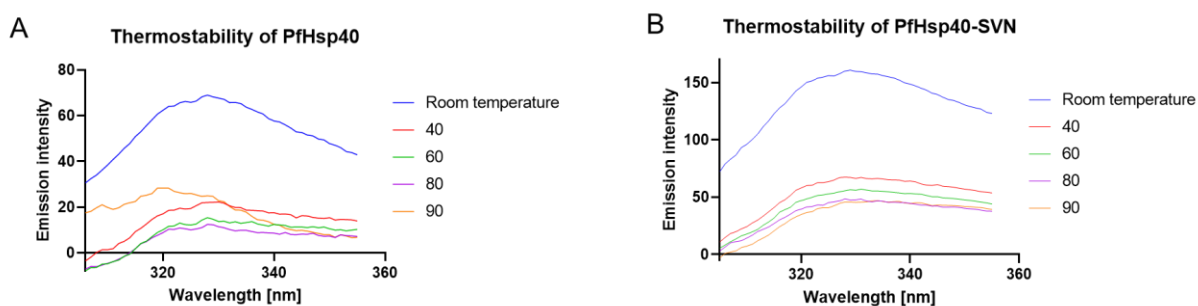


**Figure B13. Investigating the thermostability of PfHsp40 and PfHsp40-SVN.** The proteins a.) PfHsp40 and b.) PfHsp40-SVN, were subjected to increasing temperatures to investigate the stability of their tertiary structures under heat stress.



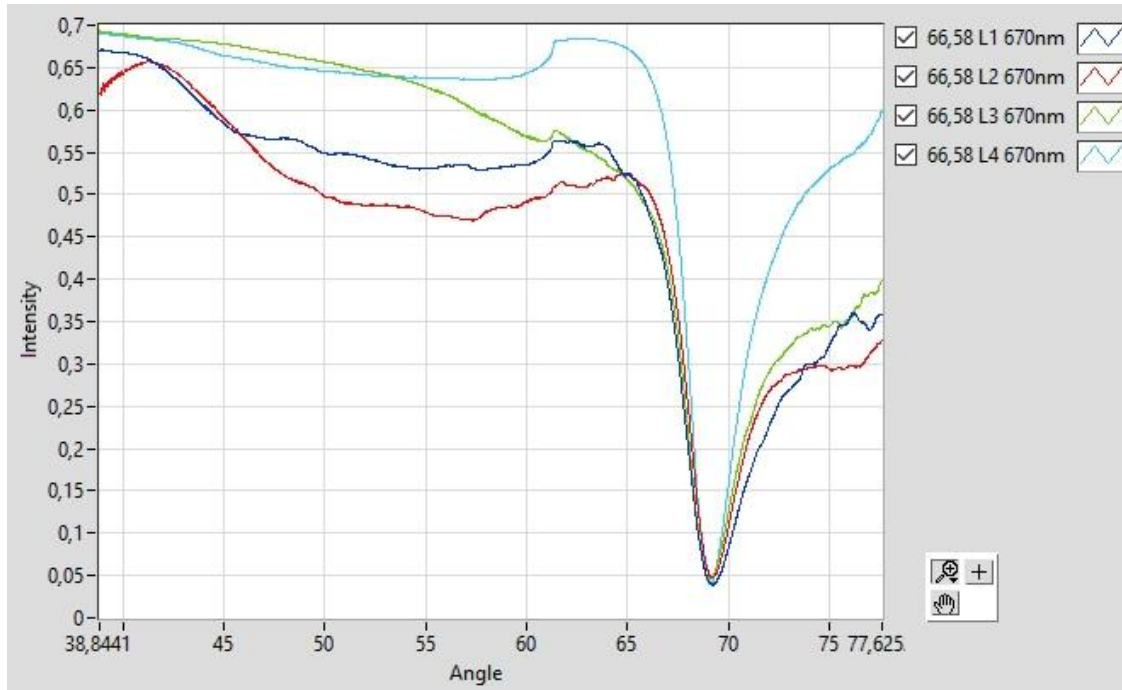


**Figure B14. SPR curve.** SPR curve indicating the reflectance intensity *versus* the incident light angle (Jang *et al*, 2015).

## Appendix C: List of Reagents

<b>REAGENT</b>	<b>SUPPLIER</b>
Acetic acid	Merck, Germany
Adenosine triphosphate	Sigma, U.S.A
Agarose	Whitehead scientific, South Africa
Ammonium molybdate	Merck, Germany
Ammonium persulphate	Merck, Germany
Ampicillin	Sigma, U.S.A
Ascorbic acid	B & M Scientific, South Africa
Bovine serum albumin	Sigma, U.S.A
Bromophenol blue	Sigma, U.S.A
Calcium chloride	Merck, Germany
Chloramphenicol	Sigma, U.S.A
Coomasie brilliant blue R250	Merck, Germany
Diethiothreitol	Sigma, U.S.A
Ethidium bromide	Sigma, U.S.A
Glacial acetic acid	Merck, Germany
Glycerol	Merck, Germany
Glycine	Merck, Germany
Guanidine hydrochloride	Merck, Germany
HEPES	Merck, Germany
Imidazole	Sigma, U.S.A
Isopropyl-1-thio-D-galacopyranoside	Sigma, U.S.A
Lysozyme	Merck, Germany

Magnesium chloride	Merck, Germany
Methanol	Merck, Germany
Monoclonal anti-His6-HRP antibodies	Sigma, U.S.A
Ni-NTA resin Thermo	Scientific, U.S.A
Nitrocellulose membrane	Pierce, U.S.A
PagerRuler Prestained Protein Ladder	Thermo Scientific, U.S.A
Peptone	Merck, Germany
Phenylmethylsulfonyl fluoride	Sigma, U.S.A
Polyacrylamide	Merck, Germany
Potassium chloride	Merck, Germany
Potassium dihydrogen phosphate	Merck, Germany
Restriction enzymes	Thermo Scientific, U.S.A
Sodium chloride	Merck, Germany
Sodium dodecyl sulphate	Merck, Germany
Sodium hydroxide	Merck, Germany
TEMED	VWR Life Science, U.S.A
Tris	Merck, Germany
Triton X-100	Merck, Germany
Tryptone	Merck, Germany
Tween 20	Merck, Germany
Urea	Merck, Germany
Yeast extract powder	Merck, Germany
$\beta$ -mercaptoethanol	Sigma, U.S.A